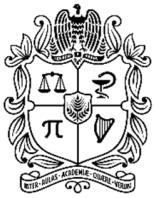

UNIVERSIDAD
NACIONAL
DE COLOMBIA

Manipulación metabólica como estrategia para el mejoramiento del biocrudo obtenido por licuefacción hidrotermal de microalgas

Alejandra Palomino Martínez

Universidad Nacional de Colombia

Facultad de Ingeniería, Departamento de Ingeniería Química y Ambiental

Bogotá, D.C., Colombia

2020

Metabolic manipulation as a strategy for the improvement of the biocrude obtained by hydrothermal liquefaction of microalgae

Alejandra Palomino Martínez

Dissertation submitted as partial requirement to obtain the degree of:

Doctor en Ingeniería – Ingeniería Química

Advisor:
Rubén Darío Godoy Silva, Ph.D.
Co-advisor:
Luis Carlos Montenegro Ruíz, Ph.D.

Research area:
Biotechnology and Chemical Processes
Research Group:
Grupo de Procesos Químicos y Bioquímicos

Universidad Nacional de Colombia
School of Engineering, Chemical and Environmental Engineering Department
Bogotá, D.C., Colombia
2020

Acknowledgements

I am grateful to all who supported me during the completion of my Ph.D. studies. I express my sincere thanks to:

- Professor Rubén Darío Godoy Silva for his guidance and support during all my doctoral studies.
- Professor Luis Carlos Montenegro Ruíz for his guidance and support during the microalgae culture stage.
- Professor Yazmin Yaneth Agámez Pertuz for her guidance and support during the liquefaction stage.
- Professor Luis Ignacio Rodríguez Valera for his technical advice on supercritical processes.
- Professor Christopher J. Chuck for giving me the opportunity of doing a research internship at the University of Bath
- All the members of the Research Group of Chemical and Biochemical Processes and the Chemical and Environmental Engineering Department, especially to engineers Fabian Rondón, Mateo Quintero, Johan Pasos and Andrés Forero, for their support in the standardization of biomass characterization techniques.
- All the members of the Algae Cultivation Laboratory of the Department of Biology, especially to biologist Edward Cano for his support in the culture of microalgae.
- All the members of the Fuel and Energy Laboratory of the Department of Chemistry, especially to Professor German Moreno, for his technical support.
- The Administrative Department of Science and Technology of Colombia – Colciencias for the Colombian Doctral Formation Grant (No. 617/2014)
- The Research Division of the Universidad Nacional de Colombia – Campus Bogotá for the financial support (Hermes Project 35768).

Abstract

Hydrothermal liquefaction of the microalga was carried out. A response surface methodology was used to explore the effect of reaction temperature, retention time, initial total solids, and biomass composition, as well as their interactions, on the yield and quality of the resultant biocrude. The maximum biocrude yield was obtained between 315–325 °C and 40–45 min, at lipid ratio and initial total solids of 0.65 and 15 %, respectively. Under these conditions, the higher heating value was 35 $MJ \cdot kg^{-1}$, the total acid number was 70 mg $KOH \cdot g^{-1}$ and the carbon, nitrogen and oxygen contents were 72 %, 3.7 % and 13 %, respectively. The inclusion of the chemical composition of the biomass as a modeling factor allowed predicting the yield and quality of the biocrude for several data sets published in the literature. The regression model predicted 61 % of the biocrude yields published within the standard deviation zone of ± 5 %. The degree of success for the models predicting quality parameters ranged from to 50-80 %.

A new quantitative model was proposed for the calculation of biocrude yield of microalgae. The new model was tested with large numbers of experimental data published over a wide range of temperatures (200–400 °C), retention times (1–120 min) and chemical composition of microalgae (0.0–66 % lipids, 9–75 % proteins, 5–64 % carbohydrates, in dry basis). This model predicted 45 % of the biocrude yields published within the standard deviation zone of ± 5 % and 78 % of the total data was within the zone of standard deviation of ± 10 %.

The effect of reaction temperature, retention time and elementary composition of the biomass was evaluated on the quality of the algae biocrude and used to propose a new quantitative model for the calculation of the elemental composition of this biocrude. The model provided information on the behavior of the reaction temperature and retention time on the carbon, nitrogen, hydrogen, and oxygen content of the algae biocrude. The new model was successful in more than 81 % for predicting the elemental composition of the macroalgae biocrude. The prediction capacity of the carbon, nitrogen, and oxygen content in the microalgae biocrude was between 53 and 81 %.

The storage stability of biocrude produced from hydrothermal liquefaction of microalgae was systematically studied over 60 days, and the effect of the storage material, feedstock species, liquefaction temperature and storage temperature were assessed. Biocrudes obtained at 300 °C and 350 °C from the microalgae Spirulina and *Chlorella vulgaris* were stored at three temperatures: cold (4 °C), ambient (20 °C) and elevated temperatures (35 °C), over the two-month period. The viscosity of the biocrudes only increased considerably at 35 °C. The reaction temperature and biomass type were also strong determining factors of the impact on biocrude stability. Biocrudes produced from *C. vulgaris* were more stable than the Spirulina, and the crudes formed at 350 °C were considerably less reactive than those produced at 300 °C.

Keywords: Response surface analysis; Combined model; Multivariable regression; Yield; Elemental composition; Ageing.

Content

List of figures

PAG.

List of tables

PAG.

List of symbols and abbreviations

Latin symbols

Symbols	Term	SI units	Definition
A	Ash	%	Equation 4-3
AP	Aqueous-phase products	%	Figure 3-1
B	Biocrude	%	Figure 3-1
C, H, O, N, S	Carbon, hydrogen, oxygen, nitrogen, sulfur	%	Table 2-2
CH	Carbohydrates	%	Equation 2-1
C_L, C_P, C_{CH}	Parameters		Equation 3-4
G	Gas	%	Figure 3-1
HB	Heavy biocrude	%	Figure 3-1
ITS	Initial total solids	%	Table 2-1
k_i	kinetic constants	min^{-1}	Figure 3-1
L	Lipid	%	Equation 2-1
LB	Light biocrude	%	Figure 3-1
Lr	Lipid ratio	-	Equation 2-1
P	Proteins	%	Equation 2-1
S	Solids (microalgae)	%	Figure 3-1
T	Temperature	°C	Table 2-1
tr	Retention time	min	Table 2-1
V	Volatiles	%	Figure 3-1
V_1	Dynamic viscosities of fresh sample	Pa·s	Equation 5-1
V_2	Dynamic viscosities of aged sample	Pa·s	Equation 5-1
X_{CH}	Content of carbohydrates	%	Equation 3-1-3-3
$X_{i,biocrude}$	Content of element i in biocrude	%	Equation 4-1
$X_{i,biomass}$	Content of element i in biomass	%	Equation 4-1
X_L	Content of lipids	%	Equation 3-1-3-3
X_P	Content of proteins	%	Equation 3-1-3-3
Y	Variable of interest		Equation 4-2
Y_B	Biocrude yield	%	Equation 3-1-3-4
Δ *Viscosity*	Index viscosity index		Equation 5-1

Subscripts

Subscript	Term
max	Maximum value
min	Minimum value

Abbreviations

Abbreviations	Meaning
ANOVA	Analysis of variance
Ch300	*C. vulgaris* biocrude obtained at 300 °C
Ch350	*C. vulgaris* biocrude obtained at 350 °C
db	Dry biomass
DCM	Dichloromethane.
FCCCD	Face-centered central composite design
GHGs	Greenhouse gases
HHV	Higher heating value
HTL	Hydrothermal Liquefaction
P-aut	Autotrophic culture
P-myx	Mixotrophic culture
RSM	Response Surface Methodology
SD	Standard deviation
Sp300	Spirulina biocrude obtained at 300 °C
Sp350	Spirulina biocrude obtained at 350 °C
TAN	Total acid number
TG	Thermogravimetric
TGA	Thermogravimetric analysis

Introduction

Biofuel is a term used to identify those liquids or gas fuels from biomass –organic matter obtained from plants, animals or microorganisms–. This term comprises fuels obtained from mature technology (also known as first generation technology), such as ethanol from starch or sugar, biodiesel from oleaginous seeds oil transesterification and biogas from anaerobic digestion of agricultural waste. Other biofuels, which are still in an experimental phase, are called to be from second and third generation, and include hydro-treated vegetal oil, biobutanol, hydrogen, lignocellulosic alcohol and biosynthesis gas [1].

The use of microalgae (microscopic photosynthetic organism) as raw material for fuel production, has some advantages in comparison with other renewable lignocellulosic materials [2,3]. Some of these advantages are:

- They can be 50 times more efficient converting sun light to biomass than terrestrial plants. The average annual rate of conversion from solar energy of fast-growth terrestrial plants is not higher than $1 W \cdot m^{-2}$, and less than the 0.5 % of the solar energy is received in a typical medium latitude region [4].
- They require no fertile ground and can grow either in fresh and salt or even residual water. For this reason, they do not compete with other agricultural activities.
- They capture between 10 and 50 times more CO_2 than terrestrial plants [5].
- They require from 6 to 10 times less water than the corn and grass crop, and the consumption can be reduced in an additional 80 % if the water is recirculated again to the culture [6].
- The nutrient can be obtained from residual water, thus reducing, on the one hand, the 55 % of the usage of nitrogen and phosphorus compared with a fresh culture and, on the other hand, the contamination of the receiving water bodies.
- Their capacity for lipids storage accumulates between 10 and 60 % of dry biomass (db), depending on the species and the culture conditions, making the microalgae an interesting option for biofuels production.

Despite these advantages, the conversion of microalgae biomass into biofuels shows some technology challenges. For example, the high moisture after the harvest (>95 %), which makes inefficient the principal paths to get liquid biofuels as the pyrolysis [7,8] or the extraction and liquid transesterification, due to the requirement of the dehydration of the biomass with a maximum of 10 % of water [9,10]. Another challenge is their different composition, because there are almost 50.000 species of microalgae already known [5]. The majority of them produces not only lipids but also proteins and carbohydrates in proportions that vary with the species and with the culture conditions (light, CO_2, pH, temperature, nutrients, just to name some of them). For these reasons, it is necessary to develop a process capable of converting the most humid biomass components to biofuel.

According to the number of publications in indexed journals, the Hydrothermal Liquefaction (HTL) of microalgae has renewed its interest for the scientific community since 2010. This process consists in transforming the biomass into biocrude (a liquid with petroleum-similar characteristics) using temperature and pressure conditions close to those of water critical point. In comparison with conventional routes of transforming biomass, the HTL has some advantages [11,12]:

- It eliminates the drying process, because the initial total solids concentration of the biomass is between 10 and 30 % w/w (90 -70 % of water).
- The resistance to the mass transfer is reduced in conditions close to the critical point (auto-diffusive coefficient $\approx 10^{-3}$ $cm^2 \cdot s^{-1}$) [13].
- Both the lipids and the other biomass components (proteins and carbohydrates) are susceptible to be converted to biocrude. For instance, in the HTL the *Chlorella pyrenoidosa* with 0.1% of lipids, obtained a biocrude yield of 39 % at 280 °C and 30 min [14]. Likewise, the *Nannochloropsis sp*. (14 % in lipids) obtained a biocrude yield of 55 % at 260 °C and 60 min [15]. However, the biomass quality in terms of its nitrogen content increases while increasing the lipids content in the microalgae used.
- Its main product is the biocrude, even though light gases (CO_2, CH_4, H_2, C_2H_6, and C_2H_4), an aqueous phase (organic acids, amino acids, and others) and insoluble residual solids (ash and carbon) are obtained.

Despite its apparent advantages, obtaining microalgae biocrude has different challenges. First, treatment and/or recirculation of aqueous phase to the culture is needed, since a process the least possible environmental impact is pursued [16]. Second, a step of post-treatment of biocrude is

required to stabilize its properties during storage and to eliminate or reduce its content of oxygen and nitrogen, in order to make it comparable to the petroleum. At this stage, high temperatures (400-500 °C) and the use of hydrogen and catalysts (mostly with active phase of noble metals and limited use) is required [17]. Third, the quantitative models that predict the yield and elemental composition of biocrude under different reaction conditions and biomass composition, which would allow to get close to a generalized process design [18,19].

In order to propose a new approach to face the second and third challenges and to contribute to a better understanding of the process of HTL of microalgae, this research will focus on gathering experimental and bibliographic information to enable the development of a selection strategy of reaction conditions based on the characteristics of the biomass. This strategy should optimize yield and quality of the biocrude, understood as a reduction of the content of elements other than carbon and hydrogen, especially nitrogen.

The hypothesis of this research was:
Microalgae are very different beings whose composition can be described in general terms by their content of 3 main blocks: lipids, carbohydrates, and proteins. In a hydrothermal liquefaction process, such components are rapidly hydrolyzed to basic components, whose number is much smaller and, depending on the reaction conditions, generate a product with defined characteristics. Consequently, the assumption is: that there is a set of reaction conditions that maximize the yield and quality of the biocrude obtained by HTL for each composition of biomass, regardless of the type of microalgae used.

If this hypothesis is corroborated, the test would materialize in the development of a model to predict the yield and the elemental composition of the biocrude from main reaction conditions and elemental and chemical composition of microalgae. Of course, the precise chemical identity of each biomass provides variations in the actual experimental results, which will result in some uncertainty of the model predictions, whose value is subjected to measurements during the Ph.D. project proposed.

The general objective of this research was to develop a strategy for the selection of reaction conditions based on the characteristics of the biomass to optimize the quality and yield of biocrude obtained by hydrothermal liquefaction of microalgae. To achieve the general objective, the following specific objectives were met:

Specific objective 1. Evaluate the effect on the elemental composition and yield of biocrude obtained by HTL of microalgae, by varying the composition of biomass and some liquefaction conditions (reaction time, initial total solids, and temperature).

The effect of the main reaction conditions and their interactions on the yield and quality of the biocrude obtained from the hydrothermal liquefaction of the *Parachlorella kessleri* microalgae was evaluated. An experimental response surface design was performed to assess how the reaction temperature, retention time, initial total solids concentration and biomass composition affect the yield and quality of the biocrude. The elementary composition, higher heating value and total acid number were used as quality indicators for the biocrude. Likewise, the level of prediction of the response surface models for the yield and the carbon, nitrogen, and oxygen contents of the biocrude was determined (Chapter 2).

Specific objective 2. Develop a predictive model of quality and yield of biocrude obtained by HTL and validate it with different species of microalgae.

An analysis of the level of prediction of the main quantitative models was performed to calculate the biocrude yield. The analysis included published data on biomass yields and chemical compositions obtained in a wide range of reaction conditions. Based on the analysis, a new model is proposed for the calculation of the biocrude yield, which includes as variables the composition of the biomass and the HTL temperature and the retention time (Chapter 3).

An analysis of the main reaction conditions of HTL was also performed in the elemental composition of the algae biocrude. From the analysis, a multivariable regression model was proposed, which included the reaction temperature, retention time and biomass composition as independent variables for the calculation of the biocrude quality of macroalgae and microalgae (Chapter 4). The proposed models for calculating the yield and quality of biocrude were validated with many published experimental data.

Specific objective 3. Evaluate the stability of biocrude obtained by HTL from microalgae *Chlorella vulgaris.*

The stability of biocrude obtained by HTL from two separate phototrophic species (Spirulina and *C. vulgaris*) at 300 and 350 °C were examined. The biocrudes were stored at three temperatures:

cold (4 °C), ambient (20 °C) and hot (35 °C), for 60 days. The dynamic viscosity, higher heating value (HHV) and thermogravimetric analysis (TGA) were measured as indicators of biocrude aging. The chemical and elemental composition of each biocrude was also analyzed at the beginning and at the end of the test period (Chapter 5).

Finally, most of the results were published or summited in peer review journals and presented at conferences.

Articles:

A. Palomino, L.C. Montenegro-Ruíz, R.D. Godoy-Silva. Evaluation of yield-predictive models of biocrude from hydrothermal liquefaction of microalgae. *Algal Res.* 44 (2019).

A. Palomino, R.D. Godoy-Silva, S. Raikova, C.J. Chuck. The storage stability of biocrude obtained by the hydrothermal liquefaction of microalgae. *Renew. Energy*. 145 (2020).

Conferences:

J. A. Pasos, A. Palomino*, L. C. Montenegro-Ruíz, R. D. Godoy-Silva, Cultivo autotrófico y mixotrófico de la microalga *Parachlorella kessleri*: efecto del tiempo de cultivo sobre la composición química (Poster). VI Congreso Latinoamericano de Biotecnología Algal, CLABA en Lima, Perú.

A. Palomino, J. A. Pasos, R. D. Godoy-Silva, L. C. Montenegro-Ruíz. Desarrollo y aplicación de una metodología para el conteo automático de la microalga *Parachlorella kessleri* empleando el programa ImageJ® (Oral presentation). VI Congreso Latinoamericano de Biotecnología Algal, CLABA en Lima, Perú.

Research stay:

I did a 6-month research stay at the Department of Chemical Engineering of the University of Bath, United Kingdom. I worked under the supervision of Dr. Christopher J. Chuck. During my research stay, I study the storage stability of biocrude.

1. Background of hydrothermal liquefaction of microalgae

The content of this chapter describes the main aspects of HTL of microalgae reported in the scientific literature specialist.

1.1 Raw materials

1.1.1 Supercritical water

The water is characterized by a relatively high critical temperature and pressure (374 °C and 22.1 MPa), in comparison with other solvents like the carbon dioxide (31 °C y 7.38 MPa), ethanol (240.8 °C y 6.14 MPa), methanol (239.5 °C y 8.09 MPa.) and acetone (235 °C y 4.7 MPa); this is due mainly to the hydrogen bridges that form between the water molecules. Physical characteristics of water like density, viscosity, and dielectric constant, change significantly as the temperature and pressure rise (Table 1-1). For example, to 25 ºC and 0.1 MPa, the water is a good solvent of the polar substances and electrolytes, while the organic compounds are little bit or nothing soluble; By the other hand, near to the critical point increases the auto-diffusion coefficient and decreases the viscosity, and especially the dielectric constant, making that the organic substances becomes soluble in water and the inorganic compounds precipitate; likewise in the supercritical water there are a higher concentration of H^+ because enhances their ionization constant, that promotes the hydrolysis reactions of organic material [3,13].

1.1.2 Microalgae

In the HTL process has utilized a great variety of species of macroalgae [20–23], microalgae [15,24–26] and, in particular cases, mixtures of them from waste-waters [27–29]. The microalgae used have been from both freshwater and saltwater with a high protein content (between 25–70 %).

One of the main problems when use microalgae as feedstock for the HLT, is the high variability in their content of proteins, lipids and carbohydrates, even if they are of the same species, affecting directly the yield and elemental composition of bio-crude, that difficult the process generalization (Table 1-2); this variation in microalgae composition attributes both the conditions which makes the culture and the species itself.

The microalgae *Chlorella vulgaris* is a unicellular spherical organism with a diameter between 2 to 10 μm; its culture can reach a productivity of biomass until 2.5 g L^{-1} day, an advantage for its use like a feedstock an industrial level. Its composition in proteins, lipids and carbohydrates varies in accordance to the culture conditions in a range between 42–58 % proteins, 5–40 % lipids and 12–58 % carbohydrates [30,31]. For the development of the present research was in particularly chosen this microalgae species because it counts with a native strain isolated in laboratory, it adapts easily in variable growth conditions, it is resistant to the pollution and counts with an extended experience related with its culture in the research group [32].

1.2 Reaction conditions on hydrothermal liquefaction

The hydrothermal liquefaction (HTL), along with the carbonization and gasification conform the processes of hydrothermal transformation of the humidity algae biomass, which differ for their operation conditions and for the final product, like the Figure 1-1.

HTL products are the biocrude (complex mixing of lineal and branched hydrocarbons C_{15}–C_{33}, cyclic nitrogenized compounds and cyclic oxygenates C_5–C_{16}), the aqueous products (soluble inorganic compounds, ammoniac, short chain hydrocarbon C_5–C_8, alcohols, ketones, carboxylate acids, aldehydes and phenols), gaseous products (mainly CO_2 and to a lesser extent CH_4, H_2, C_2H_6 and C_2H_4) and waste solids (ashes and inorganic compounds) [11].

Several authors have studied the influence of the mainly operation conditions in the yield of biocrude, among which highlight the initial total solids (5–0 %) [33–35], the reaction temperature (200–400 ºC) [34–36], the residence time (5–120 min) [15,24,37] and the homogeneous [24,36] or heterogeneous [38–40] catalyst use. In similar form, a number of authors that have focused on getting better the biocrude quality, decreasing their oxygen and nitrogen content, by a post-treatment

(des-oxygenation and/or des-nitrogenation) [41,42]. The following is a brief description in the art state of the reaction conditions of algae HTL.

1.2.1 Reaction temperature

An increase of the reaction temperature leads to a yield increase of the biocrude between 200 to 400 ºC; for higher temperatures than the critical point, enhances the gaseous phase percent and usually, decreases the biocrude fractions, aqueous and solid products [43]. With increasing the temperature in the HLT process occurs different reactions [44], influencing the biocrude yield; for example:

- A less temperatures than 220 ºC, the triglycerides, proteins and carbohydrates are hydrolyzed to more simple molecules, like fatty acids, amino acids, and sugars, respectively.
- While increases temperature between 220 to 375 ºC, occurs extra-polymerization and isomerization reactions that competes with macromolecule hydrolysis, thus obtaining the biocrude.
- Up for 374 ºC (critical temperature) are favored the decarboxylation and gasification reactions of intermediate compounds, increasing the gas yield.

Many investigators report that the optimum temperature for get the highest performance of biocrude is between 280 ºC and 350 ºC [23,33–35,45]; in that interval is favored the decreasing of oxygen in the biocrude. The optimal temperature depends on the type of algae used in every case. Unfortunately, if increase the optimal temperature in that interval it increases the content of nitrogen and sulfur in the biocrude because a high degradation of proteins, amino acids, and nucleic acids.

1.2.2 Reaction time

The reaction time affects significantly the yield of the different obtain phases in the HLT, mainly of searches have demonstrated that the biocrude yield oscillates between 30 to 120 min of reaction [15,37] but there is not a characteristic trend; in general, reaction times too longs (> 60 min) promotes the insoluble solids formation and the biocrude decomposition [24], as well as the economic unviability of the process.

As with the reaction temperature, is unknown how the time affects the distribution of nitrogen, sulfur and oxygen of the different phases of the HLT, or how influences in the macromolecule degradation

(proteins, lipids and carbohydrates) and the biocrude formation (extra-polymerization and isomerization reactions) The mostly recent searches are looking reduce the time reaction (<15 min), which leads to a smaller reactor size and reduction of the energy consumption [46,47].

1.2.3 Initial total solids

The initial total solids (ITS) mainly depend form the microalgae specie and the process economy; the studied range varies between 5 to 30 %, resulting in a major energy consumption in low concentrations (for the extra water heating) and a lower reaction capacity in higher concentrations (by the little water quantity there are for biomass dissolve).

The founded results for different authors have been contradictory and is not clear how the ITS affects the biocrude yield, for example Anastasakis & Ross [47] performed the HLT of Laminaria saccharina algae, in 350 °C, 60 min and with KOH like catalyst, varying the ITS between 5 to 20 %, finding that the biocrude yield decreased with increased the macroalgae quantity in the reactor. Contrary results reported by Li et al. [49] for the Sargassum patens macroalgae, where significantly increased the biocrude yield going form a biomass concentration of 5 to 15 %, a temperature and a time reaction of 350 °C and 15 min, respectively. On the other hand, Jena et al. [48] not found a significantly difference in the biocrude yield, increasing the ITS from 10 to 30 % in the HLT of the microalgae, in 350 °C and 60 min.

1.2.4 Initial pressure or water density

The initial pressure in the HLT reactor, has 2 mainly objectives: (1) keep the water in liquid phase (directly affecting its density) and thus improve the energetic efficiency by avoiding or reducing the water vaporization heat [13] which promotes contact between the organic matter and the reactive water and (2) accelerate the H^+ release in the medium, that catalyze the acid reactions [44]. The reported initial pressure in the reactor is typically between 2 to 5 MPa; usually is used N_2 like inert gas for maintain a free oxygen atmosphere [45,48], reducer gases like the CO or the H_2 for decreasing the oxygen content in the biocrude [38,49] or simply air. However, the effect of water density or the initial pressure on the biocrude yield is not clear, reporting in some cases that have no influence in the yield [45,50].

1.3 Separation of phases

After the reaction HTL, four different phases are obtained: aqueous, organic, solid and gases. Due to the sample size used in investigations (between 0.5 and 4 g of dry biomass) much of product remains adhered to the walls and stirrer of the reaction system; It is necessary to use an organic solvent (chloroform, dichloromethane, hexane, toluene, etc.) to separate the biocrude (organic phase) of the aqueous products and solid residue.

The type and amount of solvent used for the separation of the aqueous phase from the organic, can affect the performance and composition of biocrude. Valdez et al. [51] performed the separation of products HTL of *Nannochloropsis sp*. (350 °C, 60 min), with polar solvents (metoxiciclopentano, dichloromethane and chloroform) and nonpolar (hexadecane, hexane and cyclohexane), concluding that the hexadecane provided the highest yields of biocrude (about 39 %), but they recovered 6.7 and 9.2 % more of carbon in biocrude with chloroform or dichloromethane, respectively.

1.4 Biocrude

The biocrude is the main product of the process of HTL; its HHV ranges from 19 to 40 MJ kg^{-1} and yield between 15–70 % [11,43,44]; its properties, composition and performance are strongly dependent on the reaction conditions and the biomass [43]. In general, the biocrude is a complex mixture of compounds that can be classified according to their functional group [44]:

- Mono-aromatics and derivatives thereof, such as phenol, benzene, toluene, styrene, and others.
- Aliphatic, linear and/or branched compounds such as alkanes and alkenes of C_{15} to C_{33}.
- Fatty acids, such as palmitic, oleic, stearic, hexadecanoic, among others.
- Nitrogenous compounds such as amides and amines.
- Poly-aromatics, such as naphthalene, quinoline, fluorene, among others.
- Oxygen compounds, such as esters, aldehydes, ketones, alcohols, among others.

The quality of petroleum and its derivatives is usually related to several physicochemical characteristics such as the HHV and viscosity, both are function of elemental composition. The nitrogen and oxygen cause several problems including high density, problems of poisoning of catalysts used during petroleum hydrotreating and relatively low HHV [52–54].

Given the problems caused by nitrogen and oxygen in the biocrude, several authors have proposed different strategies for their reduction, which are summarized in Table 1-3. Such strategies include:

1. The introduction of catalysts during HTL, either homogeneous or heterogeneous.
2. A posttreatment, wherein the biocrude is subjected to catalytic hydrogenation [39,41,42,55,56]. The posttreatment achieves significantly reduce the content of O, N and S to values similar to petroleum; however it includes an additional step, which requires high temperatures (400–500 °C), long reaction times (1–4 hours) and specialized catalysts (noble metals and zeolites), affecting process economics.
3. Protein extraction of raw material, which entails an additional process, cell disruption that is highly costly in terms of energy and reduces the carbon content and hydrogen available for HTL [57].
4. Pretreatment where metabolism of microalgae and/or macroalgae is handled, in order to increase their lipid content and therefore reducing the content of nitrogen and sulfur in the raw material [58,59]. This metabolic manipulation of microalgae is a strategy easy to implement, low power consumption and does not require extra steps in the process; however, it depends on the culture conditions and the species and in many cases, the reduction of nitrogen available for the microalga significantly affect growth and productivity of crop biomass [58].

There is little information available on the behavior of biocrude during storage. The stability of the physicochemical characteristics of crude by effect of storage was studied by Jena et al. [34], finding that the viscosity of biocrude of microalgae increases linearly during the first 75 days of 191.5 cP to 578.5 cP, after which it remains more or less unchanged. The authors attributed this behavior to an aging process where there is a loss of volatiles and a series of oxidation and repolymerization reactions between oxygenates compounds.

Table 1-1. Characteristics of ambient and supercritical water [13,60].

Properties	Ambient water	Supercritical water
Dielectric constant	78	< 5
Solubility of organic compounds	Immiscible	Miscible
Solubility of inorganic compounds	Miscible	Immiscible
Diffusivity ($cm^2\ s^{-1}$)	10^{-5}	10^{-3}
Viscosity ($g\ cm^{-1}\ s^{-1}$)	10^{-2}	10^{-4}
Density ($g\ cm^{-3}$)	1.0	0.2 -0.9
Ionization constant	10^{-14}	10^{-12}

Table 1-2. Variation reported in the literature about chemical composition of the raw material and biocrude obtained by HTL of the same species of algae.

Specie	Chemical composition (daf %)			Reaction conditions (ITS, T, t)	Biocrude yield (daf %)	Elemental composition of biocrude (daf %)				Ref.
	L[1]	P	CH			N	C	H	O†	
Chlorella vulgaris	25.6	51.8	27.9	7 %, 250 °C, 5 min	33.0	5.5	70.6	9.2	14.5	[25]
Chlorella vulgaris	4.5	67.6	28.2	20 %, 250 °C, 10 min	14.6	4.1	74.7	10.4	10.7	[61]
Dunaliella tertiolecta	2.9	61.3	21.7	10 %, 360 °C, 50 min	25.8	3.7	63.6	7.7	25.1	[62]
Dunaliella tertiolecta	20.5	63.6	15.9	20 %, 340 °C, 60 min	33.6	6.9	76.3	8.4	8.4	[48]
Entermorpha prolifera	10.6	50.6	38.7	28 %, 340 °C, 40 min	14.0	4.8	79.7	8.8	6.7	[29]
Enteromorpha prolifera	2.1	20.3	65.0	15 %, 350 °C, 20 min	9.8	3.9	77.4	10.7	7.8	[63]
Nannochloropsis salina	13.0	40.0	35.7	33 %, 350 °C, 30 min	34.0	2.8	77.2	9.0	8.7	[64]
Nannochloropsis salina	37.1	43.1	9.2	20 %, 340 °C, 30 min	55.6	5.2	72.6	9.8	12.4	[52]
Tetraselmis sp	22.0	14.0	54.0	16 %, 350 °C, 5 min	58.0	5.7	71.4	9.5	12.5	[65]
Tetraselmis sp.	14.0	58.0	22.0	16 %, 350 °C, 5 min	65.0	5.0	71.0	9.5	14.0	[37]

[1]L = lipids, P = proteins, CH = carbohydrates, ITS = Initial total solids, T = Temperature, t =time. daf: dry ash-free basis. †by difference.

Figure 1-1. Hydrothermal processes transformation [11,43]

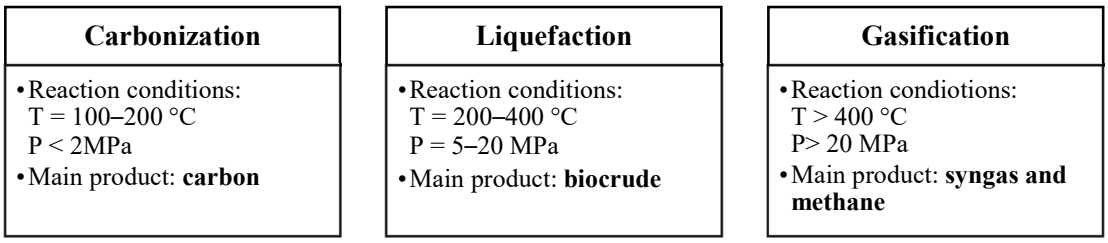

.

Table 1-3. Comparison of the processes used as strategy to improve the quality of biocrude.

Specie (strategy)[1]	Comparison	Reaction conditions (ITS, T, t)	HHV (MJ kg^{-1})	Elemental composition (daf %)			Ref.
				N	S	O	
Enteromorpha prolifera (1)	Without catalyst	13 %, 300 ºC, 30 min.	28.7	5.4	------	22.5	[23]
	With catalyst		29.89 (Na_2CO_3)	5.76 (Na_2CO_3)	------	20.15 (Na_2CO_3)	[23]
Chlorella vulgaris (1)	Without catalyst	10 %, 350 ºC, 60 min.	35.1	5.9	0.0	14.8	[18]
	With catalyst		37.1 (Na_2CO_3)	4.9 (Na_2CO_3)	0 ((Na_2CO_3)	10.7 (Na_2CO_3)	[18]
Spirulina (1)	Without catalyst	10 %, 350 ºC, 60 min.	36.8	7.0	0.0	10.4	[18]
	With catalyst		35.1 (HCOOH)	4.6 (Na_2CO_3)	0.5 (Na_2CO_3)	8.7 (Na_2CO_3)	[18]
*Nannochloropsis occulta (*1)	Without catalyst	10 %, 350 ºC, 60 min.	34.5	4.1	0.0	18.9	[18]
	With catalyst		39 (HCOOH)	3.8 (Na_2CO_3)	0 ((Na_2CO_3)	10.4 (HCOOH)	[18]
Spirulina platensis (1)	Without catalyst	20 %, 350 °C, 60 min	35.3	6.3	0.9	10.17	[26]
	With catalyst		38.4 (NiO)	4.7 ($Ca_3(PO_4)_2$)	0.9 (Na_2CO_3)	6.50 (NiO)	[26]
Nannochloropsis sp. (2)	Without catalyst	32 %, 350 °C, 60 min	38.5	4.18	0.84	9.18	[38]
	With catalyst		39.6 (Pt/C)	3.49 (Ru/C)	0.31 (Ru/C)	8.48 (Pt/C)	[38]
Chlorella vulgaris (2)	Without catalyst	10 %, 350 °C, 60 min	35.1	5.9	0.0	14.8	[39]
	With catalyst		37.9 (Pt/Al)	5.4 (Ni/Al)	0.0 (Co/Mo)	10.7 (Co/Mo)	[39]
Chlorella pyrenoidosa (2)	Without catalyst	10 %, 300 °C, 20 min	19.8	7.44	------	35.65	[40]
	With catalyst		27.7(Ce/HZSM)	0.24(Ce/HZSM)	------	32.05(Ce/HZSM)	[40]
Desmodesmus sp. (3)	Without posttreatment	500 °C, 240 min, 5 0% HZSM-5	38.4	5.3	0.56	8.35	[66]
	With posttreatment		40.3	1.6	<0.1	1.02	[66]
Chlorella sp.(3)	Without posttreatment	400 °C, 60 min, 6 MPa H_2, 5 % Pt/C-Al_2O_3	38.1	7.3	------	7.8	[67]
	With posttreatment		39.7	4.8	------	6.3	[67]
Chlorella pyrenoidosa (3)	Without posttreatment	400 °C, 240 min, 6 MPa H_2, 10 % (Ru/C+Mo_2/C)	37.4	7.05	0.68	6.07	[56]
	With posttreatment		43.3	2.87	0.087	0.63	[56]
Nannochloropsis gaditana (4)	Without pretreatment	10 %, 335 °C, 15 min	36.8	5.4	0.2	10.9	[57]
	With pretreatment		39.0	4.5	0.2	7.3	[57]
Scenedesmus almeriensis (4)	Without pretreatment	10%, 335°C, 15 min	37.2	7.2	0.3	8.9	[57]
	With pretreatment		37.1	4.9	0.4	8.1	[57]

Table 1-3. (Continued).

Specie (strategy)[1]	Comparison	Reaction conditions (ITS, T, t)	HHV (MJ kg^{-1})	Elemental composition (daf %)			Ref.
				N	S	O	
Derbesia tenuissima (5)	18 days of culture	6.6 %, 345 °C, 5 min	33.0	6.1	0.8	11.7	[58]
	36 days of culture		33.0	3.2	0.3	14.8	[58]
Ulva ohnoi (5)	18 days of culture	6.6 %, 345 °C, 5 min	32.3	6.4	0.7	12.0	[58]
	36 days of culture		32.0	2.7	0.2	16.7	[58]
Oedogonium sp. (5)	18 days of culture	6.6 %, 345 °C, 5 min	32.2	5.3	0.4	13.8	[58]
	36 days of culture		32.1	2.2	0.0	17.2	[58]
Nannochloropsis oculata (5)	3 days of culture	20 %, 300 °C, 30 min	36.5	5.5	------	12.6	[59]
	14 days of culture		40.6	2	------	10.5	[59]

[1]Strategies:

(1) HTL with homogeneous catalysts
(2) HTL with heterogeneous catalysts
(3) Post-treatment catalytic to biocrude
(4) Extraction of proteins microalgae before HTL
(5) Metabolic manipulation of microalgae in the culture to change its chemical composition

2. Yield and quality of biocrude from hydrothermal liquefaction of microalgae: Effect of main reaction conditions and their interactions

2.1 Abstract

Hydrothermal liquefaction of the microalga *Parachlorella kessleri* was carried out. A response surface methodology was used to explore the effect of reaction temperature, retention time, initial total solids, and biomass composition, as well as their interactions, on the yield and quality of the resultant biocrude. Elemental composition, higher heating value and total acid number were used as indicators of the biocrude quality. The reaction temperature was the most significant factor affecting the yield and quality of the biocrude. The response surface modeled allowed to find the optimum operating conditions required to obtain the best results. The maximum biocrude yield was obtained between 315–325 °C and 40–45 min, at lipid ratio and ITS of 0.65 and 15 %, respectively. Under these conditions, the higher heating value was 35 $MJ \cdot kg^{-1}$, the total acid number was 70 mg $KOH \cdot g^{-1}$ and the carbon, nitrogen and oxygen contents were 72 %, 3.7 % and 13 %, respectively. The inclusion of the chemical composition of the biomass as a modeling factor allowed predicting the yield and quality of the biocrude for several data sets published in the literature. The regression model predicted 61 % of the biocrude yields published within the standard deviation zone ± 5%. The degree of success for the models predicting quality parameters ranged from to 50-80 %.

Keywords: Response surface analysis; Experimental design; Total acid number; Elemental composition.

2.2 Introduction

Hydrothermal liquefaction (HTL) of microalgae is the process in which wet biomass is transformed into four products: (1) biocrude, (2) water soluble products, (3) gases and (4) solids. This process occurs at high temperatures (200–400 °C) and high pressures (5–20 MPa) [11,43]. Biocrude is the main product of HTL and is characterized as a complex mixture of organic compounds with a higher heating value (HHV) than the biomass. Due to its characteristics, the biocrude could be used as raw material for obtaining refined liquid fuels [44].

Many authors have studied the effect of diverse HTL conditions on the yield and quality of the microalgae biocrude. Such conditions include reaction temperature, retention time, initial total solids (ITS), the use of catalysts and solvents, the heating rate, the characteristics of the raw material (type, species and biochemical composition), among others [25,26,34,38,68–70]. Unfortunately, most of these investigations have carried out the analysis of the main reaction conditions, such as temperature, retention time and ITS, adopting the "one factor at a time" approach [25,34,47,71,72] or a single reaction condition for different microalgae species [18,59,73,74]. This strategy generally hinders the analysis of the interactions between the factors and the levels of optimization of the reaction conditions to obtain the maximum biocrude yield with the best possible quality.

Only very few studies of HTL of microalgae have used the Response Surface Methodology (RSM) in the analysis of the main conditions of HTL [75,76], thus allowing the establishment of optimal operating conditions for the process, based on a mathematical model that best adjusts the experimental data obtained for one or more variables of interest. For example, the RSM allowed Song et al. [75] to analyze the interactions between reaction temperature, retention time and ITS on the yields of the heavy and light biocrude obtained from the liquefaction of waste Cyanophyta biomass. The authors also examined the effect of interactions between the reaction conditions on the recovery of total organic carbon and ammonia nitrogen in the aqueous phase. Gai et al. [76] used RSM to find the optimal reaction conditions for the biocrude yield of *Chlorella pyrenoidosa*. Their analysis included the recovery of carbon and nitrogen in the biocrude and HHV. Besides the effects of the main reaction conditions and their interactions on the yield, their influence on the physicochemical properties of the biocrude are also important. Characteristics such as nitrogen and oxygen contents, viscosity and total acid number (TAN) affect the storage, transport and application

of biocrude [77,78]. Unfortunately, the study of those properties has adopted a general one factor at a time approach [48,79,80].

The objective of this study was to research the effect of the main reaction conditions and their interactions on the yield and quality of the biocrude obtained from the hydrothermal liquefaction of the microalgae *Parachlorella kessleri*. An experimental design of response surface was carried out to evaluate how reaction temperature, retention time, ITS and biomass composition affect the yield and quality of biocrude. The elementary composition, HHV and TAN, were used as quality indicators for the biocrude. Likewise, the level of prediction of the response surface models for the yield and carbon, nitrogen, and oxygen contents of the biocrude was determined.

2.3 Materials and methods

2.3.1 Microalgae culture

The microalgae *Parachlorella kessleri* (strain LAUN–2) was obtained from the collection of the Algae Cultivation Laboratory at Universidad Nacional de Colombia – Campus Bogotá. The *P. kessleri* was cultured in sterile Basal Bold Medium (BBM) in cylindric transparent vessels of glass (2 L) and plastic (4 L). Two types of culture were performed, autotrophic (P-aut) and mixotrophic (P-myx). In the medium for the P-myx culture, 1 $g \cdot L^{-1}$ of glucose was added. White LED lights were used to provide an illumination of 140 ± 5 $\mu E \cdot m^{-2}$ s^{-1}. The photoperiod was maintained in 13 light hours – 11 dark hours. The aeration flow was 1 ± 0.5 $L \cdot min^{-1}$ and the initial concentration was 1.36 $x10^6$ ± 0.05$x10^6$ $cells \cdot mL^{-1}$. The temperature was maintained at 25.8 ± 0.8 °C. The P-aut culture was maintained for 20 days, while the P-myx culture was maintained for 15 days. The biomass was harvested by centrifugation at 4,400×g for 5 min (Hermle Z206A). The centrifuged wet biomass was lyophilized (Labconco FreeZone 4.5) and the resulting solid was homogenized and stored at 4 °C.

2.3.2 Biomass characterization

All the analyses of the biomass composition were performed on lyophilized samples. The moisture content was determined gravimetrically after drying the samples at 105 °C until constant weight (Adam Equipment AMB 50). The ash content was measured after heating the dry biomass at 575 °C

for four hours in air. Elemental analysis (C, N, H, S) was performed externally at the LASAP Laboratory (Department of Chemistry at Universidad Nacional de Colombia – Campus Bogotá) using an Elementary Analyzer FLASH 2000. The oxygen content was estimated by difference. HHV was calculated from elemental composition using the equation proposed by Channiwala & Parikh [81].

The relative protein content was quantified using the Bio-Rad® Protein Assay kit and BSA was used as standard. Relative carbohydrate and lipid contents were determined according to the methods proposed by DuBois et al. [82] and Cheng et al. [83], using glucose and canola oil as standards, respectively. The materials, equipment, and procedure for quantifying the microalgae chemical composition are described in Table A 1 – Table A 5.

2.3.3 Experimental design

The main reaction conditions of the HTL of *P. kessleri* were analyzed with a face-centered central composite design (FCCCD). Reaction temperature (T), retention time (tr), initial total solids (ITS) and lipid ratio (Lr) were selected as independent factors. T was calculated from the thermodynamic tables for compressed liquid water using the final pressure and the specific volume. The factor Lr was defined according to Equation 2-1, where L, P and CH are the contents of lipids, proteins, and carbohydrates in the biomass in dry basis, respectively. The levels of each factor are shown in Table 2-1. The response variables for the biocrude were the yield, HHV, TAN and the elemental composition. The elemental composition, TAN and HHV were used as quality indicators for the biocrude.

$$\mathrm{Lr} = \mathrm{L}/(\mathrm{P} + \mathrm{CH}) \qquad (2\text{-}1)$$

2.3.4 HTL reactions

HTL experiments were carried out in a batch reactor of 43 mL (internal volume). The reaction section consisted of a tube of 3/4 in O.D. and 30.5 cm length. A cap was placed at one end and at the other end a section was fitted that consisted of a tube of ¼ in O.D. with a pressure gauge and a high-pressure valve. The total length of this section was 18 cm. All the reactor materials were 316-stainless steel (HIP, max. pressure 68 MPa).

At the beginning of each test, between 1.3 and 5.9 g of dry biomass were loaded into the reactor and between 24–34 g of distilled water were added, according to the experimental design. Then, the reactor was placed in a preheated electric furnace (Stanton Redcroft 1000c) and left until it reached the desired pressure. The average warm-up time was 32 min ± 4.5 min. The pressure was maintained for a certain retention time corresponding to the levels of the experimental design. At the end of the retention time, the reactor was immediately removed from the oven and left to cool in air to ambient temperature. The reactor was weighed before and after venting the gaseous products generated during the reaction. The yield of the gaseous product was determined from the weight difference.

The aqueous phase was filtered through an 11 μm filter to separate it from the biocrude and solids. The biocrude was recovered by washing the reactor several times with dichloromethane (DCM). DCM-biocrude solution was filtered to separate the solids and the filter was also washed with DCM until only the solids remained. The DCM-biocrude mixture was separated by evaporation under vacuum at 40 °C, to determine the mass of the biocrude. A sample of the aqueous phase (5 g) was dried at 60 °C for 24 hours to determine gravimetrically the yield of the aqueous products. The solids yield was calculated by weighing the dry filter before and after the separation of the aqueous phase and biocrude. All the yields were expressed on a dry basis of biomass.

2.3.5 Biocrude characterization

As in the biomass characterization, elemental analysis (C, N, H, S) was performed externally at LASAP Laboratory (Department of Chemistry at Universidad Nacional de Colombia – Campus Bogotá) using an Elementary Analyzer FLASH 2000. The oxygen content was estimated by difference and HHV was calculated from elemental composition using the equation proposed by Channiwala & Parikh [81]. The total acid number (TAN: milligrams of potassium hydroxide required to neutralize the acids present in one gram of biocrude) was determined by the potentiometric titration of approximately 50 mg of biocrude, previously dissolved in 25 mL of ethanol (96%), with a 0.05N solution of potassium hydroxide. The distribution of the boiling point of biocrude was analyzed using a TGA/DCS 1 Strat System, Mettler Toledo. Thermogravimetric analysis (TGA) was carried out from 30 to 800 °C at a heating rate of 10 $°C \cdot min^{-1}$, in nitrogen atmosphere (40 $mL \cdot min^{-1}$).

2.3.6 Predictive analysis of models

Regression models of yield and elemental composition of biocrude were obtained from the response surface methodology. To test their prediction capacity, data on yield and elementary composition of biocrude collected from 30 published studies were used (Table A 6). Such data were selected because they were in the same range of the biomass chemical composition and reaction conditions (reaction temperature, retention time and ITS) as this study (Table 2-1).

2.4 Results and discussion

2.4.1 Microalgae culture

The characterization of the two microalgae is shown in Table 2-2, where the chemical compositions of the biomass are normalized (the original data are shown in Table A 7). According to the hypothesis, the metabolism manipulation of the microalga *P. kessleri* had a significant effect in reducing protein content in biomass; the additional source of carbon to the culture ($1 g \cdot L^{-1}$ of glucose) reduced the protein content by 63 % and increased the lipid and carbohydrate content by 66 % and 75 %, respectively.

Table 2-2 also is shown a substantial decrease of 51% in the nitrogen content of the biomass obtained from the mixotrophic culture. The reduction in protein and nitrogen content in biomass could improve the quality of the biocrude during liquefaction This approach, which focuses on adapting the composition of the microalgae, is a first step in obtaining an improvement in the quality of the biocrude and minimizing post-treatment requirements (hydrodenitrogenation).

On the other hand, the increases of 11 % in the oxygen content and 9 % in the hydrogen content in the P-mix biomass can be attributed to the increase in its carbohydrate content. The other characteristics of the biomass such as ash content and HHV were not affected by the manipulation of nutrients during cultivation.

2.4.2 Mass balance

The global mass balance relative to the loaded dry biomass is shown in the last column of Table 2-3. It ranges between 49–97 %, with an average of 75.3 %. The larger losses were experimentally observed when handling the aqueous phase and the gases. The yield of the solids was between 8–40 %. The yield of the aqueous products and gases were between 10–27 % and 1–21 %, respectively. The highest solids yields were obtained at temperatures and retention times of 250 °C and zero min, respectively. In general, an increase in the reaction temperature or retention time decreased the yield of solids and aqueous products but increased the yield of gas and biocrude. The yields of solids, aqueous products and gases are in line with those obtained in similar studies [25,57,84,85].

2.4.3 Response surface methodology results

The results of the experimental response surface design are presented in Table 2-3 and Table 2-4 and were adjusted to the second order polynomial regression model, as presented in Table A 8. The analysis of variance (ANOVA) and the parameters of the models for the five response variables (yield, carbon, oxygen, nitrogen, HHV and TAN of the biocrude) at a confidence level of 95 % are shown in Table A 8 and Table A 9. The proposed models have an accuracy greater than 80 % in the range studied for the four factors.

2.4.4 Biocrude yield

Figure 2-1 shows the results of the response surface analysis for biocrude yield. All the factors studied have a significant and positive influence on the biocrude yield (Figure 2-1a). At 250 °C, the biocrude yield increased simultaneously with ITS, retention time and lipid ratio. However, at 350 °C, there is no difference in the biocrude yield, when the other factors are at their minimum or central values. As retention time, ITS and lipid ratio increased, the effect of the reaction temperature on the yield was less significant. Biocrude yield increased with retention time until 45 min. Times greater than 45 min decreased biocrude yield by up to 10 %. Likewise, there is a slight decrease in the biocrude yield at reaction temperatures greater than 325 °C. This can be attributed to the decomposition of intermediate products in the biocrude and formation of gases [19,50].

Gai et al. [76] and Song et al. [75], who also performed the RSM in the hydrothermal liquefaction of microalgae, reported a similar behavior for reaction temperature and retention time on biocrude yield. On the one hand, Gai et al. [76] carried out the liquefaction of the *Chlorella pyrenoidosa* microalgae. They reported that the biocrude yield increased between 260–280 °C and 30–60 min, at the maximum ITS analyzed of 35 %, followed by a slight decrease at temperatures greater than 280 °C and retention times greater than 60 minutes. On the other hand, Song et al. [75] found the maximum yield of light biocrude between 380–420 °C and 30–60 min with a biomass/water ratio of 11%, for the hydrothermal liquefaction of a *Cyanophyta*.

The ITS are another important factor that affects the biocrude yield. Figure 2-1a shows that an increase in the total solids from 5 % to 10 % kept the biocrude yield approximately constant. However, additional increases in the ITS from 10 % to 15 % favor the formation of biocrude by up to 25 %. The increase in ITS can favor interactions between the intermediate compounds formed, since the reaction medium is less diluted. Jena et al. [34] reported that there was a significant increase in biocrude yield of Spirulina when the initial solid concentration increased from 10 to 20 %. The authors attributed this increase to the optimum availability between organic compounds and H^+ and OH^- ions. Likewise, Valdez et al. [50] reported an increase in the biocrude yield of *Nannochloropsis sp* from 36 to 46 % as the concentration of microalgae increased from 5 to 35 %.

Other authors have reported an opposite behavior to the results shown by this study. For example, Hietala et al. [70] reported that the increase in ITS reduced the yield of biocrude by 6 % for 7 types of microalgae biomass, at temperatures between 100 and 250 °C. But, at temperatures higher than 300 °C, the biocrude yield increased with the ITS. Dandamudi et al. [72] also reported a decrease in the biocrude yield with the increase in solids loading from 10 to 20%, for the liquefaction of the microalga *Kirchneriella sp*. This suggests that the ITS factor depends on the intrinsic characteristics of the microalgae and each species could have an optimal point for this factor.

Unexpectedly, the yield of the biocrude decreased by 11 % when the lipid ratio was in the range of 0.15–0.40. However, the maximum yield was reached at a lipid ratio of 0.65. In general terms, the biocrude yield was favored by the increase in ITS and lipid ratio (Figure 2-1a). The maximum biocrude yield was obtained at reaction temperatures between 315–325 °C and retention times between 40–45 min, at the maximum conditions of lipid ratio and ITS, i.e. 0.65 and 15 %,

respectively. The minimum values for the biocrude yield (between 5 and 10 %) were obtained at 250 °C and zero minutes of retention time, regardless of lipid ratio and ITS.

Figure 2-1b shows the interactions between the different factors. The initial total solids did not have any significant interaction with the other factors. The interaction between the reaction temperature and the retention time affects the biocrude yield. At 250 °C, the difference in biocrude yield in the range of 0–60 min increased up to 71 %; however, at 350 °C, such difference in yield was only 2 % in the same range.

Likewise, the lipid ratio had a greater influence on the biocrude yield at low reaction temperatures. At 250 °C, a lipid ratio of 0.65 produced up to 1.4 times more biocrude than ratio of 0.15, while at 350 °C, the biocrude yield remained constant at any lipid ratio. The biocrude yield was favored by the interaction between retention time and lipid ratio. At 60 min, the biocrude yield increased from 32 to 38 % when the lipid ratio range increased from 0.15 to 0.65. However, at retention times between 0 and 10 min, there is no difference in the yield of the biocrude obtained in the same range of Lr.

2.4.5 Total acid number

Results of the experimental design for the biocrude TAN are shown in Figure 2-2. The biocrude of the microalga *P. kessleri* has a TAN between 64 and 140 mg KOH·g^{-1}. These values are within the range reported by several authors [79,80,86,87]. TAN of the biocrudes obtained are significantly high compared to the maximum value specified for the biodiesel, i.e. 0.50 mg KOH g^{-1}. TAN values above this specification may increase the likelihood of corrosion during transport, storage and use [88].

The increase of the reaction temperature, retention time, ITS and lipid ratio significantly reduced the TAN of the biocrude within the range studied for these variables. The decrease in TAN was linear for all the variables studied (Figure 2-2a). A significant reduction in TAN with the increase in reaction temperature between 250 and 350 °C was also reported by Shakya et al. [79] for three different species of microalgae: *Nannochloropsis*, *Pavlova* and *Isochrysis*, with lipid ratios of 0.25, 0.19 and 0.27, respectively. The reaction temperature favors the esterification and decarboxylation reactions of organic and fatty acids. Compounds such as alcohols, esters and hydrocarbons are formed from these reactions, which contribute to reduce the TAN [68]. The highest values of TAN

in the biocrude are between 120 and140 mg KOH·g^{-1} at temperatures of 250 °C and residence times between 0 and 30 min. The minimum values of biocrude TAN, between 64–69 mg KOH·g^{-1}, are obtained at 60 min and 15 % initial solids, regardless of the temperature and lipid ratio. The increase in the reaction temperature and the lipid ratio significantly reduces the TAN, when the retention time and ITS are in the range between 0–30 min and 5–10 %, respectively.

The increase in retention time and ITS reduced the biocrude TAN by up to 29 % (Figure 2-2a). It can be argued that longer retention times in the reactor might favor the esterification reactions of organic and fatty acids present in the biocrude, which in turn would result in an effective reduction of TAN. Likewise, by increasing the ITS, the probability that organic and fatty acids react to form more complex molecules is higher, due to the increase in the concentration of organic compounds in the reaction medium [34].

The biocrudes obtained at lipid ratio of 0.15 (protein-rich biomass) had TAN values between 70 and 140 mg KOH·g^{-1}, while the TAN for the biocrudes obtained at lipid ratio 0.65 ranged from 67 to 125 mg KOH·g^{-1}. The existing interactions between the factors were also analyzed from the response surface methodology. Figure 2-2b shows a strong interaction between the reaction temperature and the lipid ratio. For a lipid ratio of 0.15, the acidity in the biocrude decreased significantly from 120 to 75 mg KOH·g^{-1}, when the temperature increased. Nevertheless, for a lipid ratio of 0.65, the TAN remained nearly constant to 88 ± 0.7 mg KOH·g^{-1}, when the temperature increased from 250 to 350°C.

The high acidity in the biocrude obtained from protein-rich biomass at 250 °C can be explained by the general reaction network proposed by Gai et al. [68]. In this network, organic acids are produced from the deamination of amino acids. Besides, at low temperatures, the proteins in the biomass react at a faster rate than lipids and carbohydrates [19]. A similar behavior was reported by Xu et al. [87], who obtained the highest biocrude TAN for the macroalgae *Saccharina japónica* and *Pyropia yezoensis* with low lipid contents, 0.6 % and 3.20 %, respectively. This suggests that not only lipids, but also proteins and carbohydrates contribute to the formation of organic acids in the biocrude and to the increase of its acidity.

On the one hand, there is also a significant interaction between retention time and lipid ratio. At retention times of zero min, there is no significant difference in the biocrude TAN for any lipid ratio.

However, at 60 min the reduction of the TAN was 1.2 times more for a lipid ratio of 0.65. The same behavior occurs for the interaction between ITS and Lr. At 5 % initial solids, there is no significant difference in the biocrude TAN for any lipid ratio. However, at 15 % ITS, a reduction of 24 % and 7 % in the TAN biocrude is observed for Lr of 0.65 and 0.15, respectively (Figure 2-2b). On the other hand, there are no interactions between reaction temperature and retention time or temperature and ITS. Likewise, there is no interaction between retention time and ITS, in the range studied for the factors (Figure 2-2b).

2.4.6 Elemental composition and HHV

Figure 2-3 shows the behavior of the factors on the elemental composition and the HHV of the biocrude of the microalga *P. kessleri.* The reaction temperature, retention time and ITS had a significant influence on the carbon content in the biocrude. In general, the carbon content in the biocrude varied from 67 to 77 % (Figure 2-3a). The reaction temperature was the factor with the highest impact on the carbon content. Increase in reaction temperature favored the increase of the carbon content in the biocrude from 69 to 76 %, regardless of the levels of the other factors. The increase in retention time had a greater influence on the carbon content at 250 °C and 5 % ITS. At high reaction temperatures and ITS, the increase in retention time only improved the carbon content in the biocrude by 1 %. The carbon content in the biocrude decreased with the increase in the concentration of total solids, in the range of 10–15 %. The maximum carbon content in the biocrude (77 %) was obtained at 350 °C, 60 min and 8 % ITS, regardless of the lipid ratio. Likewise, the experimental carbon recovery in the biocrude varied between 7.8 and 57.7 %, following the same trend reported by several studies [70,71,89]. The maximum predicted carbon recovery was obtained between 315–325 °C for 40–45 min, at the maximum lipid ratio and ITS studied. Finally, none of the interactions between the factors had a significant influence on the carbon content in the biocrude (Figure A 1a).

The effect of the reaction temperature, retention time, ITS and ratio of lipids on nitrogen content in the biocrude is shown in Figure 2-3b. The nitrogen content in the biocrude was between 1.7–4.0 %. and increased linearly with the increase in reaction temperature, retention time and ITS. The increase in the reaction temperature increased the nitrogen content in the biocrude by 99 %, at retention times of zero minutes and ITS of 5 %. The extent of the increase in nitrogen content with reaction temperature decreased as the retention time and the ITS increased. This can be explained by the kinetic network model proposed by Valdez et al. [19]. In this model, proteins react quickly as the

temperature rises, approximately 90 % of proteins react in the first 7 min at temperatures higher than 300 °C. For this reason, at high temperatures, the retention time is less significant on the nitrogen content in the biocrude, because all the proteins (main source of nitrogen) have been consumed during the first minutes of reaction.

The interaction with the retention time reduces the rate of increase of the nitrogen content in the biocrude as a result of an increase in the reaction temperature. At 250 °C, the nitrogen content in the biocrude was 2.0 times more after 60 min than at retention times of zero minutes. At 350 °C, there was no difference in the nitrogen content in the range 0–60 min. The interactions between the other factors were not significant for the nitrogen content (Figure A 1b). Garcia Alba et al. [47] carried out the hydrothermal liquefaction of the microalgae *Desmodesmus sp*. The authors reported that both carbon and nitrogen contents in the biocrude increased from 64 to 76.5 % and from 0.4 to 5.8 %, respectively, with a temperature increase from 175 to 400 °C and a retention time of 5 min. Huang et al. [71] also reported an increase in carbon and nitrogen contents with the reaction temperature and retention time for the biocrude of two different species of microalgae.

The nitrogen recovery in the biocrude ranged widely from 2.2 to 61.3 %, following the same behavior as the biocrude yield. The model predicts a maximum nitrogen recovery at 350 °C and 40 min, for a lipid and ITS ratio of 0.65 and 15 %, respectively. The minimum nitrogen content was achieved at the lowest levels studied for reaction temperature and retention time, regardless of ITS. However, under these conditions, the biocrude yield only reached a maximum of 10 %. Hietala et al. [70] also reported low nitrogen content in the biocrude, between 1.2–2.2 %, at temperatures between 200 and 250 °C, and retention times between 1 and 3 min for different types of biomass. The maximum nitrogen content in the biocrude (4.0 %) was obtained at 350 °C and 50 min, at lipid ratio and ITS of 0.15 and 15%, respectively. At the maximum biocrude yield obtained, the nitrogen content was also close to the maximum (3.7 %). The manipulation of the reaction conditions was not enough to achieve a nitrogen content in the biocrude similar to that in petroleum (<1.5 %) [90], especially for protein-rich biomasses (> 30 %), so upgrading the biocrude is necessary for commercial fuel production [91].

The effect of reaction temperature, retention time, ITS and the lipid ratio on the calculated oxygen content in the biocrude is shown in Figure 2-3c. The oxygen content decreased significantly from 18 % to 11 % within the studied temperature range, regardless of the other factors. Increases in

retention time also reduce the oxygen content in the biocrude. This suggests that the reaction temperature and retention time promoted deoxygenation reactions [43]. However, the increase in ITS between 10 and 15 % augmented the oxygen content in the biocrude.

The maximum oxygen content in the biocrude (22 %) was obtained with an ITS of 15 % and the minimum values studied for the reaction temperature and retention time. The minimum values for the oxygen content in the biocrude were obtained at 350 °C and 60 min and ITS between 5–10 %. For the maximum biocrude yield obtained, the oxygen content in the biocrude was approximately 14 %. The interactions between the factors had no significant influence on the oxygen content in the biocrude (Figure A 1c). The oxygen content in the biocrude was significantly higher compared to the oxygen content in the petroleum (< 4.5 %). The high oxygen content decreases the HHV of the biocrude [81] and affects the storage stability of the biocrude [92,93].

Several authors have reported that, under certain circumstances, the carbon content generally increases with the lipid content in biomass, while the nitrogen content in the biocrude decreases when reducing the proteins in the biomass [59,73,80]. In this case, the biomass must have a lipid ratio higher than 0.80 (lipids> 40 % and proteins <20 %), so it is possible that the interval of lipid ratio studied was not ample enough to have a significant influence on the elemental composition of the biocrude.

None of the factors had a significant influence on the hydrogen and sulfur content in the biocrude. The hydrogen and sulfur contents in the biocrude were almost constant in the range studied, i.e. 9.3 % ± 0.3 % and 0.26 % ± 0.0 9 %, respectively (Table 2-4). This behavior is in line with those reported by other authors [70,94]. The hydrogen content of the biocrude was slightly lower when compared with the hydrogen content in oil (11.8–14.7%) [90]. However, the sulfur content of the biocrude was significantly lower when compared to the sulfur content reported for light and heavy crudes between 0–2 % and 2–5 %, respectively [95]. This is a positive aspect because it might reduce environmental pollution during the combustion of fuels.

The energy recovery varied between 9.0 and 64.7 %, following a similar behavior to the biocrude yield. The maximum energy recovery of biocrude was obtained at 350 °C for 60 minutes, at a total lipid ratio and ITS of 0.65 and 15 %, respectively. Figure 2-3d shows the effect of the factors on the biocrude HHV. The increase in reaction temperature improved the HHV of the biocrude, regardless of the levels of the other factors. The lipid ratio had no significant influence on the biocrude HHV,

neither the interactions between the factors on the HHV of the biocrude (Figure A 1d). In general terms, the HHV of the biocrude varied between 31.8–37.3 $MJ \cdot kg^{-1}$. An increase in the carbon content and a reduction of the oxygen content in the biocrude resulted in higher HHV values. The maximum predicted biocrude HHV was obtained at ITS of 8 %, at the maximum reaction temperature and retention time. Such HHV is relatively low compared to that of petroleum (42 $MJ \cdot kg^{-1}$) [96], likely as a result of the higher oxygen content in the biocrude.

2.4.7 Model analysis

The comparison between the experimental and predicted values by the regression models for yield and elementary composition of the biocrude are shown in Figure 2-4. The regression model for biocrude yield predicted 35 % and 61 % of the data within the standard deviation (SD) zone of ± 2.5 % and ± 5 %, respectively (Figure 2-4a). The prediction capacity of the biocrude carbon content model was more successful (Figure 2-4b), since 87 % of the predicted values were found within the SD zone of ± 5 %. However, the correlation between predicted and experimental values was not balanced. The model to predict the oxygen content in the biocrude (Figure 2-4c) presented a similar behavior. However, the model overestimated oxygen values less than 7 %. Figure 2-4d shows the prediction capacity of the nitrogen content model in the biocrude. The prediction capacity of the nitrogen model within the SD zone of ± 1 % was 52 %. A deficiency of this model is its inability to predict nitrogen contents greater than 4 %. Although a biomass with a high protein content was included to estimate properly the parameters of the model, the maximum experimental nitrogen content in the biocrude obtained was 4.1 %.

2.4.8 Thermogravimetric analysis

Figure 2-5 shows the TG curves for 8 samples of biocrudes obtained at 350 °C and different retention times, ITS and lipid ratio. On the one hand, at 5 % ITS, retention time have no significant effect on the quality of the biocrude (Figure 2-5a). This result is in line with the findings of previous sections, where the yield and the elementary composition remained approximately constant for ITS between 5–10 %. On the other hand, at 15 % ITS, lighter biocrudes are obtained by increasing retention time (Figure 2-5b). Heavy fractions with boiling points greater than 340 °C decreased by 17 % and 22 %, respectively, with increasing retention time from 0 to 60 min. Likewise, volatile products (< 290 °C) increased up to 1.8 times with retention time (Table 2-5). This last fraction can be used directly as

liquid fuel (gasoline and jet fuel) [97], since the increase in retention time contributes to obtain smaller molecules due to the depolymerization of larger molecules.

Figure 2-5c shows the TG curves for the biocrudes obtained at a temperature of 350 °C, 5 % ITS, 0.65 Lr and retention times of zero min and 60 min. In this case, the effect of retention time is less significant for biomass with a lipid ratio of 0.65 compared to biomass with Lr of 0.15. An increase in the lipid content in biomass augmented the volatile fraction (< 290 °C) by 49 % and 26 %, for retention times of zero min and 60 min, respectively. The intermediate fraction (290–340 °C) showed no significant variation with the increase in lipids in biomass, and the fraction obtained between 340 and 538 °C decreased considerably with the increase in lipids (Table 2-5). This can be attributed to lipids in biomass that produce compounds such as fatty acids, hydrocarbons and esters, while proteins and carbohydrates produce aromatic compounds, branched amides, nitrogenous cyclic compounds and oxygenates cyclic compounds, which are heavier and more structurally complex [98]. Finally, the biocrude obtained in comparison with petroleum can be classified as a heavy crude, since between 69.6 and 87.6 % of the compounds have a boiling point higher than 290 °C [95].

2.5 Conclusions

The reaction temperature, retention time, ITS and lipid ratio had a significant influence on the yield and TAN of biocrude of the microalga *P. kessleri.* The reaction temperature was the most influential factor in the yield and quality of the biocrude. RSM allowed to demonstrate the interaction between the factors for the yield and TAN of the biocrude. The lipids ratio had no significant influence on the elemental composition of the biocrude, in the analyzed range. The highest biocrude yield was obtained between 315 and 325 °C, and 40 and 45 min, at lipid ratio and ITS of 0.65 and 15 %, respectively. Under these conditions, the value of TAN was 70 mg $KOH \cdot g^{-1}$; the carbon, nitrogen and oxygen content were 72 %, 3.7 % and 13 %, respectively; and the HHV was 35 $MJ \cdot kg^{-1}$. The prediction of the models for the yield and content of carbon and oxygen was successful within the range studied. However, the nitrogen model failed to predict maximum values at 4 %. TGA showed that operating at increased retention times and/or lipid biomass contents is an improved strategy to obtain a lighter biocrude.

Table 2-1. Levels of independent variables.

#	Independent variables	Nomenclature	Levels		
			-1	**0**	**1**
1	Reaction temperature (°C)	T	250	300	350
2	Retention time (min)	tr	0	30	60
3	Initial total solids (% w/w)	ITS	5	10	15
4	Lipids ratio	Lr	0.15	0.40	0.65

Table 2-2. Characteristics of microalgae in percentage by mass on dry basis (%).

Properties	***P. kessleri* (P-aut)**	***P. kessleri* (P-myx)**
Moisture (%)	21.5 ± 1.3	8.3 ± 0.2
HHV ($MJ \cdot kg^{-1}$)	22.7	22.2
Elemental composition (%)		
C	54.1 ± 0.9	51.7 ± 1.1
H	5.9 ± 0.3	6.5 ± 0.0
O[1]	28.8	32.5
N	4.9 ± 0.1	2.4 ± 0.7
S	0.3 ± 0.0	0.2 ± 0.0
Ash (%)	6.0 ± 0.1	6.7 ± 0.1
Chemical composition (%)		
Lipids	12.1 ± 0.1	36.5 ± 0.2
Protein	74.8 ± 1.9	27.7 ± 0.1
Carbohydrates	7.2 ± 0.3	29.1 ± 0.2
Ash (%)	6.0 ± 0.1	6.7 ± 0.1
Lipids Ratio	0.15	0.65

[1]Calculated by difference

Table 2-3. Summary of operating conditions and yields of HTL.

# Exp.	Operating conditions			Lr	Yields (%)				Weight balance (%)
	Temperature (°C)	Retention time (min)	ITS (%)		Biocrude	Solid	Aqueous products	Gas	
1	250	0	5	0.15	8.7 ± 3.6[1]	36.6 ± 4.0	26.8 ± 8.1	1.1 ± 0.8	73.3
2	250	60	5	0.15	14.2 ± 1.6	25.7 ± 0.7	20.4 ± 1.1	6.5 ± 2.0	66.8
3	350	0	5	0.15	33.8 ± 2.0	9.4 ± 2.2	16.2 ± 5.1	8.7 ±3.1	68.1
4	350	60	5	0.15	33.0 ± 1.4	8.3 ± 0.8	11.0 ± 1.8	6.5 ± 4.6	58.8
5	250	0	15	0.15	14.8 ± 0.1	39.7 ± 0.0	15.3 ±1.7	----	69.9
6	250	60	15	0.15	20.4 ± 0.4	32.9 ± 8.0	13.7 ± 1.8	4.1	71.1
7	350	0	15	0.15	32.0 ± 0.2	16.3 ± 1.5	13.7 ± 4.1	11.3	73.3
8	350	60	15	0.15	37.1 ±2.3	11.6 ± 1.6	9.7 ±1.5	16.5 ± 1.0	74.8
9	250	0	5	0.65	12.4	39.6	28.4	5.9	86.3
10	250	60	5	0.65	29.8	22.8	24.9	19.9	97.4
11	350	0	5	0.65	35.5	15.3	19.5	12.1	82.5
12	350	60	5	0.65	30.7	8.9	9.6	----	49.2
13	250	0	15	0.65	11.2	44.2	13.4	6.5	75.2
14	250	60	15	0.65	33.6	20.0	18.5	----	72.1
15	350	0	15	0.65	35.4	17.2	14.2	13.3	80.1
16	350	60	15	0.65	38.8 ± 2.5	12.7 ± 0.5	10.8	21.0	83.3
17	300	30	10	0.40	33.7 ± 1.9	18.9 ± 5.0	16.3 ± 3.0	20.3 ± 4.7	89.1
18	250	30	10	0.40	16.7	31.5	18.0	----	66.2
19	350	30	10	0.40	33.5	14.3	10.0	9.4	67.2
20	300	0	10	0.40	17.5 ± 2.0	36.2 ± 2.5	16.4 ± 0.6	----	70.1
21	300	60	10	0.40	32.2	16.8	15.9	19.7	84.6
22	300	30	5	0.40	31.1	18.4	18.5	----	68.0
23	300	30	15	0.40	36.4	17.2	20.6	8.6	82.8
24	300	30	10	0.15	35.6 ± 0.7	19.5 ± 2.7	14.9 ± 0.7	7.3 ± 1.5	77.2
25	300	30	10	0.65	38.2 ± 0.7	26.5 ± 0.4	20.3 ± 1.2	10.4 ± 0.4	95.4
26[2]	350	30	15	0.15	38.0 ± 1.2	11.8 ± 0.8	11.5 ± 0.8	14.3 ± 3.1	75.5
27[2]	350	30	5	0.15	34.2 ± 0.5	9.0 ± 1.6	13.4 ± 0.2	6.8 ± 0.4	63.6

[1] Some points of the experimental design were performed by duplicate. The central point (#17) was repeated 7 times. The values in the table are the average and standard deviation. [2] Additional points.

Table 2-4. Summary of operating conditions of HTL and quality indicators of biocrude.

# Exp.	Operating conditions				Elemental composition				TAN	HHV
	Temperature (°C)	Retention time (min)	ITS (%)	Lr	C (%)	H (%)	N (%)	S (%)	(mg KOH·g^{-1})	(MJ·kg^{-1})
1	250	0	5	0.15	67.9 ± 0.3[1]	10.0 ± 0.5	1.7 ± 0.5	0.17 ± 0.02	138.2 ± 7.40	33.1 ± 0.5
2	250	60	5	0.15	74.5 ± 0.3	9.4 ± 0.2	2.5 ± 0.3	0.24 ± 0.00	109.8 ± 3.2	35.3 ± 0.6
3	350	0	5	0.15	74.5 ± 0.0	9.6 ± 0.0	3.5 ± 0.2	0.26 ± 0.03	87.8 ± 0.9	36.5 ± 0.6
4	350	60	5	0.15	77.4 ± 0.4	9.2 ± 0.2	3.4 ± 0.1	0.24 ± 0.02	82.1 ± 5.7	37.1 ± 0.7
5	250	0	15	0.15	68.1 ± 0.8	9.0 ± 0.7	1.8 ± 0.3	0.24	131.1 ± 4.1	32.3 ± 1.1
6	250	60	15	0.15	70.5 ± 0.5	9.3 ± 0.3	3.2 ± 0.2	0.16	113.2 ± 1.5	35.0 ± 0.3
7	350	0	15	0.15	73.5 ± 0.4	9.1 ± 0.2	3.7 ± 0.0	0.36 ± 0.03	75.4 ± 3.4	35.2 ± 0.3
8	350	60	15	0.15	74.9 ± 0.5	9.2 ± 0.1	4.1 ± 0.2	0.13 ± 0.01	68.2 ± 1.2	35.8 ± 0.4
9	250	0	5	0.65	71.3	9.5	2.0	0.23	119.5	34.3
10	250	60	5	0.65	74.3	9.6	2.6	ND[2]	86.2	35.9
11	350	0	5	0.65	74.6	9.7	3.3	ND	134.1	36.1
12	350	60	5	0.65	75.7	9.6	3.5	0.47	73.9	36.7
13	250	0	15	0.65	68.4	9.5	1.5	0.23	92.3	33.0
14	250	60	15	0.65	68.7	8.9	3.0	0.26	61.4	32.5
15	350	0	15	0.65	73.9	9.2	4.0	0.28	83.9	35.3
16	350	60	15	0.65	76.9 ± 0.0	9.5 ± 0.1	3.8 ± 0.1	0.29 ± 0.05	79.7 ± 3.2	37.0 ± 0.1
17	300	30	10	0.4	72.6 ± 1.6	9.1 ±0 .5	3.3 ± 0.1	0.31 ± 0.08	93.5 ± 4.4	35.3 ± 0.2
18	250	30	10	0.4	68.3	9.1	2.3	ND	115.2	32.4
19	350	30	10	0.4	75.5	9.0	3.9	0.14	66.1	35.7
20	300	0	10	0.4	71.3 ± 1.0	9.6 ± 0.5	2.8 ± 0.0	0.28	108.7 ± 7.2	33.8 ± 0.9
21	300	60	10	0.4	72.0	9.1	3.5	ND	68.2	34.2
22	300	30	5	0.4	72.4	9.2	3.2	ND	96.0	34.5
23	300	30	15	0.4	68.4	8.5	3.2	ND	82.9	31.8
24	300	30	10	0.15	73.8 ± 0.8	8.8 ± 0.5	3.6 ± 0.3	0.27	88.1 ± 4.0	35.5 ± 0.2
25	300	30	10	0.65	71.6 ± 0.5	9.1 ± 0.0	3.0 ± 0.2	0.42	90.4 ± 3.0	34.0 ± 0.2

[1] Some points of the experimental design were performed by duplicate. The central point (#17) was repeated 7 times. The values in the table are the average and standard deviation. [2]ND: not detected.

Table 2-5. Boiling point distribution of biocrude identified by TGA.

Product	Boiling Point Range	Fraction (%)							
		Exp. 3[1]	Exp. 27[2]	Exp. 4[3]	Exp. 7[4]	Exp. 26[5]	Exp. 8[6]	Exp. 15[7]	Exp. 16[8]
Gasoline	< 190°C	2.6	3.1	2.5	0.6	3.1	2.8	6.6	6.5
Jet fuel	190–290°C	15.1	18.5	14.7	11.8	18.5	19.8	17.8	23.9
Diesel	290–340°C	22.0	20.9	19.5	20.9	20.9	23.6	22.7	23.1
Vacuum gas oil	340–538°C	40.5	35.1	42.1	42.0	35.1	34.7	32.7	26.8
Vacuum residue	>538°C	19.8	22.4	21.2	24.7	22.4	19.1	20.2	19.7

[1] HTL performed at temperature of 350 °C, ITS of 5 %, Lr of 0.15 and retention time 0 min.
[2] HTL performed at temperature of 350 °C, ITS of 5 %, Lr of 0.15 and retention time 30 min.
[3] HTL performed at temperature of 350 °C, ITS of 5 %, Lr of 0.15 and retention time 60 min.
[4] HTL performed at temperature of 350 °C, ITS of 15 %, Lr of 0.15 and retention time 0 min.
[5] HTL performed at temperature of 350 °C, ITS of 15 %, Lr of 0.15 and retention time 30 min.
[6] HTL performed at temperature of 350 °C, ITS of 15 %, Lr of 0.15 and retention time 60 min.
[7] HTL performed at temperature of 350 °C, ITS of 15 %, Lr of 0.65 and retention time 0 min.
[8] HTL performed at temperature of 350 °C, ITS of 15 %, Lr of 0.65 and retention time 60 min.

Figure 2-1. Response surface analysis for biocrude yield: (a) principal effects, where the interest factor is varied from its lowest level to its highest level, while the other factors remain constant in their value (high: red solid line, central: blue medium-dashed line, and low: black dashed-dotted line), and (b) interactions between factors, where, in each lane, the first factor was varied from its lowest level to its highest level, while the second factor remains in its lowest level (red medium-dashed line) or highest level (black solid line). All the other factors, except those involved in the interaction, remain constant in their central values.

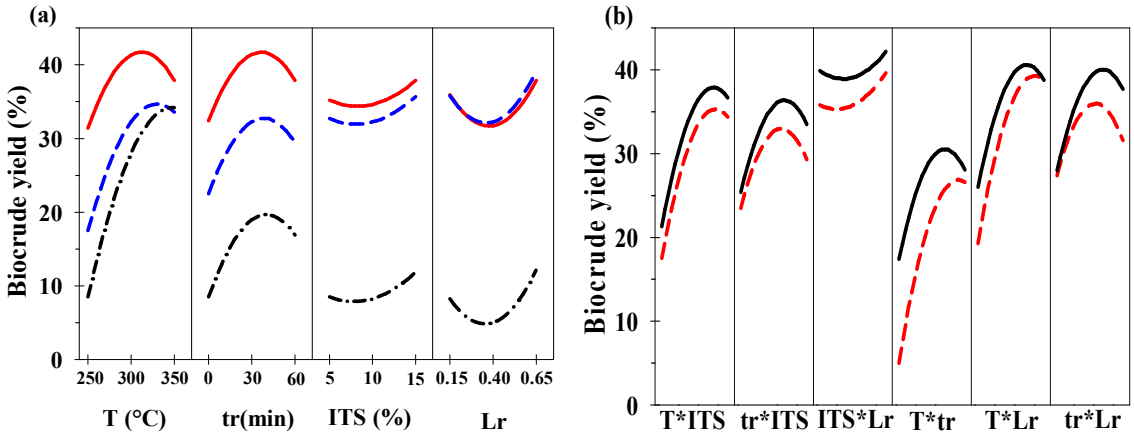

Figure 2-2. Response surface analysis for biocrude TAN: (a) principal effects, where the interest factor is varied from its lowest level to its highest level, while the other factors remain constant in their value (high: red solid line, central: blue medium-dashed line, and low: black dashed-dotted line), and (b) interactions between factors, where, in each lane, the first factor was varied from its lowest level to its highest level, while the second factor remains in its lowest level (red medium-dashed line) or highest level (black solid line). All the other factors, except those involved in the interaction, remain constant in their central values.

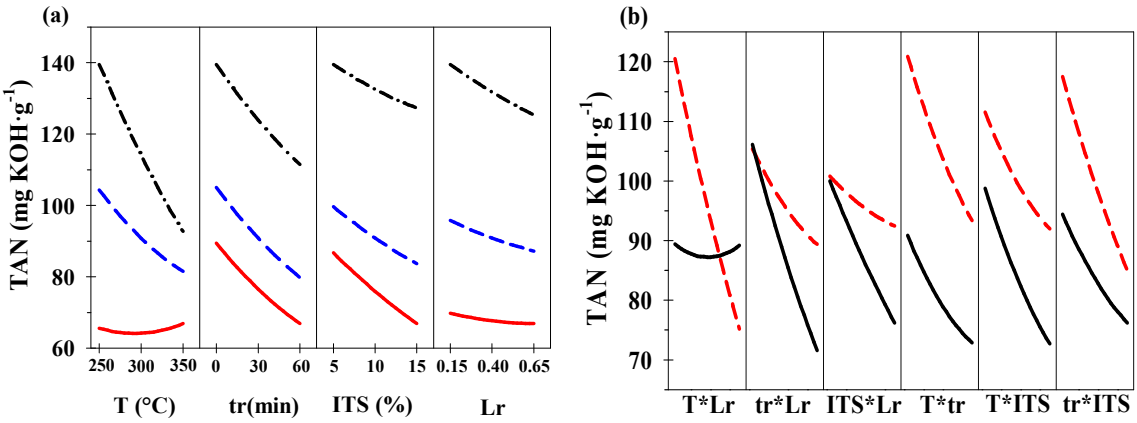

Figure 2-3. Response surface analysis for elemental composition and HHV of biocrude: (a) principal effects for carbon content, (b) principal effects for nitrogen content, (c) principal effects for oxygen content, and (d) principal effects for HHV. The interest factor is varied from its lowest level to its highest level, while the other factors remain constant in its values: high (red solid line), central (blue medium-dashed line) and low (black dashed-dotted line).

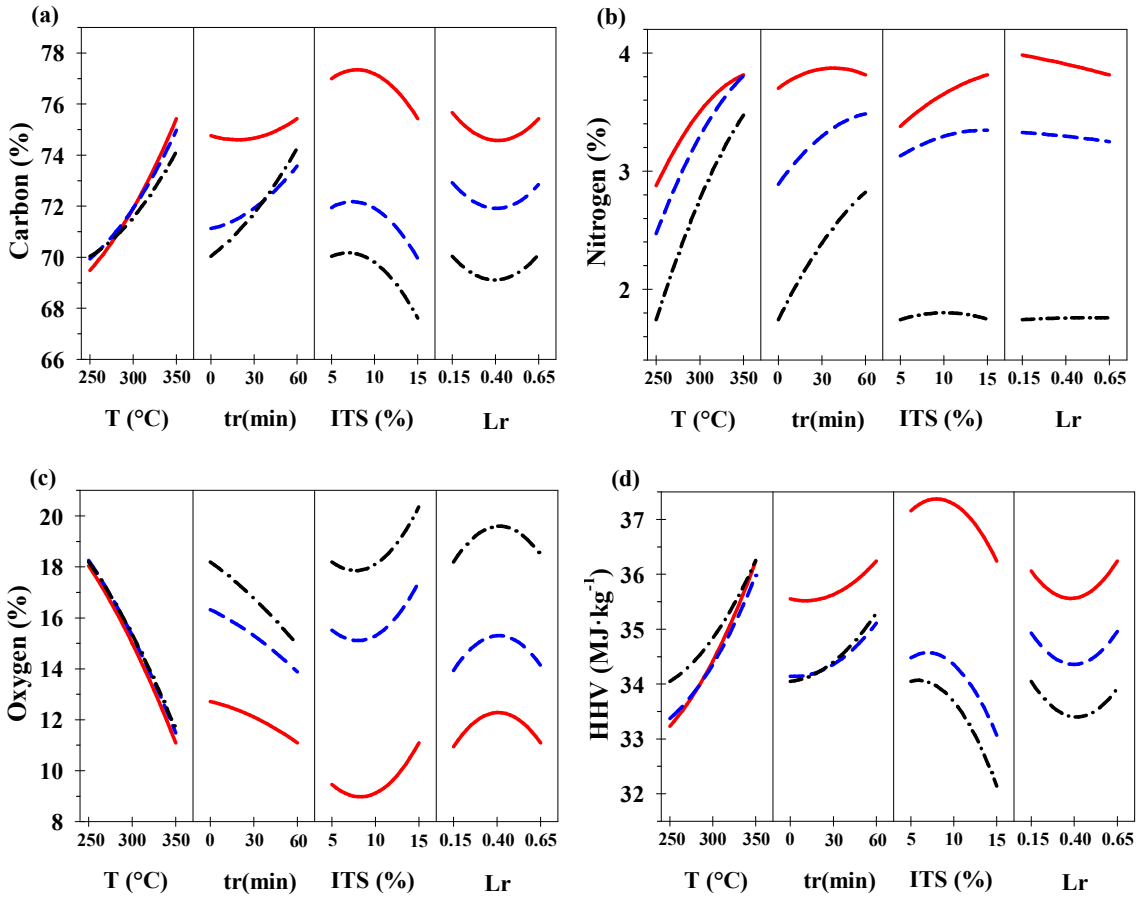

Figure 2-4. Comparison of predictions obtained using RSM model for: (a) yield. (b) carbon. (c) oxygen and (d) nitrogen. Gray circle: literature data and red triangle: data of this study. The continuous black line represents an exact match between the model and the experimental data. The red dotted lines and the blue dashed lines for the graphs (a)–(c) represent a SD of ± 2.5 % and ± 5 %, respectively. The red dotted lines and the blue dashed lines in the graph (d) represent a SD of ± 0.5 % and ± 1 %, respectively.

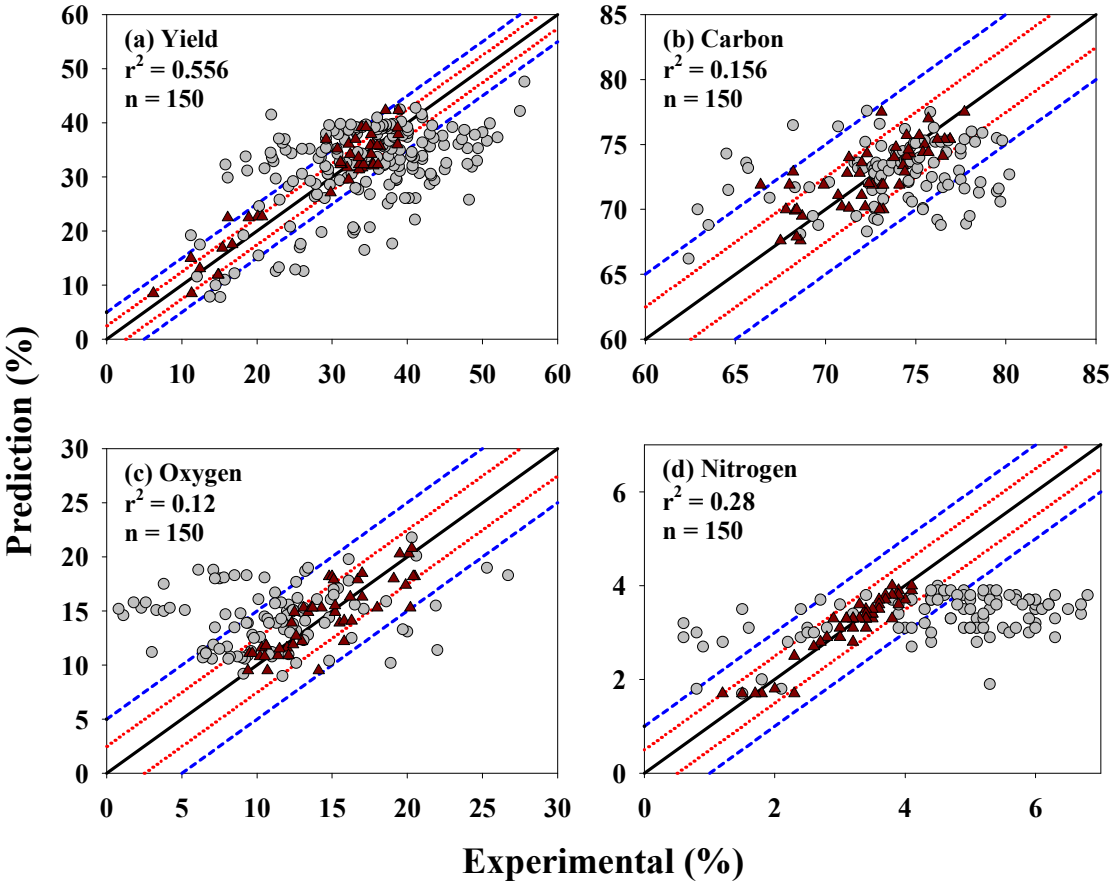

Figure 2-5. TG curves of biocrudes obtained at different retention times. (a) HTL performed at a temperature of 350 °C, ITS of 5 % and Lr of 0.15, (b) HTL performed at a temperature of 350 °C, ITS of 15 % and Lr of 0.15, and (c) HTL performed at a temperature of 350°C, ITS of 5 % and Lr of 0.65.

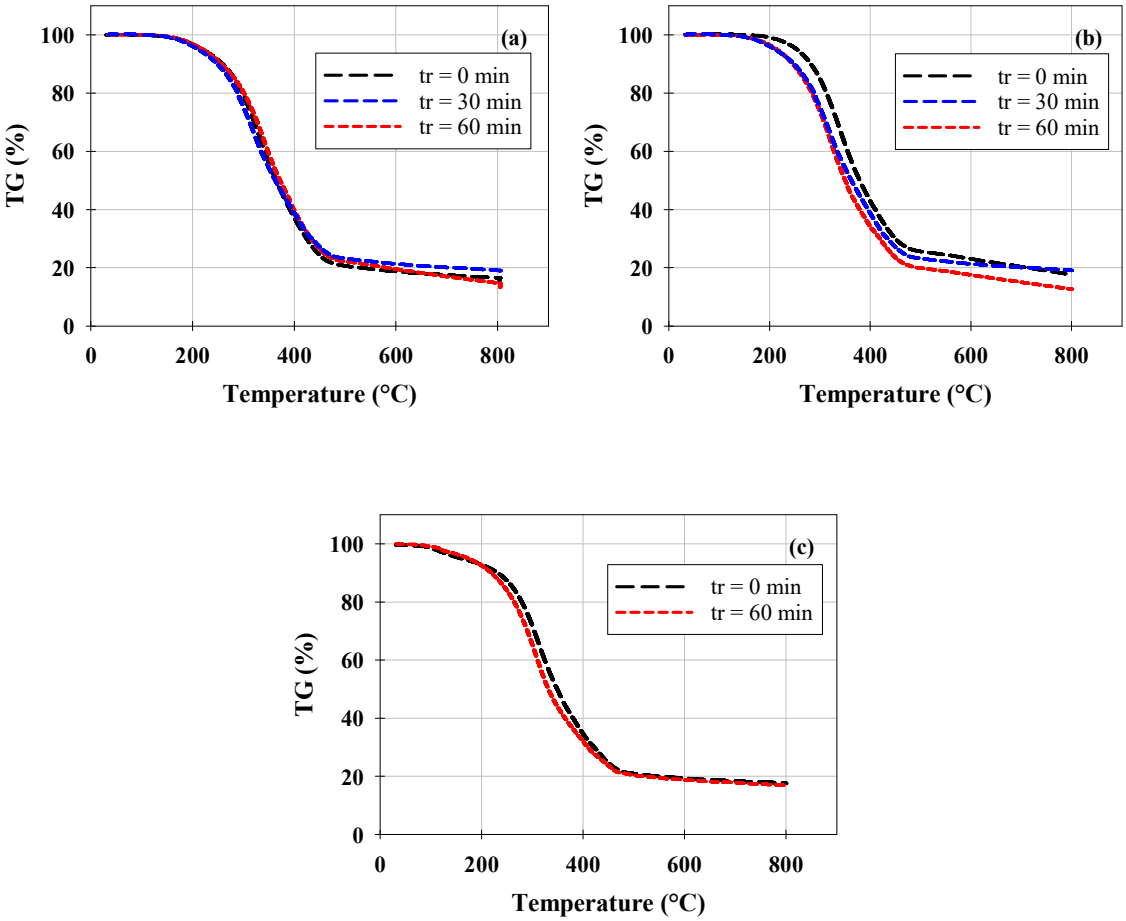

3. Evaluation of yield-predictive models of biocrude from hydrothermal liquefaction of microalgae

The content of this chapter is published in the Algal Research journal.

3.1 Abstract

The prediction capacity of published component additivity and kinetic models was analyzed for calculation of the biocrude yield of hydrothermal liquefaction of microalgae. Their advantages and limitations were identified. Likewise, the effect of reaction temperature and retention time was evaluated on the yield of the biocrude for the kinetic models for four hypothetical biomasses. From the analysis of the component additivity and kinetic models, a new quantitative model was proposed for the calculation of biocrude yield of microalgae. The new model was tested with large numbers of experimental data published over a wide range of temperatures (200–400 °C), retention times (1–120 min) and chemical composition of microalgae (0.0–66 % lipids, 9–75 % proteins, 5–64 % carbohydrates, in dry basis). The predictive capacity of the new model was compared with component additivity and kinetic models. Results show that the model captures better the trend of the experimental data. This model predicted 45 % of the biocrude yields published within the standard deviation zone ± 5 % and 78 % of the total data was within the zone of standard deviation ± 10%. The combined model predicts yields of up to 60 % for lipid-rich biomasses and shows a better linear distribution between experimental and predicted yields than any other currently available model.

Keywords: Reaction network; Kinetic model; Component additivity model; Model compound.

3.2 Introduction

Microalgae are a promising raw material for biofuels production, due to the flexibility and high productivity of their cultivation [2,99]. Hydrothermal liquefaction (HTL) of microalgae is a process in which wet biomass is transformed at high temperatures (200–400 °C) and pressures (5–20 MPa) [43]. The main product of HTL is the biocrude, which is characterized by a complex mixture of organic compounds with a higher heating value (HHV) than biomass [44].

The temperature (T), retention time (tr), initial total solids (ITS), use of catalysts, characteristics of biomass (type, species and biochemical composition), among others, are some of the main variables of HTL that affect significantly the biocrude yield and have been studied by different authors [25,26,34,38,68–71]. The results obtained have allowed to advance in the understanding of the mechanism of the reaction and in the projection of HTL at a pilot and/or industrial scale [100]. However, mathematical equations relate the characteristics of the biomass with the yield and those of the biocrude that are needed for the scaling and economic analysis of the microalgae HTL.

The mathematical models published to date to predict the biocrude yield have biomass composition, temperature and/or reaction time as main variables. Biller & Ross [18] proposed a component additivity model for the calculation of the biocrude yield from the fractions of lipids (X_L), proteins (X_P) and carbohydrates (X_{CH}) of the biomass (Equation 3-1). The coefficients a, b and c are individual yields for the different model compounds of lipids (sunflower oil), proteins (soy protein, albumin and glutamine) and carbohydrates (glucose and starch), obtained at a temperature and reaction time of 350 °C and 60 min, respectively:

$$\text{Biocrude yield (\%)}: Y_B = aX_L + bX_P + cX_{CH}. \quad (3\text{-}1)$$

On the one hand, several authors have proposed different values for the parameters of the linear model, when varying the reaction conditions and/or when using other model compounds or microalgae (Table 3-1) [59,73,80,101]. Other versions of the component additivity model include three additional terms that represent the effect of the interactions between lipids, proteins and carbohydrates of the biomass in the biocrude yield (Equation 3-2 and Equation 3-3), where d, e and f are the parameters of interaction among them (Table 3-1) [102–104]. All these models proved to be reasonably successful within the scope of their studies and, because of their simplicity, are widely

popular. However, they only apply at a specific temperature and reaction time and their coefficients must be determined for each set of reaction conditions of interest:

$$\text{Biocrude yield (\%)}: Y_B = aX_L + bX_P + cX_{CH} + dX_LX_{CH} + eX_LX_P + fX_PX_{CH}, \quad (3\text{-}2)$$

$$\text{Biocrude yield (\%)}: Y_B = aX_L + bX_P + cX_{CH} + d(X_LX_{CH}/|X_L - X_{CH}|) + e(X_LX_P/|X_L - X_P|) + f(X_PX_{CH}/|X_P - X_{CH}|). \quad (3\text{-}3)$$

On the other hand, kinetic models can predict the biocrude yield over a wide range of temperatures and reaction times. Valdez et al. [105] proposed a reaction network for the liquefaction of the microalga *Nannochloropsis sp.* (Figure 3-1a), where the solids (microalgae) react to form aqueous products, biocrude (light and heavy) and gases. The result was a system of differential equations constructed from the kinetic network, the design equation of an isothermal batch reactor and assuming first-order kinetics. This model allowed calculating the yields of each of the HTL products in a range of temperature and reaction times between 250–400 °C and 10–90 min, respectively.

Likewise, Valdez et al. [19] modified their reaction network and correlated the biochemical composition of three species of microalgae (*Nannochloropsis sp.*, *Chlorella protothecoides* and *Scenedesmus sp.)* with the yields of the three products of the HTL (Figure 3-1b). The content of lipids, proteins and carbohydrates of biomass allowed to extend the applicability of the kinetic model to other species of algae. From the kinetic networks proposed by Valdez et al., Vo et al. [84,85] proposed different values for the kinetic constants from the correlation of the yields of the HTL products of the microalgae *Tetraselmis sp*. (Figure 3-1a) and *Aurantiochytrium sp*. KRS 101 (Figure 3-1b). These models maintain the assumption that each macromolecule of the microalga reacts independently during HTL. Likewise, Sheehan & Savage [106] updated and modified the differential equations system for the network shown in Figure 3-1b, by calculating their own kinetic parameters and including interaction terms between the biomass macro-compounds represented as a second order reaction, to improve the prediction level of the kinetic model. This update of the kinetic model was successful, since it predicted 70 out of 133 experimental yields published by other authors. The values of the kinetic parameters for the kinetic network of Figure 3-1b. proposed by Valdez et al. [19], Vo et al. [24] and Sheehan & Savage [106] are shown in Table B 1.

Hietala et al. [107] proposed the first model for fast HTL, accounting for temperature variation (between 200–400 °C), reaction times (from 10 s) and heating rate (between 110–350 °C·min^{-1}).

Additionally, its kinetic network included a solid path to gas reaction and the formation of a new volatile fraction from the aqueous phase (Figure 3-1c). This model showed great success within the study scope; however, it does not take into account the chemical composition of the biomass, which restricts its applicability. There are also other models that calculate the yield of the biocrude from other variables such as heating rate [46] or content and type of fatty acids in the biomass (saturated, monounsaturated and polyunsaturated) [59,74]. These models are restricted to a single reaction condition and to obtaining additional data during experimentation.

In this article, an analysis was made of the prediction level of the main quantitative models to calculate the yield of the biocrude. The analysis included published data on yields and chemical compositions of biomass obtained in a wide range of reaction conditions. Likewise, from the analysis, a new model is proposed for the calculation of the yield of the biocrude, which includes as variables the composition of the raw material, and the HTL temperature and the retention time.

3.3 Material and methods

3.3.1 Predictive analysis of yield models

The prediction capacity was analyzed in the additivity models of components proposed by Biller & Ross [18], Leow et al. [59], Wagner et al. [101], Li et al. [73], Shakya et al. [80], Teri et al. [102], Lu et al. [103] and Sheng et al. [104] (Table 3-1). For this purpose, the published yields of 60 papers were compiled, in which the biomass chemical composition data were available and reaction conditions (temperature, time and ITS, among others) were similar (Table B 2). In total, these studies included 130 types of biomass with different chemical compositions (0.0–59.9 % lipids, 9.3–74.7 % proteins, 5.8–63.6 % carbohydrates and 2.0–47.5 % ash, in dry basis).

The effect of the HTL temperature and retention time was analyzed on the biocrude yields using the kinetic models proposed by Valdez et al. [19], Vo et al. [85] and Sheehan & Savage [106] (Figure 3-1b and Table B 1), simulating each model with four hypothetical biomasses with very different chemical composition, as show in Table 3-2. These four hypothetical biomass compositions were established according to those reported in different hydrothermal liquefaction articles (Table B 2 and Figure B 1). Likewise, the prediction capacity of the kinetic models was analyzed. The calculated yield of the different models was compared with 450 experimental biocrude yields

from 73 published studies (Table B 2). The selected experimental yields were obtained from 176 types of biomass with different chemical compositions (0.0–66.3 % lipids, 9.3–74.7 % proteins, 5.4–63.6 % carbohydrates and 0.3–47.5 % ash, in dry basis), at temperatures of 250, 300, 350 and 400 °C and retention times between 1.0–120 min.

3.4 Results and discussion

3.4.1 Component additivity models

The yield predictions for the component additivity models described in Table 3-1 are shown in Figure 3-2. The predictions of the models proposed by Biller & Ross and Wagner et al. at 350 °C and 60 min are shown in Figure 3-2a and Figure 3-2b, respectively. Figure 3-2b includes some additional experimental data obtained at the same model temperature (360 °C). These models do not include the terms of interaction between macromolecules. In general terms, these two models underestimated 83% and 61% of the experimental data, respectively, and only 15 % and 26 % of the analyzed data were within the standard deviation (SD) zone ± 5%. The additional interaction terms proposed by Teri et al. and Lu et al. significantly improved the prediction level for the same data set (at 350 °C and 60 min); 50 % and 32 % of the analyzed data were found in the SD zone of ± 5%. The prediction capacity of the Lu model did not improve with the additional points (Figure 3-2c and Figure 3-2d).

Figure 3-2e – Figure 3-2l show the predictions for the models whose parameters were obtained at temperatures around 300°C and retention times around 30 min. The yields calculated by these models were compared with experimental data obtained at the experimental conditions of temperature and retention time close and/or equal to 300 °C and 30 min. The experimental and predicted data by the models of additivity of components without interaction are shown in Figure 3-2e – Figure 3-2i.

The model proposed by Leow et al. was able to predict 67 % of published data at the conditions of the model within the area of SD ± 5 % (Figure 3-2e), followed by the model proposed by Shakya et al. at 320 °C and Li et al., with 60 % and 54 % of the data in the SD zone ± 5 %, respectively (Figure 3-2f and Figure 3-2g). The success of these models can be attributed to the fact that their parameters were calculated from the results obtained in the direct liquefaction of different microalgae

species with variable chemical compositions, since the type of macromolecules and their cross-interactions were more representative than the results obtained from the liquefaction of model compounds or their mixtures. However, the Shakya et al. model predicted 31 % of the experimental data at 280 °C, including the data obtained from the same conditions of the model (Figure 3-2h). Additionally, the Wagner et al. model at 300 °C underestimated 87 % of the experimental data obtained at a temperature of 300 °C and retention time of 30 min (Figure 3-2i). The same trend was maintained independently of the retention time (Figure B 2). The models that include interactions did not improve the prediction level for this data set, equal and/or near at 300 °C and 30 min (Figure 3-2j–Figure 3-2l).

In general, predictions of component additivity models underestimate experimental results. The difference between the calculated and experimental yields might be attributed to the varied amount of conditions involved in HTL. Several of the experimental data were obtained at ITS and heating rates different from those used in the experiments that determined the parameters of the models. Other data sets differ in the method and solvent used during the separation of the products and in the type of reactor. Despite the success of some of these models, they are only applicable to a set of specific conditions.

3.4.2 Kinetic models

Figure 3-3 depicts the effect of temperature and reaction time on the yield of the biocrude predicted by the Valdez et al. model for four types of hypothetical biomasses with different composition. In general terms, the biochemical composition of microalgae only had a significant effect on the yield of the biocrude at temperatures between 250–270 °C. In this temperature range, the highest yields predicted by the model are achieved for protein-rich biomass, between 37–42 % (Figure 3-3a). The yields predicted at 250 °C by the model decrease down to 24% when the lipid content in the biomass increases (Figure 3-3b and Figure 3-3c), while for carbohydrate-rich biomass the yield reaches 21 % at the same temperature. Similarly, the retention time has an almost linear effect on the yield in the interval 0–10 min (Figure 3-3d).

At temperatures and reaction times above 300 °C and 10 min, the chemical composition of the biomass does not significantly affect the yield of the biocrude. The maximum biocrude yield

predicted by the model was 43 % and is reached between 300–350 °C and times above 20 min, independently of the composition of the biomass.

This behavior is contrary to what has been evidenced experimentally by several authors, where the chemical composition of the biomass has a significant effect on the biocrude yield in a wider range of temperatures, between 250–400 °C [25,34,47,68,70]. Likewise, yields higher than 50 % have been reported, especially for lipid-rich biomass [59,73,80]. At more severe conditions (370 ° C > T, 30 min > t), the predicted biocrude yield is reduced as it is transformed into aqueous products and gases, congruent with published experimental data [47,89,108].

Likewise, the effect of temperature and reaction time on the biocrude yield calculated from the models proposed by Vo et al. and Sheehan & Savage was analyzed. The biomass composition only has a small effect on the yield calculated by the Vo et al. model (between 2–5 %) at temperatures and retention times less than 300 °C and 30 min, respectively. The maximum biocrude yield predicted by the Vo et al. model is approximately 50 % in a range of temperatures and reaction times between 300–350 °C and 10–30 min, respectively (Figure B 3).

The chemical composition of the biomass has a significant effect on the maximum yield of biocrude when using the model proposed by Sheehan & Savage (Figure 3-3e – Figure 3-3h). According to the model, the yield of the biocrude is higher than 30 % at temperatures between 250–300 °C and times of 1 min when the liquefaction is carried out on protein-rich microalgae (Figure 3-3e). This observation indicates that at retention times of less than 10 min, protein-rich microalgae (> 50 %) are preferred for obtaining biocrude. As the lipid content in the biomass increases, longer retention times (> 14 min at 250 °C and > 5 min at 300 °C) are needed to achieve similar yields in the same temperatures range between 250–300 °C (Figure 3-3f and Figure 3-3g). Independently of the content of lipids and/or proteins in the microalga, the maximum biocrude yield achieved with the model is around 45% at temperatures and retention times greater than 300 °C and 30 min. The opposite occurs in component additivity models where, according to the magnitude of the parameters, it is preferable to have lipid-rich microalgae. On average, 92 % of the lipid content in the microalgae reacts to form the biocrude, followed by the proteins (32 %) and carbohydrates (11 %) (Table 3-1). For the liquefaction of carbohydrate-rich microalgae, more severe conditions are needed (> 350 °C and > 50 min) to achieve yields close to 40 % (Figure 3-3h). This behavior is described by several researchers [70,73,109].

Figure 3-4 shows the predictive capacity of the Valdez et al., Vo et al. and Sheehan & Savage models without interactions at different temperatures. At 250 ° C, the Valdez et al, Vo et al. and Sheehan & Savage models predict 30 %, 28 % and 45 % of the experimental data within the SD zone ± 5 %, respectively (Figure 3-4a – Figure 3-4c). The successful percentage of the kinetic models at 300 °C is 34 % ±3 % (Figure 3-4d – Figure 3-4f). At this temperature, all models underestimate the biocrude yield when the microalgae biomass has a lipid content greater than 45 % (Figure B 4). Likewise, when comparing the experimental and calculated yields by the Sheehan & Savage model at temperatures of 250 and 300 °C, 90 and 57 % of the data are overestimated, respectively when the microalgae is protein-rich (Figure B 5). A similar trend occurs for Valdez et al. and Vo et al. models.

At 350 °C, Valdez et al. and Vo et al. models predict 30 % and 26 % of the experimental data, respectively (Figure 3-4g and Figure 3-4h). The Sheehan & Savage model improves the prediction level of the experimental data for each reaction temperature analyzed, especially at 350 °C, where 71 % of the data is within the SD zone ± 5 % (Figure 3-4i). At 400 °C, the prediction level of the models is between 30–60 %, Valdez et al. > Vo et al. > Sheehan & Savage (Figure 3-4j – Figure 3-4l). In general terms, the model proposed by Sheehan & Savage predicts 54 % within the SD zone ± 5 % of the total experimental data analyzed, significantly improving the prediction capacity of the Valdez (31 %) and Vo (30 %) models.

The success of the Sheehan & Savage model can be attributed to the fact that the chemical composition of the biomass influences the calculated yields in the analyzed range of temperatures. However, the linear correlation between all the experimental and calculated values is not balanced. The coefficients of determination (r^2) in Figure 3-4 are all less than 0.30, thus values calculated between 42–48 % correspond to high experimental yields (> 55 %), while at experimental values lower than 30 %, there is an overestimation of 70 % of the data. The same happens for Valdez et al. and Vo et al. models. The general predictive capacity of Sheehan & Savage model did not improve when including the terms of interaction. Only at 250 °C and 300 °C, the inclusion of interaction terms increased in 10 % of data within the SD zone ± 5 %. However, at 350 °C and 400 °C the percentage of data within the SD zone ± 5 % was reduced in 15 % (Figure B 6).

3.4.3 A new model

A new model for the calculation of the yield of biocrude is proposed from the previous analysis. The new model is the result of the combination between a component additivity model and a kinetic model (Equation 3-4). A series of new terms with the form (1-exp (-k_i t)) are analogous to the formation of biocrude from main components following a first-order reaction (i → B), where i corresponds to either L: lipids, P: proteins and CH: carbohydrates. These new terms include the variables of retention time (tr) and reaction temperature (k_i (T)) to the component additivity model. Likewise, the kinetic model is simplified to a single equation, as shown in Equation 2-4:

$$\text{Biocrude yield (\%)}: Y_B = C_L X_L\left(1 - \exp(-k_L tr)\right) + C_P X_P\left(1 - \exp(-k_P tr)\right) + C_{CH} X_{CH}\left(1 - \exp(-k_{CH} tr)\right). \quad (3\text{-}4)$$

The kinetic constants (k_i) were calculated from the Arrhenius parameters proposed by Sheehan & Savage [106] (Table 3-1). Parameters C_i were calculated from the multiple regression analysis involving 830 experimental yield data collected from 93 articles (Table B 2). The experimental yields were obtained in a wide range of temperatures (200–400 °C) and retention times (1–120 min). Likewise, they involved other variables that might influence the yield of biocrude, but are not specified in the models (i.e. ITS, heating rate, type of separation solvent, initial pressure, agitation, among others). For the multiple regression analysis, the built-in Microsoft Excel Regression Analysis Toolbox® was used. Table 3-3 shows the values of the regressed parameters for Equation 2-4. The parameters C_i are similar to those obtained by other authors for the component additivity model (Table 3-1). In general, these parameters represent an average of how much lipids, proteins and carbohydrates reacted to produce biocrude. The remaining fraction is assumed to be equivalent to the formation of aqueous products and gases.

The effect of temperature and retention time on the biocrude yield predicted by the combined model is similar to that presented by the Sheehan & Savage model (Figure 3-5). However, with the combined model, a greater influence of the composition of the microalga on the biocrude yield is appreciated, especially for lipid-rich and protein-rich biomasses. As in the Sheehan & Savage model, in the combined model, protein-rich microalgae reacted rapidly (1 min) even at low temperatures (250 °C). However, the biocrude yield predicted by the combined model is 1.7 times lower than that predicted by the Sheehan & Savage model (Figure 3-5a and Figure 3-5e). The yields predicted by

the combined model for a protein-rich biomass are 38 % ± 2 % on average, between 300–400 °C and retention times higher than 30 min (Figure 3-5b – Figure 3-5d).

As the lipid content in the microalga increases, the maximum biocrude yield predicted by the combined model also increases (up to 62 %), for temperatures and retention times higher than 350 °C and 20 min, respectively (Figure 3-5c and Figure 3-5d). This is the main difference between the combined and the Sheehan & Savage models, since the maximum yield predicted by the latter does not exceed 45 % for lipid-rich microalgae. The biocrude yield predicted by the combined model for lipid-rich microalgae is higher than that for protein-rich microalgae at >300 ° C and >5 min (Figure 3-5f). With the Sheehan & Savage model, there is no difference between the predicted yield for these two biomasses in the same range of temperatures and retention times.

In the HTL of a carbohydrate-rich biomass, the yields predicted by Sheehan & Savage model and by the combined model are similar throughout the range of temperature and times. At temperatures and retention times higher than 350 °C and 30 min, respectively, the biocrude yield predicted by the combined model for carbohydrate-rich microalgae is slightly higher than that predicted for protein-rich microalgae (Figure 3-5g and Figure 3-5h). This can be attributed to the fact that the magnitude of the parameters (C_P and C_{CH}) of the combined model is similar for the reaction of these macromolecules. Likewise, at high temperatures (> 350 °C) the reaction rate of carbohydrates increases by an order of magnitude [19,85]. After 30 min, the biocrude yield predicted by the combined model remains constant on time, for every biomass composition and the reaction temperature (Figure 3-5).

The predictive capacity of the combined model at different temperatures is shown in Figure 3-6. At 250 °C, the combined model significantly improves the prediction capacity of the Valdez et al. and Vo et al. kinetic models. However, the percentage of success of the combined model is 15 % less than the Sheehan & Savage model within the SD zone ± 5 % (Figure 3-6a). At 300, 350 and 400 °C, the same trend is maintained. When expanding the SD zone to ± 10 %, the percentage of success of the combined model and the Sheehan model is similar and the difference between them is not higher than 2 % for temperatures of 250 and 350 °C (Figure 3-6a and Figure 3-6c). At 300 °C, the prediction level of the combined model within the SD zone ±10 % improves, compared to the Sheehan & Savage model, since predicted biocrude yields are higher than 50 %, which is closer to the experimental yields obtained for lipid-rich biomasses (Figure 3-6b).

At 400 °C, the prediction level of the combined model is 37 %, overestimating 56 % of the experimental data (Figure 3-6d). This overestimation can be attributed to the fact that at higher temperatures, other reactions like the formation of gases from the biocrude have a higher influence [19,85]. This decrease in the biocrude at high temperatures and retention times is not observed in the combined model (Figure 3-5).

Although the percentage of data predicted by the combined model within the SD zone ± 5 % is slightly lower than the percentage of success of the Sheehan & Savage model, the data predicted by the combined model *vs.* experimental data show a more balanced linear distribution, when compared with all the other kinetic and linear models analyzed. This distribution can be better appreciated involving all the collected experimental data (n = 830) and comparing them with the predicted values for the Leow et al., Sheehan & Savage and combined models (Figure B 7). A slope equal to one and an intercept equal to zero means that there is an exact match between the data predicted by the models and experimental data. The lineal distribution of the combined model is further verified by its r^2 value of 0.47, which exceeds the other models. The three models predict 45 % ± 1 % of the data calculated within the SD zone ± 5 %. Likewise, 78 % of the data calculated by the combined model are within the ±10 % zone, followed by the models of Sheehan & Savage (71 %) and Leow et al. (68 %).

3.5 Conclusions

Component additivity models to predict biocrude yield on HTL of microalgae showed acceptable success, especially those whose parameters were calculated from the results obtained for direct liquefaction of different microalgae species with variable chemical compositions, as opposed to model compounds. The biocrude yield, calculated by the kinetic models at temperatures higher than 300 °C and 10 min, was independent of the chemical composition of the biomass, especially, when it is protein-rich or lipid-rich. This behavior is contrary to the experimental data presented in different published articles. The new model proposed for the microalgae HTL can predict biocrude yields for biomasses with variable chemical compositions in a wide range of reaction conditions (HTL temperature and retention time). The combined model predicts yields of up to 60 % for lipid-rich biomasses and shows a better linear distribution between the experimental and the predicted yields.

Table 3-1. Parameter values for correlating biocrude yields from component additivity model.

Model	Eq.	HTL conditions (Temperature, time, ITS[1])	Model compounds (L, P, CH)[2]	Parameter						Ref.
				a	b	c	d	e	f	
Biller & Ross	3-1	350 °C, 60 min, 10 %	Sunflower oil, soy protein, glucose	0.80	0.18	0.06	-	-	-	[18]
Leow et al.	3-1	300 °C, 30 min, 20 %	*Nannochloropsis oculata* (L: 0–59 %. P: 17–75 %. CH: 12–22 %)	0.97	0.42	0.17	-	-	-	[59]
Wagner et al.	3-1	300 °C, NR[3], 16.7 %	Rapeseed oil, soy protein, corn flour	0.96	0.161	0.024	-	-	-	[101]
Wagner et al.	3-1	360 °C, NR, 16.7 %	Rapeseed oil, soy protein, corn flour	1.013	0.286	0.036	-	-	-	
Shakya et al.	3-1	280 °C, 30 min, 15 %	9 types of biomass (L: 14–55 %. P: 7–63 %. CH: 9–50 %)	0.90	0.32	0.22	-	-	-	[80]
Shakya et al.	3-1	320 °C, 30 min,15 %	9 types of biomass (L: 14 – 55 %. P: 7 - 63%. CH: 9 – 50 %)	0.96	0.43	0.30	-	-	-	
Li et al.	3-1	300 °C, 30 min, 20 %	24 types of biomass (L: 0–43 %. P: 11–70 %. CH: 10–64 %)	0.85	0.45	0.22	-	-	-	[73]
Teri et al.	3-2	300 °C, 20 min, 15 %	Sunflower oil, soy protein, cornstarch	0.951	0.334	0.058	-0.00016	0.271	-0.00019	[102]
Teri et al.	3-2	350 °C, 60 min, 15 %	Sunflower oil, soy protein, cornstarch	0.949	0.316	0.061	-0.212	0.359	0.00038	
Lu et al.	3-2	350 °C, 30 min, 20 %	Soybean oil, soy protein, cellulose	0.82	0.211	0.0457	0.000	0.000	0.479	[103]
Sheng et al.	3-3	280 °C, 60 min, 10 %	Castor oil, soy protein, glucose	0.90	0.385	0.025	0.052	0.093	0.003	[104]

[1] ITS: Initial total solids. [2] L, P and CH: lipids, proteins, and carbohydrates content in biomass, respectively. [3] NR: not reported

Table 3-2. Composition of the different model biomasses.

Biomass	Composition (%)[1]			
	Proteins	**Lipids**	**Carbohydrates**	**Ash**
1	60.0	10.0	25.0	5.0
2	35.0	35.0	25.0	5.0
3	10.0	60.0	25.0	5.0
4	17.5	17.5	60.0	5.0

[1]db: dry biomass

Table 3-3. Parameter values for the proposed combined model (Equation 3-4).

Component i	$\log_{10}[A_i]$ (min^{-1})	E_{ai} ($kJ \cdot mol^{-1}$)	C_i
Lipids (L)	5.32	65.8	0.813
Proteins (P)	5.29	51.9	0.397
Carbohydrates (CH)	5.25	78.6	0.367

Figure 3-1. Hydrothermal liquefaction reaction network. (a) Valdez et al. [105]. (b) Valdez et al. [19]. (c) Hietala et al. [107]. S: solids (microalgae), AP: aqueous-phase products, LB: light biocrude, HB: heavy biocrude, B: biocrude, G: gas and V: volatiles. L, P and C: lipids, proteins and carbohydrates content in biomass, respectively. k_i are kinetics constants.

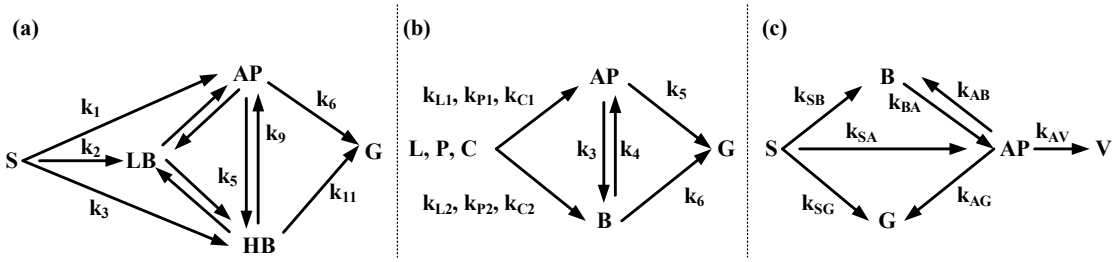

Figure 3-2. Comparison of yield predictions obtained by the component additivity models from: (a) Biller & Ross [18] at 350 °C and 60 min, (b) Wagner et al. [101] at 360 °C, (c) Teri et al. [102] at 350 °C and 60 min, (d) Lu et al. [103] at 350 °C and 30 min, (e) Leow et al. [59] at 300°C and 30 min, (f) Wagner et al. [101] at 300 °C, (g) Shakya et al. [80] at 280 °C and 30 min, (h) Shakya et al. [80] at 320°C and 30 min, (i) Li et al. [73] at 300 °C and 30 min, (j) Teri et al. at [102] 300 °C and 20 min, (k) Sheng et al. [104] at 280 °C and 60 min, and (l) Lu et al. [103] at 350 °C and 30 min. The continuous black line represents an exact match between the model and experimental data. The red dotted lines represent a SD of ± 5 %. The r^2 explain the variance of the experimental and predicted data for a linear regression with the intercept equal to zero. Gray circle: points obtained from the HTL of microalgae at the same experimental and modeled temperature and retention times. Blue triangle up: experimental points obtained from HTL of microalgae at 350 °C and 60 min, but modeled at the conditions of every graph. Blue triangle down: experimental points obtained from HTL of microalgae at 300 °C and 30 min, but modeled at the conditions of every graph.

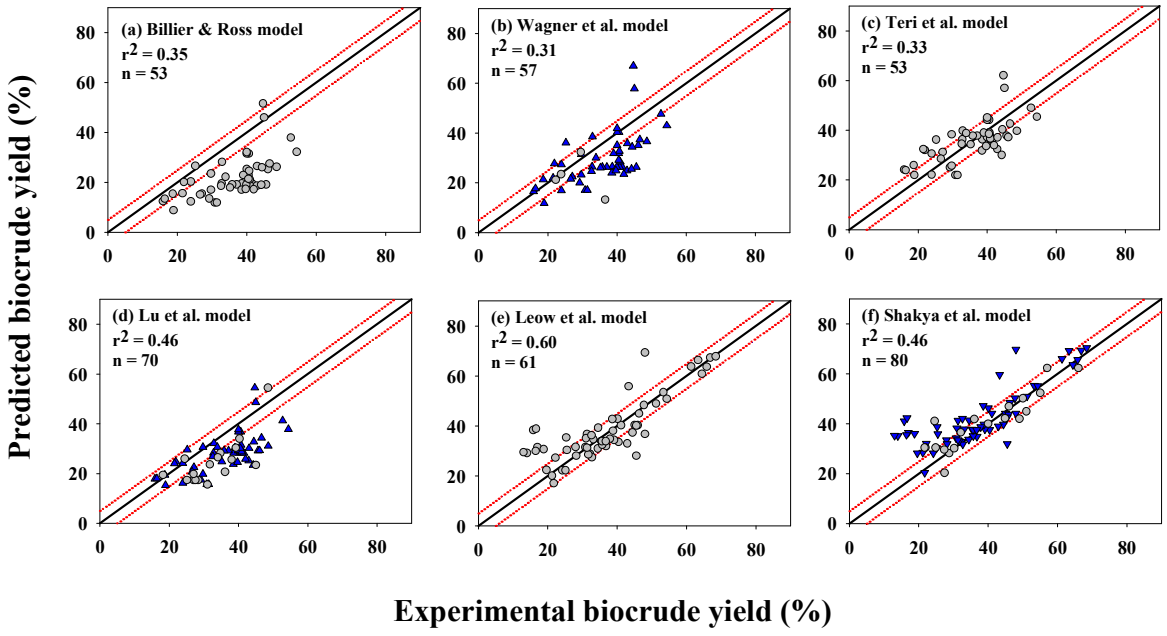

Figure 3-2. (Continued).

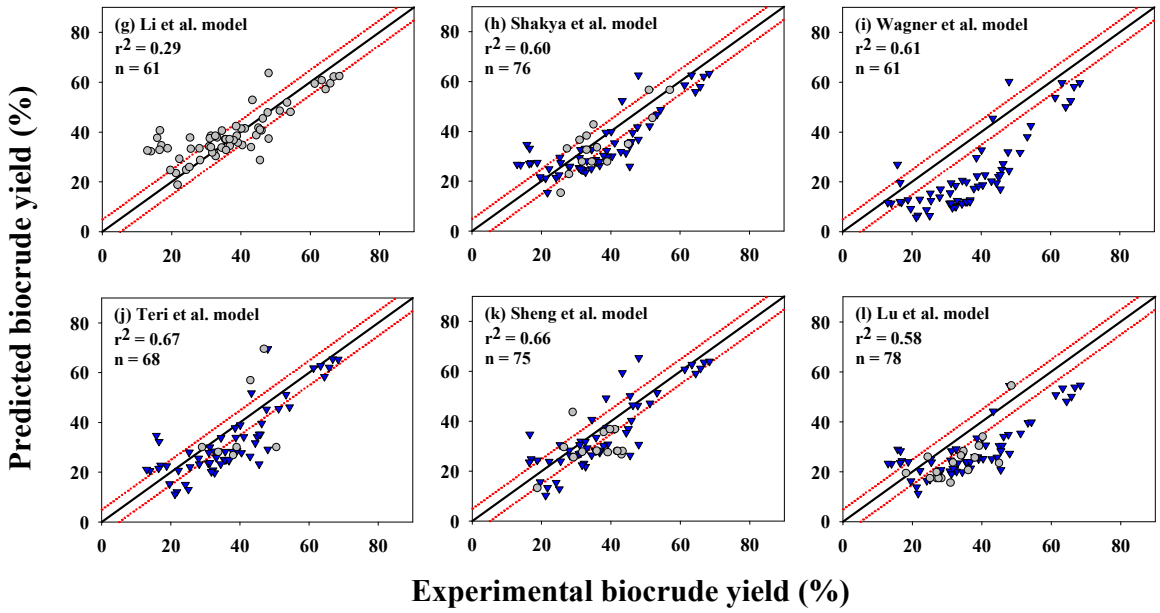

Figure 3-3. Effect of temperature and retention time on calculated biocrude yields by the models: (a) – (d) Valdez et al. [19], and (e) – (h) and Sheehan & Savage [106] from hydrothermal liquefaction of four hypothetical biomass. (a) and (e) Biomass 1: 10% lipids, 60 % proteins and 25 % carbohydrates. (b) and (f) Biomass 2: 35 % of each lipids and proteins and 25 % carbohydrates. (c) and (g) Biomass 3: 60 % lipids, 10 % proteins and 25 % carbohydrates. (d) and (h) Biomass 4: 60 % carbohydrates and 17.5 % of each lipids and proteins.

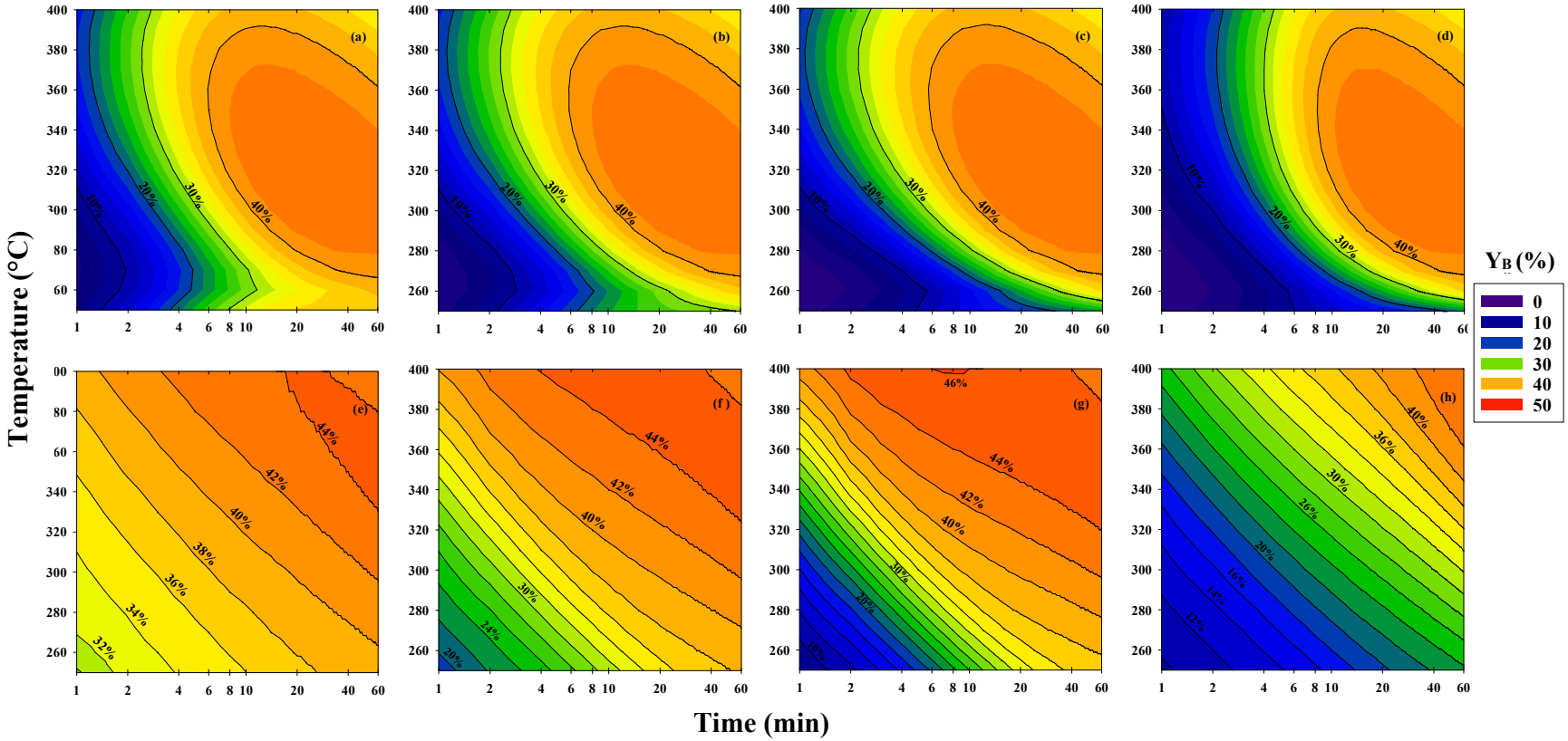

Figure 3-4. Comparison of yield predictions obtained using kinetic models from Valdez et al. [19], Vo et al. [85] and Sheehan & Savage [106] without interactions at different HTL temperatures: (a) – (c) 250 °C, (d) – (f) 300 °C, (g) – (i) 350 °C, and (j) – (l) 400 °C. The continuous black line represents an exact match between the model and experimental data. The red dotted lines represent a SD of ± 5 %. The r^2 explains the correlation between the experimental and the predicted data.

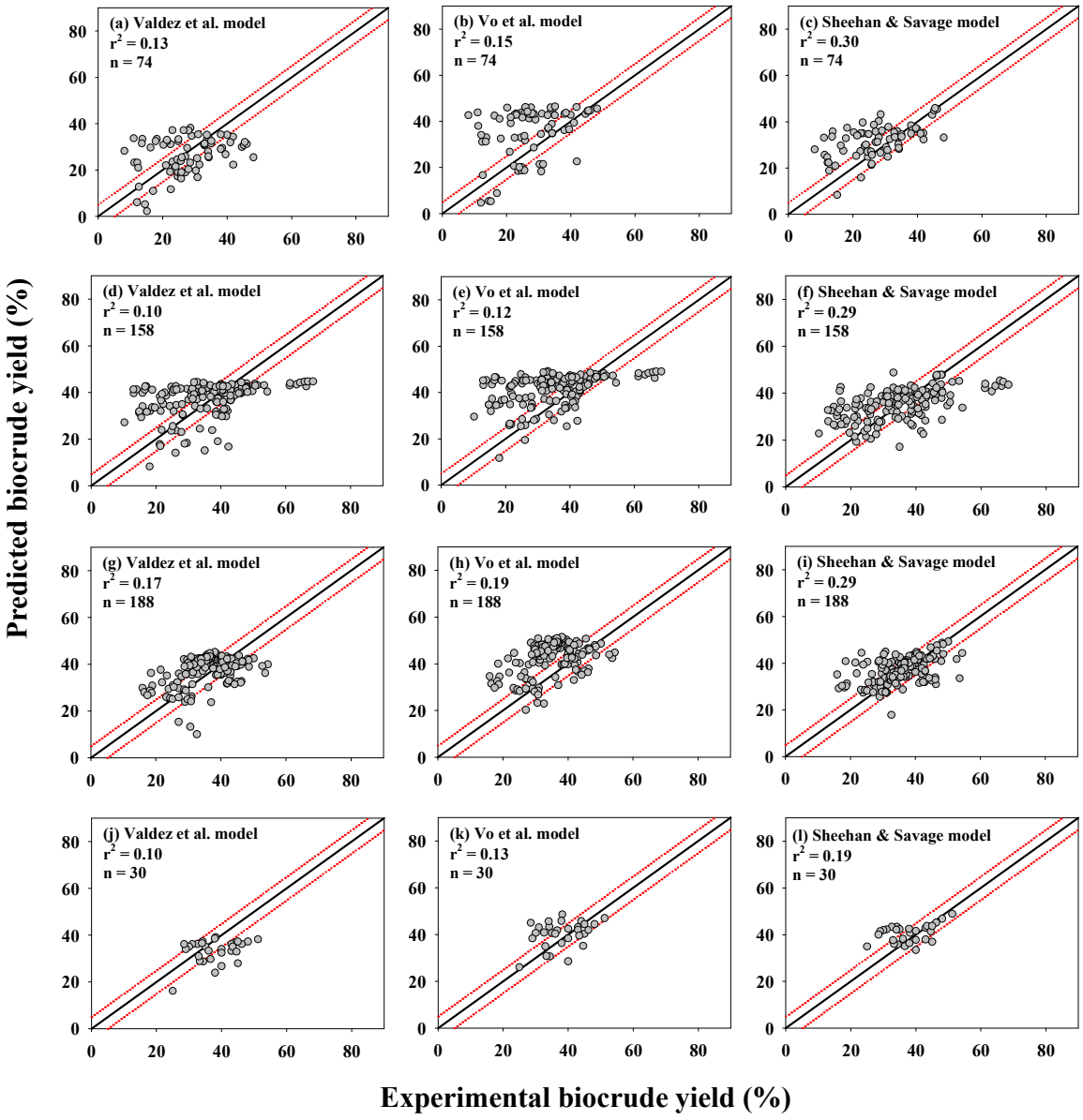

Figure 3-5. Effect of temperature and retention time on calculated biocrude yields using the model proposed in this study (Eq. 4) for hydrothermal liquefaction of four hypothetical biomasses. (a) – (d) at constant temperature, and (e) – (h) at constant retention time. Biomass 1: 10 % lipids, 60 % proteins and 25 % carbohydrates. Biomass 2: 35 % of each lipids and proteins and 25 % carbohydrates. Biomass 3: 60 % lipids, 10 % proteins and 25 % carbohydrates. Biomass 4: 60 % carbohydrates and 17.5 % of each lipids and proteins.

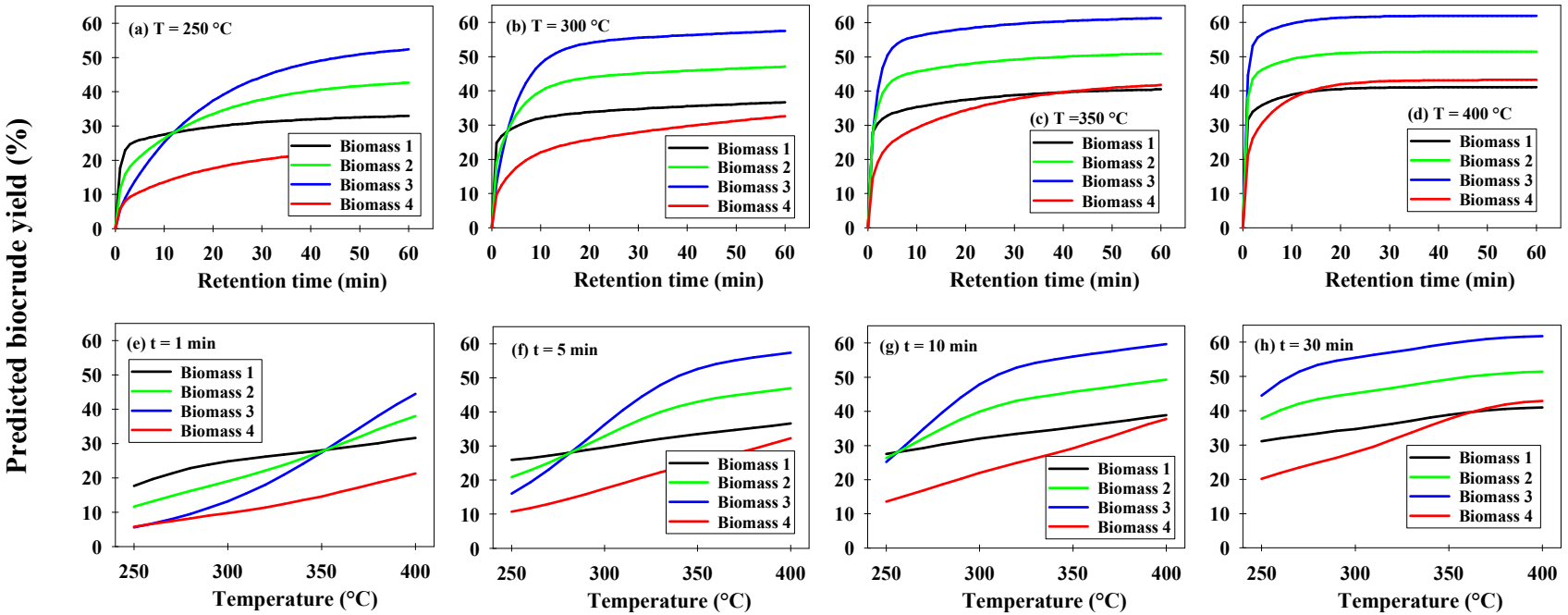

Figure 3-6. Comparison of yield predictions obtained by kinetic models from this study at different HTL temperatures: (a) 250 °C, (b) 300 °C, (c) 350 °C and (d) 400 °C. The continuous black line represents an exact match between the model and the experimental data. The red dotted lines represent a SD of ± 5 %. The blue dashed lines represent a SD of ± 10 %. The r^2 explains the correlation between the experimental and the predicted data.

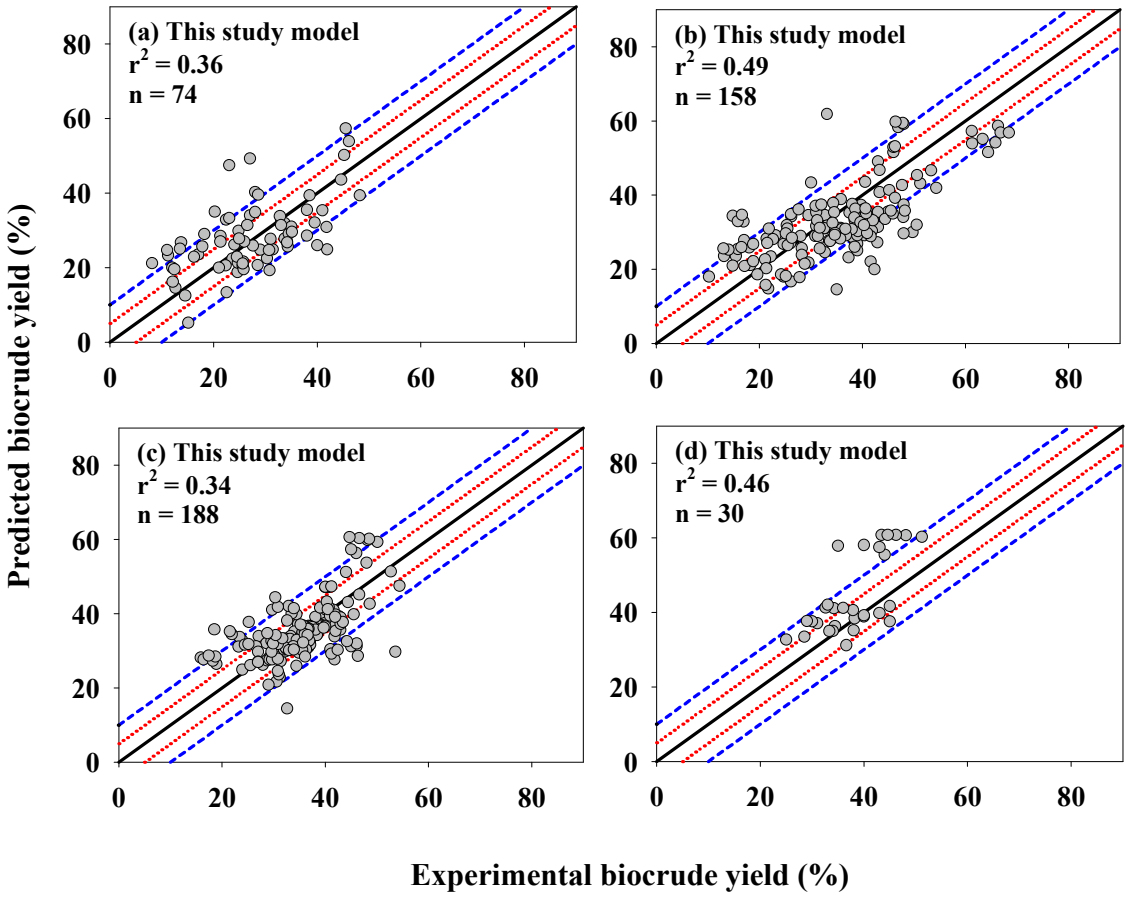

.

4. Quality-predictive models of biocrude from hydrothermal liquefaction of algae

4.1 Abstract

The effect of reaction temperature, retention time and elementary composition of the biomass was evaluated on the quality of the algae biocrude and used to propose a new quantitative model for the calculation of the elemental composition of this biocrude. The model provided information on the behavior of the reaction temperature and retention time in the carbon, nitrogen, and oxygen content of the algae biocrude. The new model was tested with more than 400 experimental data published over a wide range of temperatures (200–400 °C), retention times (0–120 min) and biomass elemental composition (30–70 % carbon, 1 –13 % nitrogen, 8–55 % oxygen, dry ash free). The new model was successful in more than 85 % for predicting the elemental composition of the macroalgae biocrude. The prediction capacity of the carbon, nitrogen, and oxygen content in the microalgae biocrude was between 53 and 81 %.

Keywords: Elemental Composition; Multivariable Regression; Microalgae; Macroalgae.

4.2 Introduction

Biofuel is a term used to identify solid, liquid or gaseous fuels obtained from biomass [1]. Microalgae (microscopic photosynthetic organism) have been used as raw material to produce fuels, such as biodiesel and biocrude, given the efficiency and versatility of their culture [13,110]. In comparison, macroalgae are multicellular organisms that have plant-like characteristics. Macroalgae are used to produce biofuels such as bioethanol and biocrude, due to their composition (mainly carbohydrates) and their easy harvesting [111,112]. Hydrothermal liquefaction (HTL) transforms biomass into biocrude by contact with water at severe conditions of temperature (200–400 °C) and pressure (10–20 MPa) [11].

The biocrude of algae is a liquid mixture of different organic compounds, like petroleum. The obtained biocrude has a Higher Heating Value (HHV), between 19 and 40 $MJ \cdot kg^{-1}$, and its yield varies between 15 and 60 % of the initial dry biomass. The remainder is gas, solid or water-soluble products. Both yield and quality of the biocrude depend largely on the reaction conditions (reaction temperature and retention time) and the characteristics of the raw material (type, species and chemical composition) [12,44].

Like petroleum, the quality of the biocrude can be expressed based on characteristics such as elemental composition, HHV, viscosity, API gravity, among others. These characteristics affect the storage, transport and application of biocrude as source of fuel [93,113]. For example, the biocrude has a higher content of nitrogen (up to 7 %) and oxygen (up to 19 %), compared to petroleum. The oxygen content in the biocrude reduces HHV [81] and nitrogen can form NO_2 compounds during combustion [91]. Therefore, the use of additional stages to upgrade biocrude (catalytic hydrotreatment) is necessary [77,78]. Both the yield and quality of the biocrude are important when scaling and designing the HTL process.

For the design and scaling of HTL process, mathematical equations are needed to relate the characteristics of the biomass and reaction conditions with the yield and quality of the biocrude. The main mathematical models for predicting biocrude yield are component additivity model [18,59,73,80,102] and kinetic model [19,85,106,107]. These models have as variables the composition of the biomass, the reaction temperature and/or the retention time, and they have shown acceptable success in predicting biocrude yield [114].

Several models have been proposed to predict the quality of the biocrude and have focused mainly on predicting the elementary composition and HHV. In general terms, those models are linear and depend on the elemental composition or protein content of the biomass. Leow et al. [59] performed HTL at 300 °C and 30 min to several batches of the microalga *Nannochloropsis oculata* with a wide range of compositions (23–59 % lipids, 58–17 % protein, 12–22 % carbohydrates) and a defatted batch (0 % lipids, 75 % protein, 19 % carbohydrates). The authors reported that there is a strong relationship between the profiles of the fatty acids of both, the biocrude and the biomass, and proposed a model to calculate a number of characteristics of the biocrude (carbon, oxygen, hydrogen, HHV, boiling point) from the fatty acids present in the microalgae. The nitrogen content in the biocrude was calculated from the protein content in the biomass. Hietala et al. [74] proposed different

linear multiple regression models for the calculation of the elemental composition of biocrude using the data obtained from the HTL of mixed microalgae at 350 °C and 20 min.

The mentioned models have several limitations. On the one hand, they only apply to a specific reaction temperature and retention time. On the other hand, they require additional experimental information, such as the fatty acid profile or, at least, the fatty acid attributes (saturated, mono-unsaturated, poly-unsaturated), which severely restricts their applicability, since that information is not readily available in algae HTL-related published literature.

From HTL, Li et al. [73] obtained data at 300 °C and 30 min for 24 microalgae biomasses of different chemical compositions. The authors proposed a Multiphase Component Additivity model in which the elemental composition of the biocrude was correlated with the average oxidation state of the raw material carbon. More recently, Lu et al. [103] performed the HTL of pure compounds and their binary, ternary, quaternary and quinary mixtures for lipids, proteins and carbohydrates (soybean oil, soy protein, cellulose, xylose and lignin) at 350 °C for 30 min. Based on the results of the individual compounds and their binary mixtures, they proposed a new model to predict the content of carbon, hydrogen and nitrogen of the HTL biocrude. In both cases, the prediction level of the models has not been thoroughly tested.

The parameters of the four models previously described have been calculated following different methodologies, but all of them have the characteristics of the raw material as independent variables. These models only apply to a specific set of reaction temperature and retention time. Therefore, every model coefficient must be experimentally determined if the reaction conditions of interest deviate from the original set. Likewise, these models have only been developed to predict the elementary composition of biocrude from microalgae, but not from macroalgae. Due to the large difference existing between the chemical compositions of these two biomasses, it is deemed appropriate to develop models that can be used to determine the quality of the macroalgae biocrude as well.

Therefore, the objective of this article is to provide an analysis of the main reaction conditions of HTL on the elemental composition of the biocrude of algae. From the analysis, a multivariable regression model is proposed that includes as independent variables the reaction temperature, retention time and biomass composition for the calculation of the biocrude quality from both macroalgae and microalgae.

4.3 Materials and methods

4.3.1 Data

Data for the analysis of the quality of the biocrude of algae were obtained from 84 published articles, containing 59 data sets for macroalgae biocrude (Table C 1) and 404 data sets for microalgae biocrude (Table C 2). The reaction temperature, retention time and the elementary composition of the biomass were the variables of interest in the analysis of the quality of algae biocrude. The selected articles included HTL reactions carried out with real algae biomass in batches, without catalyst nor solvent, at a wide range of reaction temperatures (200–400 °C), retention times (0–120 min), atmospheres (nitrogen, helium, air or unspecified) and biomass elemental composition (30.7–64.0 % carbon, 4.3–9.9 % hydrogen, 8.8–55.0 % oxygen, 1.0–12.6 % nitrogen and 0.0–7.1 % sulfur). Other variables such as the initial total solids, heating rate, type of separation solvent, initial pressure, or reactor type, were not considered in the analysis of the biocrude quality. The elementary composition was used as an indicator of the quality of the biocrude.

4.3.2 Multivariable regression

For the calculation of the content of carbon, nitrogen, hydrogen and oxygen in the algae biocrude ($X_{i,biocrude}$), a second-order multivariable regression model (Equation 4-1) was proposed, which is analogous to a Response Surface Model without interactions between the factors. The regression model includes the normalized variables: reaction temperature (T′), retention time (tr′) and elementary composition of biomass ($X_i'_{,biomass}$). The subscript i refers to the element of interest (carbon, nitrogen, hydrogen or oxygen). The normalization of the variables was carried out according to Equation 4-2, where Y is the variable of interest (reaction temperature, retention time or elemental composition in biomass). The maximum and minimum values for the normalization of the variables are shown in Table 4-1:

$$X_{i,Biocrude}\,(\%) = a_{0i} + a_{1i}T' + a_{2i}T'^{2} + a_{3i}t_r' + a_{4i}t_r'^{2} + a_{5i}X_{i,Biomass}' + a_{6i}X_{i,Biomass}'^{2}, \quad (4\text{-}1)$$

$$Y' = (Y - Y_{min})/(Y_{max} - Y_{min}). \quad (4\text{-}2)$$

For the multiple regression analysis, the built-in Microsoft Excel Regression Analysis Toolbox® was used. The parameters of the elemental composition models of the algae biocrude were estimated from the multiple regression analysis that involved 286 data sets obtained from 58 articles published between 2010 and 2017 (model calibration point, Table C 1 and Table C 2). 177 data sets from 26 articles published between 2017 and 2019 were used to validate the elementary composition models (validation point, Table C 1 and Table C 2).

4.3.3 Data trend analysis

The symmetry and dispersion of the data collected from the elemental composition of biomass and biocrude were analyzed based on the calculation of the average, median, maximum, minimum and percentiles (5^{th}, 10^{th}, 25^{th}, 75^{th}, 90^{th} and 95^{th}) (Table C 3). The graphical representation of these data is shown in a box plot.

The influence of the main reaction conditions on the elemental composition of the algae biocrude was analyzed by grouping data into a series of subsets. Each subset had in common the same value for a variable (reaction temperature, retention time or biomass elementary composition), independently of the value taken by the other reaction variables, as described in Figure C 1a. Each subset was named sequentially (a, b, c, ...) (Table C 1 and Table C 2) and its experimental average was plotted to inquiry for a trend. Similarly, the trend of the data calculated by the proposed models of elementary composition was analyzed by performing a second-order regression in the calculated averages of every subset, as described in Figure C 1b.

4.4 Results and discussion

4.4.1 Multivariable regression analysis

Table 4-2 shows the parameters of Equation 4-1 for the calculation of the carbon, nitrogen, and oxygen content in the macroalgae and microalgae biocrude. The analysis of the 463 data sets (Table C 1 and Table C 2) revealed that the elemental composition of micro- and macroalgae, as well as the corresponding derived biocrudes, ranges significantly, probably due to the characteristics of every specie, as well as culture and HTL conditions. The average empirical formula of macroalgae and microalgae biomass can be expressed as $CH_{1.90}N_{0.09}O_{0.72}S_{0.02}$ and $CH_{1.72}N_{0.13}O_{0.42}S_{0.01}$, respectively.

Likewise, the average empirical formula of biocrude from macroalgae and microalgae was $CH_{1.34}N_{0.06}O_{0.11}S_{0.001}$ and $CH_{1.58}N_{0.06}O_{0.13}S_{0.002}$, respectively. In order to analyze the results and understand the influence of every variable on the elemental composition of the biocrude, each element will be discussed separately.

4.4.2 Carbon (C)

Carbon content in the biocrude contributes to a higher value of HHV, as indicated by the positive coefficient in Equation 4-3, proposed by Channiwala & Parikh [81]. Figure 4-1a shows the symmetry and dispersion of the data corresponding to the carbon content in the biomass and in the biocrude for both types of algae. The dispersion of carbon data in the biomass is attributed to the type, species, and culture conditions of the algae, while the dispersion of data in the biocrude is due to the reaction conditions and biomass characteristics. The carbon content ranges between 67 and 77 % in the microalgae biocrude, and between 71 and 80 % in macroalgae biocrude. In general terms, the carbon in the biocrude increases between 24–58 %, with respect to the initial biomass (Figure 4-1a):

$$\mathrm{HHV}\ (\mathrm{MJ}\cdot\mathrm{kg}^{-1}) = 0.3491\mathrm{C}(\%) + 1.1783\mathrm{H}(\%) + 0.1005\mathrm{S}(\%) - 0.1034\mathrm{O}(\%) - 0.0151\mathrm{N}(\%) - 0.0211\mathrm{A}(\%). \quad (4\text{-}3)$$

The reaction temperature and retention time affect the carbon content in the biocrude. When the temperature rises from 200 to 400 °C, the C content increases by 7 % for microalgae biocrude and by 10 % for macroalgae biocrude (Figure 4-1b). According to the trend, a higher carbon content in the biocrude could be expected as the reaction temperature increases. The prediction capacity of the regression model seems satisfactory for the calculation of carbon in the algae biocrude with respect to the reaction temperature. The average of the data predicted by the model shows the same trend as the average of the experimental data for each temperature. However, at low temperatures (~200°C), the model overestimates the carbon content in the microalgae biocrude (Figure 4-1b).

Regarding retention time, the C content in the macroalgae biocrude increases up to 40 min, after which (between 40–90 min) the carbon percentage decreases by up to 6 %. The carbon content in the microalgae biocrude increases from 67 % to 73 % for retention times between 0 and 20 min. At retention times greater than 20 min, the carbon content remains relatively constant. The model also overestimates the carbon content in the microalgae biocrude for retention times between 0 and

5 min. In the range 5–90 min, the model predicts the carbon content in the algae biocrude within 1 % of the experimental value (Figure 4-1c).

The carbon content in the original biomass also has a significant effect on the carbon content of the biocrude. The increase in the carbon content in biomass has a positive influence on the carbon content of the microalgae and macroalgae biocrude. As in the reaction temperature and retention time, the model is incapable of predicting carbon contents less than 70 % in the biocrude of microalgae (Figure 4-1d).

4.4.3 Nitrogen (N)

The content of N in microalgae and macroalgae biocrude varies in ranges between 1.6–7.9 % and 2.3–7.0 %, respectively (Figure 4-2a). An analysis of the reported experimental data (data not shown) allows to conclude that a significant part of the N present in the original algae (up to 74 % for microalgae and 64 % for macroalgae) is transferred to the biocrude during HTL. Compared to the nitrogen content of petroleum (<1.5 %) [90], the necessity of reducing the nitrogen content in the biocrude is evident, since this element would contribute to the formation of greenhouse gases (NO_X) during the eventual combustion of the fuel.

A rise in HTL temperature increases the nitrogen content in the biocrude up to 49%, when microalgae are used as raw material (Figure 4-2b). This behavior might be explained through the reaction scheme proposed by Gai et al. [68], where the temperature favors the reaction of ammonia (found in the aqueous phase after the hydrolysis of the amino acids) with cyclic oxygenated compounds (carbohydrates derivatives), fatty acids and glycerol (lipid derivatives), to form cyclic nitrogenous compounds, indoles and long chain amides. This occurs because these compounds have larger molecular weight and are structurally more complex, hence they become insoluble in water and are transferred to the biocrude, increasing the amount of nitrogen in it. Unexpectedly, N in the macroalgae biocrude presents an opposite behavior: when the reaction temperature increases from 250 to 400 °C, the nitrogen content decreases by 47 % (Figure 4-2b).

With respect to the effect of retention time, during the first 5 min of HTL, the nitrogen content in the microalgae biocrude increases up to 6 %, due to the rapid breakdown of proteins [115,116]. Between 5 and 60 min, the nitrogen in the biocrude remains approximately constant. After 60 min, a slight decrease in the nitrogen content is observed. The nitrogen content in the macroalgae biocrude also

increases slightly with the reaction time, but at a slower rate, also reaching approximately 6 % nitrogen after 60 min (Figure 4-2c).

Proteins in the biomass of the algae appear to be the main type of N-containing compounds. Several studies show that the proteins may account for 41–87 %, and 38–69 % of the total N in the biomass of microalgae and macroalgae, respectively [117–119]. Therefore, it seems plausible that the proteins contribute the most as nitrogen source of the biocrude. In this case, the nitrogen content of biocrude could be significantly diminished by reducing the nitrogen content in the biomass (reduction of protein content), as supported by Figure 4-2d. This can be achieved by means of nutrient starvation during the culture [58,59,73] or the extraction of proteins in the biomass previous to HTL [57,120].

The regression model for predicting the nitrogen content in the microalgae biocrude has a notable deficiency at low reaction temperatures (<250 °C), retention times (<5 min) and nitrogen contents in the biomass (<2 %). Under these conditions, the model overestimates the nitrogen content in the biocrude between 29 and 43 % (Figure 4-2b and Figure 4-2c). The model for predicting the nitrogen content in macroalgae had an acceptable success in the range of reaction temperature and retention time analyzed. However, when the nitrogen content in macroalgae is greater than 6%, the model underestimates the nitrogen content in the biocrude by 11 % (Figure 4-2d).

4.4.4 Oxygen (O)

The oxygen content in the biocrude is the main responsible for the lower HHV of the biocrude compared to petroleum (Equation 4-3). It also affects the stability of the biocrude during storage and transport, limiting its use as a raw material for obtaining liquid fuels [77,78]. The reported oxygen content in microalgae and macroalgae biocrude varies within the ranges of 7.1–19 % and 6.1–16 %, respectively (Figure 4-3a). Generally, between 2–12 % and between 6–30 % of the oxygen present in macroalgae and microalgae is transferred to the biocrude, respectively (data not shown). However, compared to petroleum (0.1–4.5 %) [90], the O in the biocrude is considerably higher. It should be noted that, in most cases, oxygen is not measured directly, but its concentration in the biomass or in the biocrude is estimated by subtracting at 100 % the concentrations of all the other measured elements (C, H, N, S). Therefore, in some cases it can be overestimated if the content of ash and water in the biomass and biocrude has not been measured.

During HTL, an increase in reaction temperature from 200 to 400 °C considerably decreases the O content in the biocrude, from 20 to 10 % for microalgae and from 14 to 6 % for macroalgae (Figure 4-3b). A rise in retention time of up to 40 minutes also contributes to considerably reduce the O content in the biocrude (Figure 4-3c), supporting the hypothesis that the reaction time contributes significantly to improve the quality of the biocrude. An increase in the oxygen content in the biomass of microalgae and macroalgae increases the proportion of this element in the algae biocrude (Figure 4-3d).

In general, the proposed model for the calculation of the oxygen content in the algae biocrude successfully predicts the experimental data, except at temperatures below 250 °C or retention times between 0 and 10 min. Under such conditions, the oxygen content in the microalgae biocrude is greater than 15 %. The model also underestimates the oxygen content in the microalgae biocrude when the oxygen content in the biomass is greater than 40 %.

4.4.5 Hydrogen (H)

Like carbon, hydrogen in the biocrude favors HHV (Equation 4-3). The hydrogen content in microalgae and macroalgae biocrudes shows a relatively narrow distribution with 90 % of the data reported between 8.3–12 % and 7.2–10.8 %, respectively. Such values are about 21–27 % larger compared with the hydrogen content in the respective initial biomass (Figure 4-4a). In the case of microalgae, the hydrogen content remains almost constant in 9.2 % ± 1.2 %, regardless of the retention time and reaction temperature (Figure C 2a–2b). In consequence, the biomass hydrogen content becomes the sole parameter that correlates the increase in hydrogen content in the biocrude (Figure C 2c). Conversely, the hydrogen content in macroalgae biocrude appears to be influenced by all three variables (temperature, retention time, hydrogen content in the biomass), as shown in Figure C 2a–2c.

4.4.6 Sulfur (S)

Sulfur and nitrogen are vital macronutrients in the cultivation of algae and contribute to protein synthesis and cell growth [121]. However, the content of S in the biocrude participates in the formation of SO_X emissions during combustion and contribute to air pollution [44]. The sulfur content in the biocrude of microalgae and macroalgae is in the range of 0 (below the detection limit) and up to 2 % (Figure 4-4b). Analysis of published data shows that approximately 65 % of the sulfur

present in the biomass is transferred to the biocrude (data not shown). In comparison to light and heavy petroleum containing amounts of S between 0–2 % and 2–5 %, respectively [95], the algae biocrude obtained by HTL can be classified as light crude in terms of its sulfur content.

4.4.7 Accuracy analysis of the proposed model

To evaluate the ability of the model to predict the quality of biocrudes from micro and macroalgae, the predictive abilities were compared with new experimental data and the predictions of previously published models.

- **Validation of the model**

Figure 4-5 shows the comparison between the set of experimental validation values and those predicted by the regression model of this study for the elementary composition of algae biocrude. The regression model had a significant success in predicting the carbon, nitrogen, and oxygen contents of the macroalgae biocrude. In general terms, the model predicted 92 % and 90 % of the data related to carbon and oxygen contents, respectively, within the standard deviation (SD) zone of ± 3.0 % (Figure 4-5a and Figure 4-5b). The capacity of the model to predict the nitrogen and hydrogen content was 85 % and 75 %, respectively, within the SD zone of ± 1.0 % (Figure 4-5c and Figure 4-5d).

The ability of the model for predicting the elemental composition in the microalgae biocrude was less successful. The regression model for the carbon content in microalgae biocrude predicted 48 % and 75 % of the data within the SD zone ± 1.5 % and ± 3.0 %, respectively (Figure 4-5e). The main deficiency of the model to predict the carbon content in the microalgae biocrude occurs when the carbon content is less than 68 %. In this case, 93 % of the data are overestimated by the model with absolute errors between 3.5–14 %. Basically, C contents of less than 68 % were obtained at temperatures of 200–250 °C and retention times between 0 and 5 min. Likewise, the capacity of the model to predict oxygen content in the microalgae biocrude was 68 % within the SD zone of ± 3.0 %. The largest errors are evidenced when the oxygen content in the biocrude is less than 5 % or greater than 15 % (Figure 4-5f). The success of the regression model for the nitrogen content was 53 % within the SD zone of ± 1.0 %. However, there is a high dispersion of the data predicted by the model when the nitrogen content in the biocrude is less than 2 % (Figure 4-5g). The success of the

regression model to predict the hydrogen content was 81 %, though there is a dispersion higher than 12 % in the data for hydrogen content in biocrude (Figure 4-5h).

- **Comparison with other models**

Figure 4-6 shows the comparison of this model with those proposed by Li et al. [73] and Lu et al. [103] for the calculation of the carbon, nitrogen and hydrogen content in the microalgae biocrude. The model for the calculation of the carbon content proposed by Li et al. predicts 28 % of the experimental data within the SD zone of ±1.5 %, while 52 % of the data are within the SD zone of ± 3 %. These experimental data were obtained at a reaction temperature of 300 °C and retention time of 30 min. The multivariable regression model proposed in this study shows a significant improvement in the calculation of the carbon content of the microalgae biocrude because it predicts 76 % of the data within the SD zone of ± 3 % (Figure 4-6a).

The success of the Li et al. model to predict the nitrogen content of the biocrude was 61 %, while the success of the multivariable regression model was slightly lower (52 % of the data are within the SD zone of ± 1 %) (Figure 4-6b). The capacity to predict hydrogen content by the Li et al. model and by the multivariable regression model was similar, since both models predict more than 90 % of the experimental data within the SD zone of ± 1 % (91 % and 94 %, respectively) (Figure 4-6c). It should be noted that, although satisfactory results are obtained with the Li model, it is only applicable to a specific reaction condition (300 °C and 30 min), while the regression model can be used in a wider range of reaction conditions.

Lu et al. model for predicting the carbon, nitrogen and hydrogen content in microalgae biocrude used reaction conditions of 350 °C and 30 min, but was less successful when compared with the two models described above. Lu et al. model only predicted 27 % of the carbon data within the SD zone of ± 3 %, and 55 % for both nitrogen and hydrogen content data within the SD zone of ± 1 %. Under these reaction conditions (350 °C and 30 min), the success of the multivariable regression model to predict the carbon, nitrogen and hydrogen content in the microalgae biocrude was 64 %, 36 % and 81 %, respectively (Figure 4-6d – Figure 4-6f).

4.5 Conclusions

The extensive analysis of published data revealed clear trends. For example, the biocrude obtained from the HTL of algae contains a much higher content of nitrogen and oxygen than petroleum. An

increase in reaction temperature and retention time increased the carbon content in the algae biocrude. The hydrogen and sulfur contents in the algae biocrude remain approximately constant with reaction temperature and retention time.

With these trends, a new regression model was proposed to provide information about the influence of the reaction temperature, retention time and elementary composition of biomass on the elemental composition of the biocrude. The proposed regression model was built using 286 data sets and validated using 177 data sets. The proposed regression model showed an acceptable success in predicting the elemental composition of algae-derived biocrude, especially in the case of macroalgae biocrude, where its success rate was greater than 85 %. The proposed model has a larger set of variables (reaction temperature, retention time and elementary composition of the biomass) than previously published models. However, in the range of 200–250 °C and 0–5 min, the regression model had a notable deficiency to predict the elemental composition of the microalgae biocrude.

Table 4-1. Normalization of the variables for the proposed quality-predicting model of algae biocrude (Equation 4-1 and Equation 4-2).

Variable (Y)	Nomenclature	Levels	
		Y_{min}	Y_{max}
Temperature (°C)	T	200	400
Retention time (min)	tr	0.0	120
Carbon (%) [1]	X_C	30	70
Oxygen (%)	X_O	8.0	55
Nitrogen (%)	X_N	1.0	13
Hydrogen (%)	X_H	4.0	10

[1]daf: dry ash free

Table 4-2. Parameter values for the proposed model of the elemental composition of algae biocrude (Equation 4-1).

Type	Element	Parameter						
		a_0	a_1	a_2	a_3	a_4	a_5	a_6
Macroalgae	Carbon (%)[1]	64.22	7.83	5.03	26.65	-26.98	-3.32	2.41
	Oxygen (%)	21.54	-1.89	-8.61	-27.46	28.09	-3.82	2.81
	Nitrogen (%)	3.04	0.08	-1.68	-3.43	3.56	16.47	-15.38
	Hydrogen (%)	12.21	-9.65	8.90	8.95	-10.15	-8.66	6.28
Microalgae	Carbon (%)	62.19	3.89	0.65	6.96	-5.24	16.55	-6.90
	Oxygen (%)	15.33	-8.66	2.70	-9.00	7.24	-2.48	12.40
	Nitrogen (%)	0.26	6.31	-5.19	2.97	-5.31	6.61	-1.48
	Hydrogen (%)	8.38	-1.37	1.46	-0,85	2.26	-0.74	4.88

[1]daf: dry ash free

Figure 4-1. Carbon content in the biocrude via algae HTL. (a) Comparison between the algae C content and the C content of the biocrude. The box represents the range where 50 % of data are located. The black and red lines are the median and average, respectively. The error bars above and below the box indicate the 90th and 10th percentiles. The black points are the 5th and 95th percentiles. The gray band represents the petroleum composition range [90]. (b) Effect of reaction temperature on C content of biocrude. (c) Effect of retention time on C content of biocrude. (d) Effect of algae C content on C content of the biocrude. The dotted lines in (b)-(d) represent the C content predicted by the model.

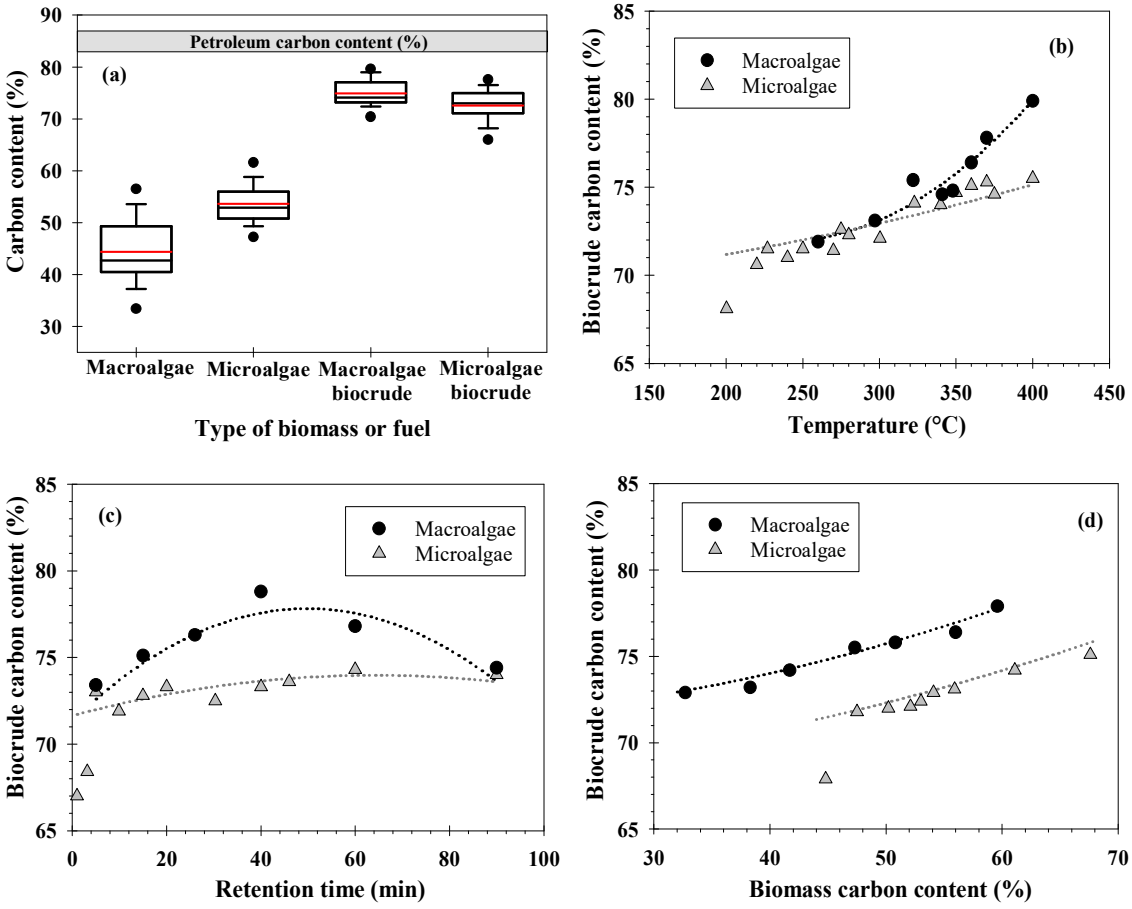

Figure 4-2. Nitrogen content in the biocrude via algae HTL. (a) Comparison between the N content of algae and N content of biocrude. The box represents the range where 50 % of data are located. The black and red lines are the median and average, respectively. The error bars above and below the box indicate the 90th and 10th percentiles. The black points are the 5th and 95th percentiles. The gray band represents the petroleum composition range [90]. (b) Effect of reaction temperature on N content of the biocrude. (c) Effect of retention time on N content of the biocrude and (d) effect of algae N content on N content of the biocrude. The dotted lines in (b)-(d) represent N content predicted by the model.

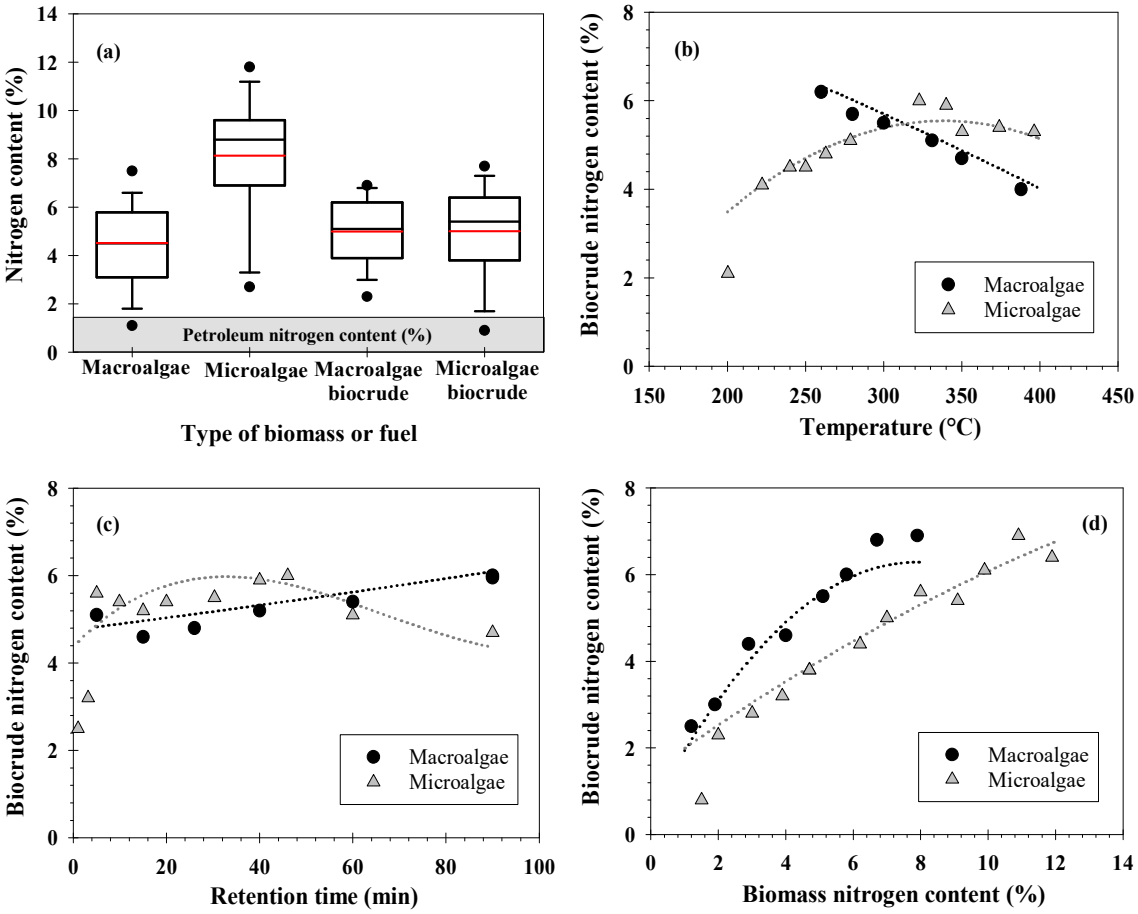

Figure 4-3. Oxygen content in the biocrude via algae HTL. (a) Comparison between the O content of algae and O content of biocrude. The box represents the range where 50 % of data are located. The black and red lines are the median and average, respectively. The error bars above and below the box indicate the 90th and 10th percentiles. The black points are the 5th and 95th percentiles. The gray band represents the petroleum composition range [90]. (b) Effect of reaction temperature on O content of biocrude. (c) Effect of retention time on O content of biocrude. (d) Effect of algae O content on O content of the biocrude. The dotted lines in (b)-(d) represent O content predicted by the model.

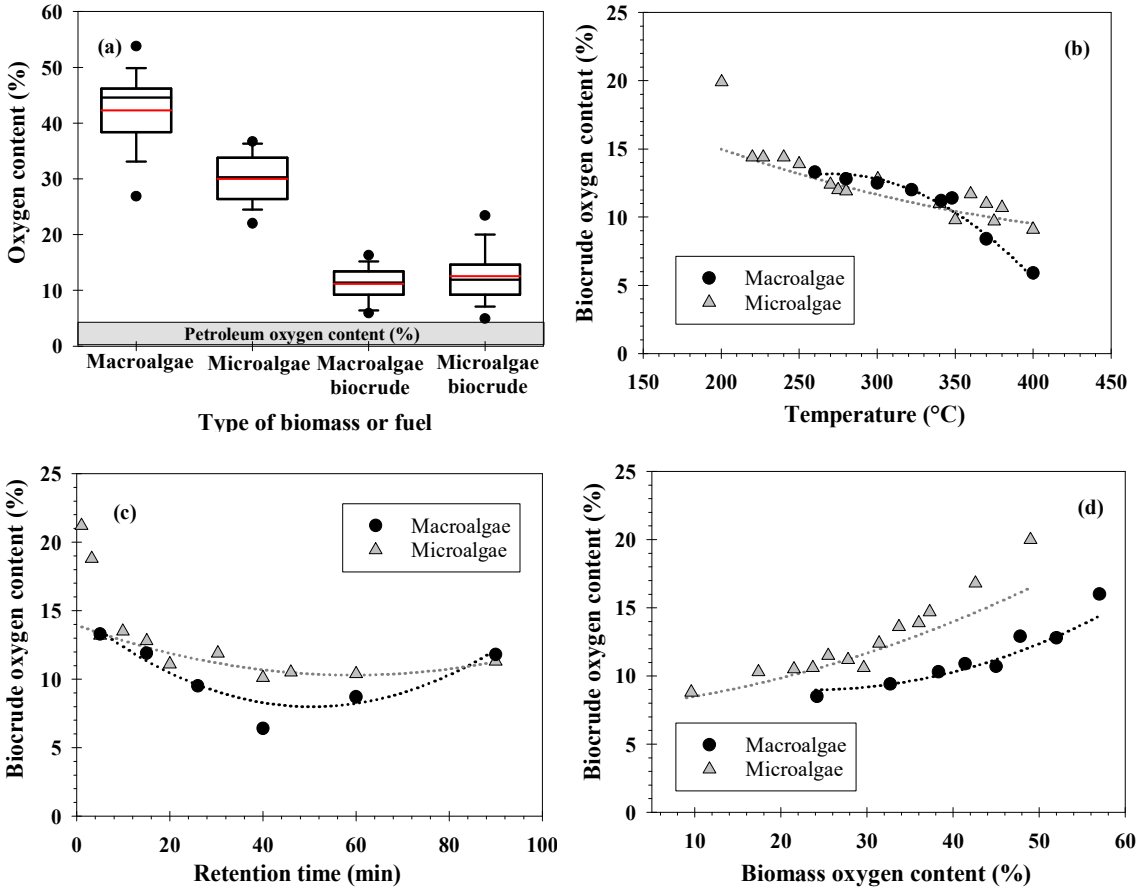

Figure 4-4. Hydrogen and sulfur content in the biocrude via algae HTL. (a) Comparison between the hydrogen content of algae and biocrude. (b) Comparison between the sulfur content of algae and biocrude. The box represents the range where 50 % of data are located. The black and red line are the median and average, respectively. The error bars above and below the box indicate the 90th and 10th percentiles. The black points are the 5th and 95th percentiles. The gray band represents the petroleum composition range [90].

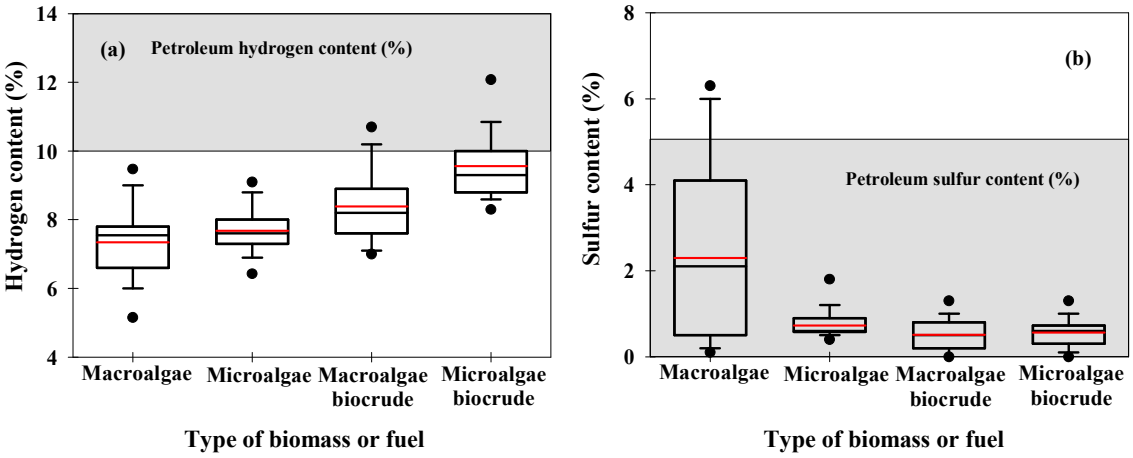

Figure 4-5. Prediction of the elemental composition in biocrude of: (a) – (d) macroalgae and (e) – (h) microalgae. Gray circle: calibration points for Equation 3-1. Red triangle: validation data points. The continuous black line represents an exact match between the model and the experimental data. In the graphs (a), (b), (e) and (f), the red dotted lines and the blue dashed lines represent a SD of ± 1.5 % and ± 3 %, respectively. In the graphs (c), (d), (g) and (h), the red dotted lines and the blue dashed lines represent a SD of ± 0.5 % and ± 1 %, respectively. The term r^2 explains the correlation between the experimental and the predicted data.

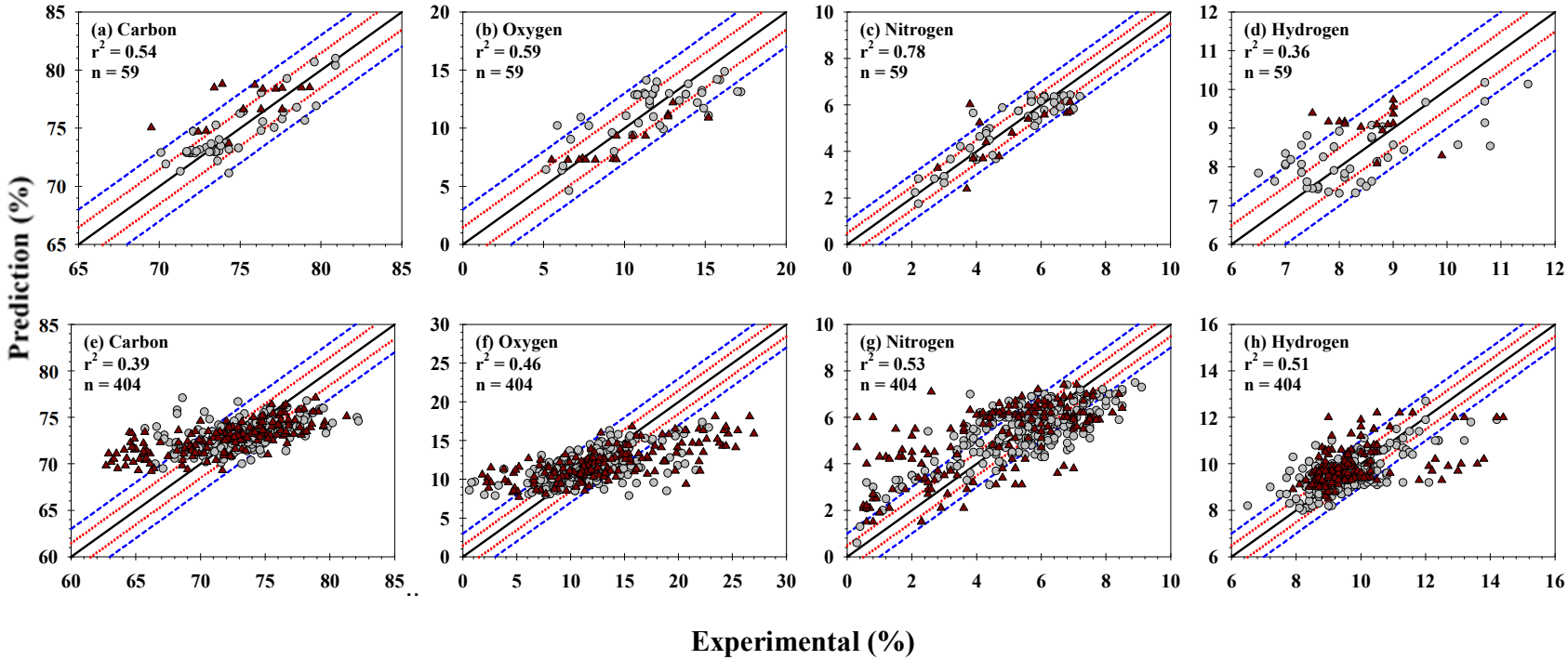

Figure 4-6. Prediction of carbon, nitrogen and hydrogen content in biocrude by: (a) – (c) Li et al. model at 300 °C and 30 min, and (d) – (f) Lu et al. model at 350°C and 30 min. Gray circles: points calculated by Li et al. model. Gray squares: points calculated by Lu et al. model. Red triangles: points calculated by the model proposed in this study. The continuous black line represents an exact match between the models and the experimental data. In the graphs (a) and (d), the red dotted lines and the blue dashed lines represent a SD of ± 1.5 % and ± 3 %, respectively. In the graphs (b), (c), (e) and (f), the red dotted lines and the blue dashed lines represent a SD of ± 0.5 % and ± 1 %, respectively. The term r^2 explains the correlation between the experimental and the predicted data.

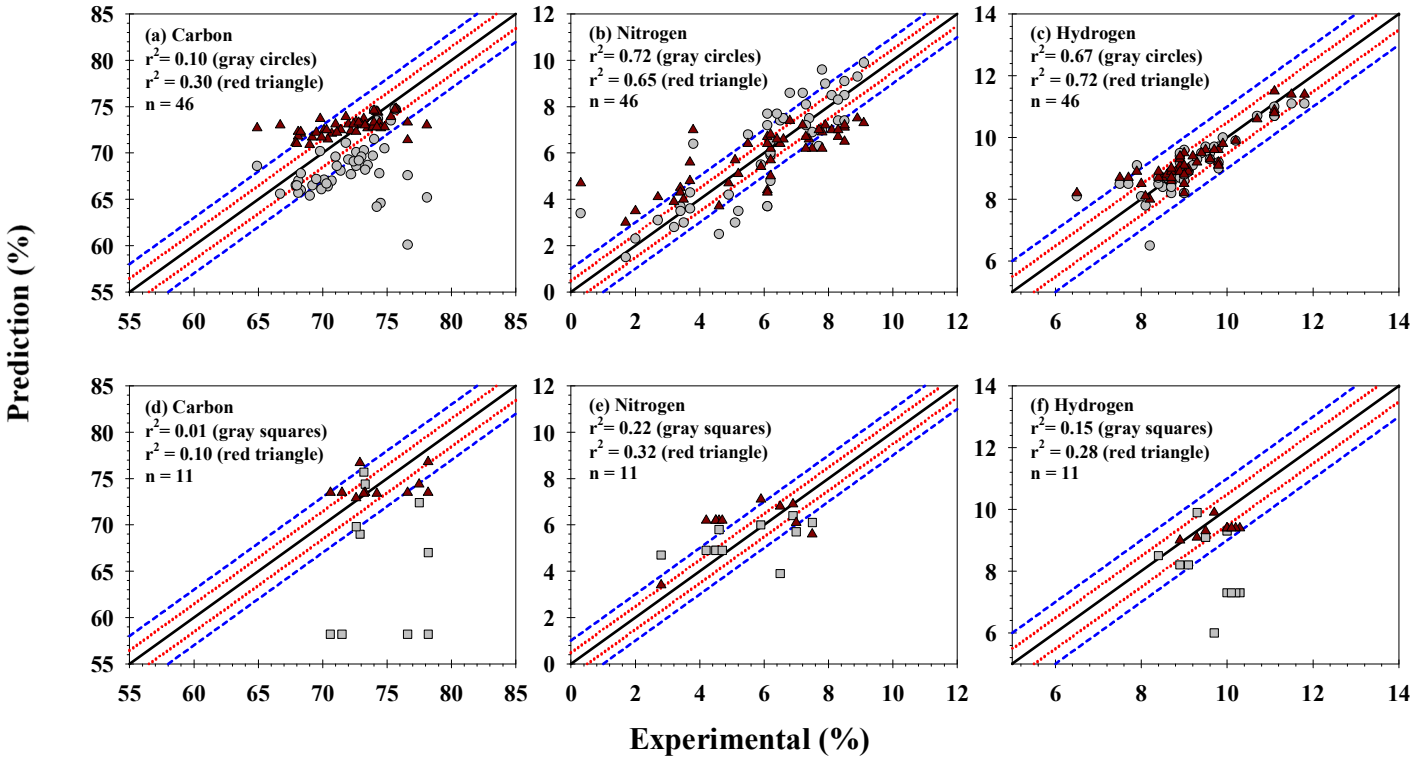

5. The storage stability of biocrude obtained by the hydrothermal liquefaction of microalgae

The content of this chapter is published in the Renewable Energy journal.

5.1 Abstract

Hydrothermal liquefaction is a promising technology that can produce biocrude oil from wet biomass. The biocrudes, while generally acknowledged to be more stable than pyrolysis oils, are still thought to degrade relatively quickly, which limits their applicability. In this investigation, the storage stability of biocrude produced from hydrothermal liquefaction of microalgae was systematically studied over 60 days, and the effect of the storage material, feedstock species, liquefaction temperature and storage temperature were assessed. Biocrudes obtained at 300 °C and 350 °C from the microalgae Spirulina and *Chlorella vulgaris* were stored at three temperatures: cold (4 °C), ambient (20 °C) and elevated temperatures (35 °C), over the two-month period. The dynamic viscosity, higher heating value, thermogravimetric analysis and elemental and chemical composition were assessed. The viscosity of the biocrudes only increased considerably at 35 °C. The reaction temperature and biomass type were also strong determining factors of the impact on biocrude stability. Biocrudes produced from *C. vulgaris* were more stable than the Spirulina, and the crudes formed at 350 °C were considerably less reactive than those produced at 300 °C. This demonstrates that biocrudes can be stored without substantial degradation, allowing a more flexible approach to upgrading to value products.

Keywords: Spirulina; *Chlorella*; Biocrude; HTL; Ageing; Polymerization.

5.2 Introduction

Advanced drop-in biofuels are an alternative to fossil-derived fuels, giving similar performance while reducing net emissions of CO_2 and other greenhouse gases (GHGs) [1]. Microalgae are a viable feedstock for biofuel production, some species have shown up to 50 times higher photosynthetic efficiencies compared to terrestrial plants, and do not require fertile soil for cultivation, posing no competition to other agricultural activities. However, the use of microalgae as a feedstock for "traditional" biofuels, such as biodiesel or bioethanol, is limited by poor economics and the extremely dilute nature of cultivated algae (0.1–2.5 $g \cdot L^{-1}$), requiring energy-intensive dewatering [2,3].

One promising conversion technology is hydrothermal liquefaction (HTL), which can convert wet microalgal biomass into a petroleum-like liquid (biocrude) with a heating value higher than the original raw material. The biocrude can then be converted into hydrocarbon fuels separately or alternatively co-refined with fossil fuels [17,122]. Yields vary depending on feedstock but are typically between 30 and 40 % with respect to the dry microalgal biomass. The HTL reaction occurs at conditions close to the critical point of water, with loadings between 5 and 20 % solids and reaction temperatures and pressures between 200–400 °C and 10–20 MPa, respectively. The physicochemical properties, yield and elemental and chemical composition of the biocrude are strongly dependent on the reaction conditions (HTL temperature and time) and the characteristics of the raw material [11,43].

The biocrude is a complex mixture of linear and branched hydrocarbons, nitrogenated and oxygenated cyclic compounds, fatty acids, esters, phenolic derivatives and alternative oxygenates [44]. The biocrude is similar to heavy oil, though has a higher nitrogen and oxygen content, up to 7 % and 19 %, respectively [11,43,44]. The dynamic viscosity typically falls between 35 and 6,200 mPa·s at 40 °C, whilst the densities generally range between 0.9 and 1.3 $gm \cdot L^{-1}$. HHV values of around 31–39 $MJ \cdot kg^{-1}$ are typical, depending on the carbon content [79,113,123–126].

In the large-scale production of microalgal biocrude, it is also necessary to consider its stability during transport and long-term storage, since thermal and storage stability studies of similar fuels report an increase in their viscosity, density and molecular weight, among other properties [127–130]. The change in the physicochemical properties of the biocrude during storage is known as aging, and is attributed to the polymerization, esterification and condensation reactions between the volatile

and oxygenated compounds found in biocrude [96,131,132]. One of the key requirements for HTL biocrudes is the potential to co-refine with fossil resources, which would potentially require longer-term storage and transport.

Several studies on the stability of bio-oil obtained from pyrolysis of lignocellulosic biomass have been published to date, in which two main evaluation methods are used: prolonged storage under controlled conditions, and accelerated aging at 80 or 90 °C. The main metrics for bio-oil stability are viscosity, water content, pH and total acid number (TAN) [127–130,133–138]. Whilst it has been noted that due to the lower levels of reactive oxygenated species, HTL biocrudes tend to be more stable than the corresponding pyrolysis bio-oils [113], no investigations have yet examined the long-term storage of biocrude from the HTL of microalgae, or the effect of the various parameters on the physical and chemical properties during storage. This is key to determining how biocrudes will fit into the existing transportation infrastructure. In this investigation, the stability of biocrude obtained by HTL of two separate phototrophic species (Spirulina and *C. vulgaris*) at 300 and 350 °C were examined. The biocrudes were stored at three temperatures: cold (4 °C), ambient (20 °C) and hot (35 °C), over 60 days. The dynamic viscosity, higher heating value (HHV) and thermogravimetric analysis (TGA) were measured as indicators of biocrude aging. The chemical and elemental composition of each biocrude was also analyzed at the beginning and at the end of the test period.

5.3 Material and methods

5.3.1 Materials

The cyanobacteria *Arthrospira platensis* (Spirulina) and microalgae *Chlorella vulgaris* were obtained from Naturya (Bath, United Kingdom). Feedstock chemical compositions were provided by the supplier. The ash and moisture content of the biomass was quantified using TGA; the mass loss between 20 and 105 °C was used to determine the sample moisture content and the percentage mass residual at the end of the TGA was taken to be the ash (Figure D 1). Quantification of the elemental analysis and HHV is described in section 4.3.4. The characterization of the two microalgae is shown in Table 5-1. All other reagents were purchased from Sigma Aldrich and used without further purification.

5.3.2 HTL reactions

Biocrude for the stability study was obtained at two different reaction temperatures (300 and 350 °C), using two different biomass types (Spirulina and *Chlorella vulgaris*). Liquefaction was carried out in a 50 mL batch reactor. The reactor consisted of a section of 1" stainless-steel tubing fitted with a pressure gauge, a thermocouple, a needle valve for venting gaseous products at the end of the reaction, and a pressure relief valve. The design of the reactor and reaction procedures have been previously reported [139]. In a typical reaction, the reactor was charged with 5 g (dry weight) of microalgae and 20 mL of deionized water (20% total initial solids). The reactor was then introduced into a vertical tubular furnace pre-heated to 550 °C and left until it reached the desired reaction temperature. HTL was performed at two temperatures 300 °C (10 MPa) and 350 °C (17 MPa), with an average heating speed of 13 and 10 °C·min^{-1}, respectively. Once the reaction temperature was reached, the reactor was immediately removed from the oven and allowed to cool to ambient temperature. A typical HTL thermal profile can be found in Figure D 2. After the reaction, gaseous products were released via the needle valve; aqueous phase products were subsequently decanted and filtered to separate them from the biocrude and solid products. The biocrude was recovered by washing the reactor and filter paper several times with chloroform. The chloroform-biocrude solution was filtered and the solvent was removed in vacuo at 35 °C.

5.3.3 Storage stability test

The storage stability test was performed on four types of biocrude: *C. vulgaris* biocrude obtained at 300 °C (Ch300) and 350 °C (Ch350), and Spirulina biocrude obtained at 300 °C (Sp300) and 350 °C (Sp350). Each sample of biocrude was stored for 60 days in a sealed glass vial, in the dark and at controlled temperatures: cold (4 °C), ambient (20 °C) and hot (35 °C). A further stability test was performed on the *Chlorella* biocrude obtained at 300 °C (Ch300m) and 350 °C (Ch350m): a stainless-steel strip (2.0 cm x 1.6 cm x 0.025 cm thickness) was added to the vial containing biocrude and stored for the same time interval at 20 °C. This was to establish whether biocrude aging was influenced by corrosion effects (which would affect the type of storage container used industrially). The stainless-steel plate was weighed before and after the test. The dynamic viscosity was primarily used to determine the stability of the biocrude. Elemental and chemical composition and HHV of the biocrude were recorded at the start (0 days) and end of the aging study (60 days). All measurements were made in duplicate. TGA was carried out during the first 15 and 20 days of the test.

5.3.4 Analytical methods

The dynamic viscosity, TGA, HHV and chemical and elemental composition of the biocrude were analyzed during the storage stability test. The dynamic viscosity of the biocrude was measured using a Bohlin C-VOR rheometer, using a CP 1°/20mm spindle, and a gap width of 0.07 mm. The value of shear stress was chosen empirically, depending on the expected viscosity of the biocrude, generally between 8 and 800 Pa. The viscosity measurements were made at a temperature of 40 °C and the viscosity index is defined in Equation 5-1, where V_1 and V_2 are the dynamic viscosities of fresh sample and aged sample, respectively:

$$\Delta \text{Viscosity} = V_2 - V_1 \,/\, V_1 . \quad (5\text{-}1)$$

TGA of the biocrude was performed on a Setaram TG-92 thermogravimetric analyzer. The sample was heated from ambient temperature to 800 °C at a heating rate of 10 °C·min^{-1}, with 1.5 bar nitrogen as carrier gas and 0.5 bar argon supplied as furnace gas. Elemental analysis of the biomass and biocrude were carried out externally in OEA Laboratories Limited (Cornwall, United Kingdom). HHV was calculated from elemental composition using equation proposed by Channiwala & Parikh [81].

Biocrude samples were analyzed by Gas Chromatography-Mass Spectrometry (GC–MS) (Agilent Technologies 7890A–5975C). An HP-5MS capillary column (30m x 250 mm x 0.25 mm) was used to separate the compounds. The biocrude samples were diluted in tetrahydrofuran (THF) to a concentration of1 mg·mL^{-1}. The injection volume was 1 mL, with a split ratio of 1:10 and an inlet temperature of 250 °C. The initial temperature of the column was held at 50 °C for 1 min, then ramped at 7.5 °C·min^{-1} to 290 °C, and held at 290 °C for 3 min. The major compounds were identified according to the National Institute of Standards and Technology (NIST11) spectral database.

5.4 Results and discussion

In this study we selected the two highest industrially produced photosynthetic micro-organisms for the liquefaction; the eukaryotic *Chlorella vulgaris* and prokaryotic Spirulina. The yields of biocrude and solid residue for HTL reactions of microalgae at different temperatures are shown in Table 5-2. The yields obtained are in line with those obtained in similar studies [18,34,73,140].

5.4.1 Dynamic viscosity

Biocrude yields were higher for *C. vulgaris* than Spirulina, increasing slightly with increasing temperature for both species. To assess the stability, the samples were stored at three different temperatures, 4 °C, chosen as the coldest reasonable refrigeration temperature, 20 °C, room temperature and 35 °C, realistically the highest temperature the crude would be exposed to over long periods of time if stored poorly in hot climates. The biocrude viscosity and behavior, however, were significantly different for the two species, and changed significantly during storage (Figure 5-1). All samples showed Newtonian behavior in the shear stress range 8–800 Pa. The initial viscosity of the biocrude decreased considerably with increasing reaction temperature for both microalgae. This behavior is similar to previous observations [34,48,141,142] and is presumably due to more extensive depolymerization of larger macromolecules into smaller, less viscous fragments at higher temperatures. In general, the viscosity of the biocrude increased with time and storage temperature, which suggests that condensation and polymerization reactions were occurring [96,132,143]. For both species, the biocrudes generated at lower temperatures polymerized to a much greater extent than the crudes formed at 350 °C. Microalgal biocrude obtained at 350 °C remained liquid throughout the entire 60 days storage period.

The Sp300 sample was considerably more viscous than the Ch300 sample. However, at 4 °C, both samples changed, on average, at a rate of 7 % day^{-1} (Figure 5-2a). The rate of repolymerization was heavily influenced by storage temperature. At 20 °C and 35 °C, the change in dynamic viscosity in Ch300 was 5 and 20 times higher than in the Sp300 sample, respectively (Figure 5-2c and Figure 5-2e). Sp300 solidified before the end of the test period, independent of the storage temperature.

At 4 °C, the dynamic viscosity of the Sp350 and Ch350 biocrudes remained unchanged during the first 10 days of storage. This demonstrates that biocrudes could potentially be stored and transported under temperature-controlled conditions if transportation times were relatively short. However, after 10 days, the viscosity of the samples increased linearly at a rate of approximately 10%·day^{-1}. After 35 days of storage, the viscosity increase rate of the Sp350 was 2.6 times higher compared to the change in viscosity of Ch350 (Figure 5-2b). At 20 °C, the viscosity of samples Ch350 and Sp350 do not show this lag time, and rather, start reacting immediately. The viscosity of Ch350 increased 3.7 times faster than the viscosity of Sp350 during the first 20 days. After this point, the viscosity increase rate of the Ch350 stabilized (9 %·day^{-1}), while the viscosity growth rate of the Sp350 sample

increased from 11 to 26 %·day^{-1}. At the end of the storage period, both biocrudes had a similar viscosity (Figure 5-2d).

At 35 °C, the viscosity of Sp350 and Ch350 increased at an average rate of 28 %·day^{-1} during the first 15 days. During the period be- tween 20 and 35 days, the viscosity for both samples stabilized to a degree. After this point the dynamic viscosity increased dramatically for both Sp350 and Ch350 samples, at an average rate of 70 and 43 %·day^{-1}, respectively (Figure 5-2f). Although it is difficult to make a direct comparison with literature due to the lack of information available on the stability of microalgal biocrude, Spirulina biocrude produced by Jena et al. showed a similarly rapid and linear increase in viscosity during the first 75 days of storage [113].

The effect of the storage material on the viscosity of the biocrude is shown in Figure 5-3. In general, the presence of metals did not have a significant effect on the viscosity of the *C. vulgaris* biocrude during storage at 20 °C. Likewise, there was no corrosion damage to the steel plate and its weight remained unchanged. A slight increase in viscosity for the samples stored with metal was observed at the start of the test, and once again at the end of the 60 days storage period. This behavior can be attributed to the fact that metals can act as a catalyst, accelerating biocrude aging. The biocrudes showed a similar behavior to those observed in a study by Garcìa-Pèrez et al. examining the effect of stainless steel and copper on the rheological characteristics of biocrude obtained by pyrolysis of wood residues, during accelerated aging [144].

5.4.2 Thermogravimetric analysis

To assess the impact of storage on the biocrude properties, the crudes were also examined by TGA. The thermogravimetric curves (TG) of the biocrudes Ch300 and Ch350 stored at 35 °C for 15 days are shown in Figure 5-4a and Figure 5-4b. Thermogravimetric weight loss in biocrudes is commonly divided into three stages: (1) evaporation of volatile compounds between 20 and 200 °C, (2) decomposition of intermediate compounds between 200 and 480 °C, and (3) formation of solid residues at 535 °C [138,145,146].

For the crude Ch300, over 10 % of the weight was lost prior to 200 °C for samples at the early stages of storage. These more volatile fractions were depleted slightly within the first 7 days of storage but disappeared entirely by day 9. This corresponds with the sharp increases in the viscosity. Over the entire storage period, the volatility of the sample increased slightly, suggesting that the volatiles react

with the alternative components and the molecular weight of the crude increases over the storage time. In the Ch350 sample, the loss of volatile compounds was lower, and as such, the viscosity increased substantially less. The residual mass fraction increased slightly for both biocrudes from 20 % to 24 %. The weight loss of the volatile fraction and the increase in the generation of solid residue in the biocrude during storage show the degree of aging of the biocrude, which can be attributed the volatile com- pounds, such as ketones, alcohols and aldehydes, phenol, furfural and their derivatives reacting to obtain higher molecular weight compounds [96,132,143].

Samples Ch300 and Ch350 stored at 4 °C and 20 °C showed similar behavior to that described above. At 20 °C, the solid residue increased by 3 % and 2 % for Ch300 and Ch350 samples, respectively. The level of volatile compounds decreased by 51 % in the Ch300 sample during 12 days of storage, whereas the volatile fraction remained unchanged in Ch350 (Figure 5-4c and Figure 5-4d). At 4 °C, the volatile fraction, and the solid residue in the Ch350 sample remained un- changed during 15 days of storage. The solid residue content of the Ch300 sample remained constant, and the volatile fraction only decreased by 25 % (Figure 5-4e and Figure 5-4f). The TG curves for Sp350 stored at 4, 20 and 35 °C are given in the supporting information (Figure D 3); where the volatile and solid fractions had changes like those shown in Ch350 during the first 15 days of storage.

5.4.3 Elemental composition and HHV

Generally, heteroatoms such as bound oxygen and nitrogen are responsible for the instability of biocrudes during storage and transport, since most nitrogenated and oxygenated compounds are comparatively more reactive [132]. Some studies have shown that a reduction in oxygen content makes the biocrude more stable during storage, in addition to improving other properties, such as viscosity and HHV [92,147].

Changes in elemental composition during storage of the microalgal biocrudes are shown in Table 5-3. In general, there was a slight increase in carbon content with storage time and temperature, as well as a small reduction in oxygen content in the biocrude. This suggests that condensation reactions are occurring and removing oxygen. The nitrogen and hydrogen content in the bio- crude remained relatively unchanged during storage. Although the elemental composition remained relatively stable with time and storage temperature, the structure of the compounds changed, evidenced by the increase in the viscosity of the biocrude (Section 5.4.4).

These results are comparable with lignocellulosic bio-oils, where the elemental composition of the bio-oils remained approximately unchanged during the first 2 months of storage [130,131,148]. However, Jo et al. reported that the oxygen content of biocrudes decreased significantly from 42 % to 27 %, and the carbon content increased from 42 % to 63 %, when the storage time was greater than 6 months [147]. This reduction of the oxygen content in biocrude can be attributed to condensation and esterification reactions that eliminate oxygen in the form of water, and the loss of volatile compounds by evaporation [132].

HHV of the microalgal biocrudes before and after storage is shown in Figure 5-5. The HHV of the fresh biocrude samples before commencing the stability test was (in descending order) Ch350 > Ch300 > Sp350 > Sp300; increasing the HTL processing temperature favored the deoxygenation and denitrogenation of biocrudes (Table 5-3). Comparing the HHV values before and after storage, HHV of Sp300 increased by 1 %, 2 % and 2.4 % when the sample was stored at 4 °C, 20 °C and 35 °C, respectively. Similarly, for Sp350 and Ch350, small but positive changes in HHV (0.1–4 %) were observed when storage temperature was increased. However, the opposite behavior was observed in the sample Ch300: HHV decreased with increasing storage temperature.

These small changes in the energy content of the biocrudes during storage are congruent with the changes in elemental composition, particularly the oxygen content. In general, HHV fluctuated by ± 4 % with respect to samples at the beginning of the aging period, demonstrating that HHV remains relatively stable over 2 months of storage. Since, the storage of the biocrude in the industry will occur in tanks built mainly of steel, it was possible to demonstrate that the presence of metals did not significantly affect the elemental composition and HHV of the Ch300m sample stored at 20 °C. Only a small decrease (4 %) in the HHV of the Ch350m sample was observed (Table 5-4). This suggests that storage in glass lined vessels will potentially not be necessary.

5.4.4 Chemical composition

The results of the GC-MS analysis for the samples Ch300 and Ch350 before and after storage are shown in Figure 5-6a and Figure 5-6b. GC–MS was used as a qualitative tool to demonstrate the changes in the main volatile components of the biocrude during storage. It is evident from the chromatograms of the two samples that HTL temperature had an impact on the chemical composition of the biocrude. The Ch350 sample contained a greater variety of volatile compounds than the Ch300

sample (Figure 5-6a and Figure 5-6b). This could be the reason for the significant difference between the viscosity of the two samples.

In both samples, a decrease in the overall number and area of the main peaks is observed with increasing storage temperature, which could be attributed to the formation of other compounds of higher molecular weight (polymerization) [96,131]. The peaks corresponding to oxygenated and nitrogenated compounds such as phenol, pyrazine, pyrrole, pyrimidine and indole and their derivatives (5–15 min), were significantly reduced with increasing storage temperature, especially in the Ch350 sample stored at 35 °C (Figure 5-6b). Likewise, a reduction was observed in the peaks detected between 21 and 23 min corresponding to fatty acid derivatives, such as esters, as well as some unsaturated hydrocarbons and amides. In general, increasing storage temperature caused the loss of many light components, corresponding to retention times between 5 and 30 min.

In the Ch350 biocrude, a significant reduction in volatile compounds was observed when the sample was stored at 20 °C and 35 °C, compared to sample stored at 4 °C, where only a slight variation of these compounds is observed, suggesting that cooling the biocrude can delay the polymerization reactions. The decrease in the level of compounds such as phenol (6.5 min), 4-methyl- phenol (8.4 min) and indole (13 min) indicate that they may be involved in polymerization reactions that can occur at temperatures as low as 20 °C [149].

These results suggest that aging of the microalgal biocrude could be due to the presence of phenolic, nitrogenated and unsaturated compounds, which continue to react during storage until they reach equilibrium [147,148]. Unlike biocrude obtained from lignocellulosic biomass, the biocrude produced from microalgae contains up to 8 times more nitrogen, so that other reactions involving nitrogenous species could occur, such as the polymerization of indoles [150]. These reactions involving nitrogenous species could be the reason that the increase in viscosity was 5 times faster, on average, in biocrude obtained from microalgae than bio-oil obtained by pyrolysis of lignocellulosic biomass [129,148,151].

Results obtained by GC-MS were consistent with the changes evidenced by macroscopic properties, such as viscosity. However, although the larger molecules generated by polymerization re- actions in the biocrude were expected to appear in the chromato- grams at higher retention times, these expected new peaks were not observed, as the compounds were probability too large or insufficiently

volatile to be detected by GC-MS. Similar results were observed for the Sp300 and Sp350 samples (Figure 5-6c and Figure 5-6d). The presence of steel during biocrude storage did not seem to affect the chemical composition of the biocrude. (Figure 5-6e and Figure 5-6f).

5.5 Conclusions

HTL processing temperature and biomass type were determining factors in the initial physicochemical characteristics of the biocrude. According to the type of biomass, HTL temperature and storage temperature, the stability of the biocrude was *Chlorella* > Spirulina, 350 °C > 300 °C and 4 °C > 20 °C > 35 °C, respectively. The viscosity of the Ch350 and Sp350 biocrudes stored at 4 °C did not show any significant change throughout the 60-day storage period. However, biocrude viscosity increased considerably when stored at 35 °C, especially for the Ch300 biocrude. The increase in the viscosity of the biocrude with storage time and temperature can be attributed to the loss of volatile compounds and the increase of the residual fraction, as demonstrated by TGA, suggesting that polymerization and esterification reactions were occurring between the biocrude compounds. The presence of stainless-steel strips did not affect the aging of the biocrude during storage at 20 °C for two months, suggesting that bio-crudes could be stored in steel vessels. The elemental composition and HHV of the biocrude changed slightly over the storage period for all storage temperatures. GC-MS analysis revealed that storage temperature had a significant influence on the reduction of volatile compounds in the biocrudes. Ultimately, biocrude upgrading is necessary to improve its long-term stability and displace traditional fossil-based fuels. However, this work demonstrates that, with careful handling, algal biocrudes are stable enough for storage and transportation and could be shipped from point of production to a traditional refinery or biorefinery for further upgrading

Table 5-1. Characterization of biomass in percentage by mass on dry basis (%).

Properties	**Spirulina**	***C. vulgaris***
Moisture (%)	5.2	3.4
Ash (%)	7.7	8.7
HHV ($MJ \cdot kg^{-1}$)	23.0	24.0
Elemental composition (%)		
C	49.7	51.4
H	7.2	7.4
O[1]	24.3	22.1
N	11.3	10.2
Chemical composition (%)[2]		
Lipids	1.1	2.3
Protein	70.2	61.8
Carbohydrates	19.3	26.7
Others	0.7	0.4

[1]by difference. [2]from supplier.

Table 5-2. Yield of biocrude and biochar of microalgae Spirulina and *C. vulgaris* in percent by mass on dry basis (%).

Microalgae	HTL Temperature (°C)	Biocrude (%)	Solid (%)
Spirulina	300	31.0 ± 1.6	10.0 ± 0.8
	350	36.2 ± 1.3	6.8 ± 1.2
C. vulgaris	300	39.6 ± 1.9	8.1 ± 0.8
	350	42.1 ± 1.5	5.5 ± 0.7

Table 5-3. Change in elemental composition during storage (0 and 60 days) of microalgae biocrude.

Biomass	HTL Temperature (°C)	Element	Composition (%)			
			Before storage	After storage		
				4 °C	20°C	35°C
Spirulina	300	C	67.2 ± 0.1	67.7 ± 0.1	68.6 ± 0.03	69.2 ± 0.03
		H	8.7 ± 0.03	8.8 ± 0.04	8.7 ± 0.03	8.6 ± 0.05
		O[1]	15.6 ± 0.03	15.0 ± 0.03	14.0 ± 0.03	14.0 ± 0.1
		N	8.4 ± 0.03	8.5 ± 0.03	8.7 ± 0.03	8.1 ± 0.03
	350	C	68.2 ± 0.05	69.4 ± 0.1	69.0 ± 0.2	70.0 ± 0.1
		H	8.7 ± 0.05	8.9 ± 0.04	8.4 ± 0.1	8.9 ± 0.04
		O[1]	16.1 ± 0.03	14.4 ± 0.04	15.5 ± 0.2	14.0 ± 0.03
		N	7.0 ± 0.04	7.4 ± 0.03	7.0 ± 0.03	7.2 ± 0.03
C. vulgaris	300	C	68.8 ± 0.1	66.9 ± 0.2	67.8 ± 0.1	67.5 ± 0.03
		H	8.9 ± 0.03	8.6 ± 0.1	8.7 ± 0.03	8.7 ± 0.1
		O[1]	15.1 ± 0.1	17.2 ± 0.3	15.7 ± 0.1	16.6 ± 0.03
		N	7.2 ± 0.1	7.4 ± 0.03	7.9 ±0.03	7.3 ± 0.03
	350	C	70.8 ± 0.1	72.3 ± 0.2	72.8 ± 0.03	73.3 ± 0.03
		H	9.0 ± 0.03	9.3 ± 0.03	9.1 ± 0.03	9.1 ± 0.2
		O[1]	13.6 ± 0.03	11.7 ± 0.2	11.5 ± 0.03	10.8 ± 0.03
		N	6.6 ± 0.05	6.6 ± 0.03	6.7 ± 0.03	6.8 ± 0.03

[1]by difference.

Table 5-4. Elemental composition (%) and HHV ($MJ \cdot kg^{-1}$) of biocrude from *C. vulgaris* stored with and without metal.

HTL temperature (°C)	Characteristic	Before storage	After storage at 20°C	
			Without metal	With metal
300	C	68.8 ± 0.1	67.8 ± 0.1	69.5 ± 0.1
	H	8.9 ± 0.03	8.7 ± 0.03	8.7 ± 0.04
	O[1]	15.1 ± 0.1	15.7 ± 0.1	14.7 ± 0.04
	N	7.2 ± 0.1	7.9 ± 0.03	7.1 ± 0.03
	HHV	32.8 ± 0.03	32.1 ± 0.05	32.9 ± 0.03
350	C	70.8 ± 0.1	72.8 ± 0.03	69.2 ± 0.2
	H	9.0 ± 0.03	9.1 ± 0.03	8.5 ± 0.03
	O[1]	13.6 ± 0.03	11.5 ± 0.03	15.3 ± 0.03
	N	6.6 ± 0.05	6.7 ± 0.03	6.9 ± 0.03
	HHV	33.8 ± 0.03	34.8 ± 0.05	32.5 ± 0.1

[1]by difference.

Figure 5-1. Change of dynamic viscosity of biocrude of microalgae: (a) Ch300, (b) Ch350, (c) Sp300, and (d) Sp350. The biocrude was stored at 4 °C (square), 20 °C (triangle) and 35 °C (circle). Error bars indicate standard deviation.

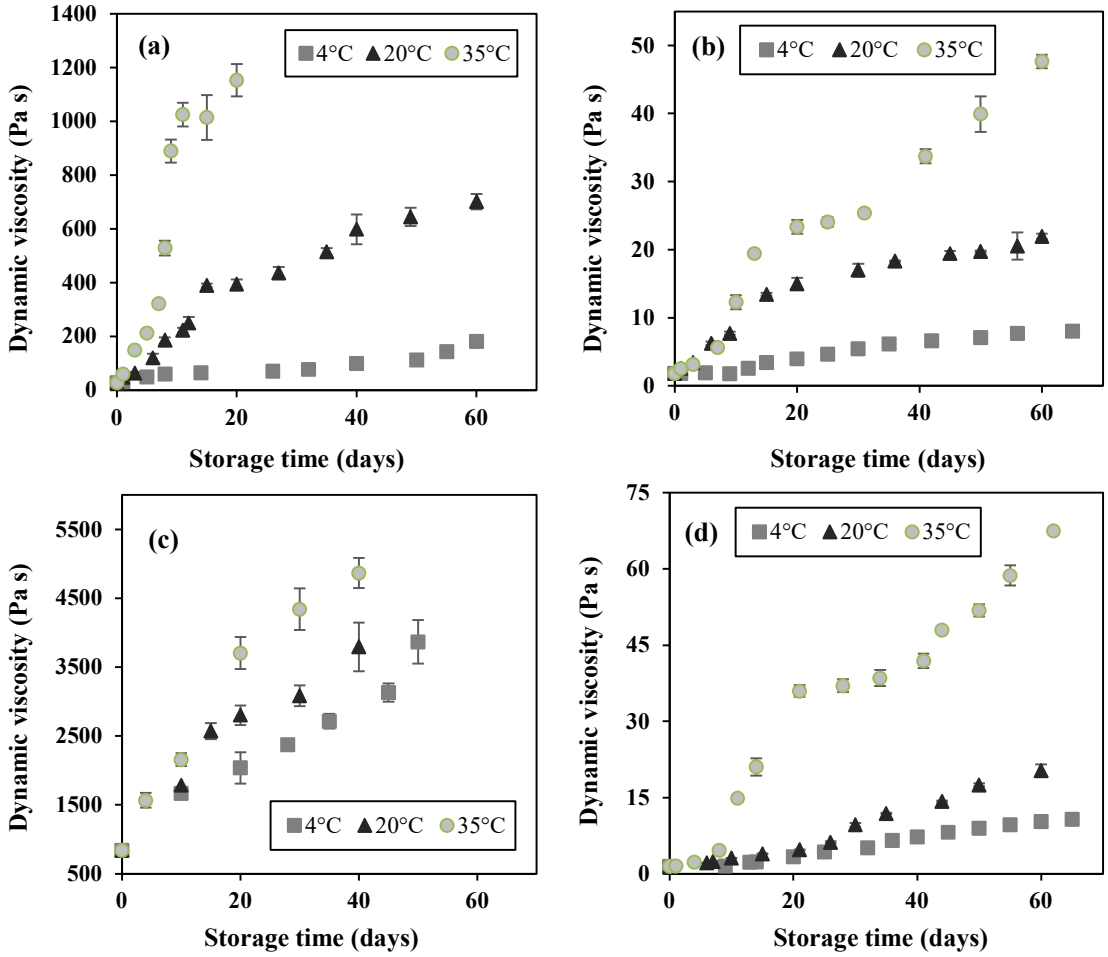

Figure 5-2. Viscosity index of biocrude of microalgae: (a) and (b) e biocrude stored at 4 °C, (c) and (d) e biocrude stored at 20 °C, (e) and (f) e biocrude stored at 35 °C. Error bars indicate standard deviation.

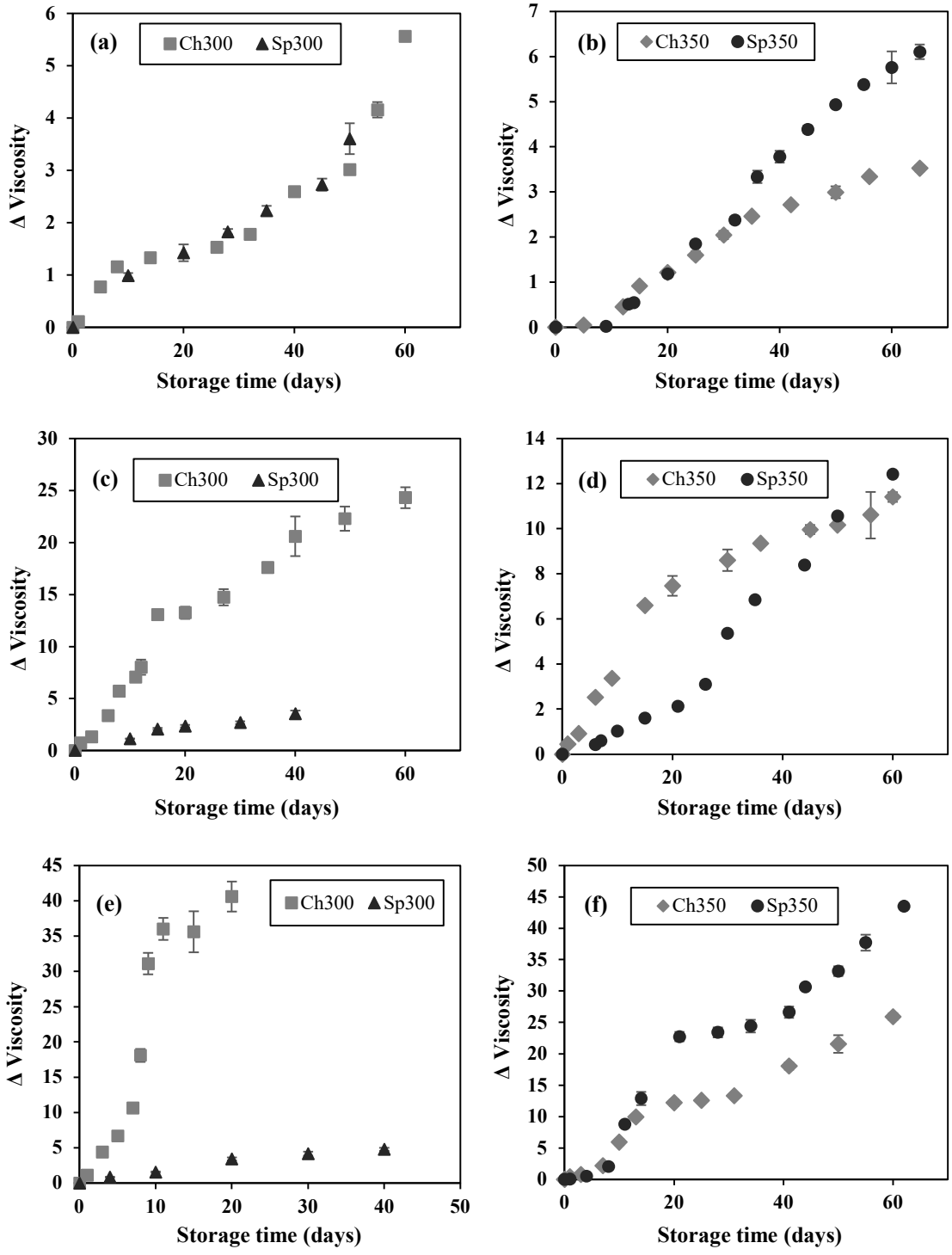

Figure 5-3. Change of dynamic viscosity of biocrude of *C. vulgaris* obtained to different HTL temperature (a) 300 °C, and (b) 350 °C with (circle) and without (triangle) contact with a stainless-steel plate. The biocrude was stored at 20 °C. Error bars indicate standard deviation.

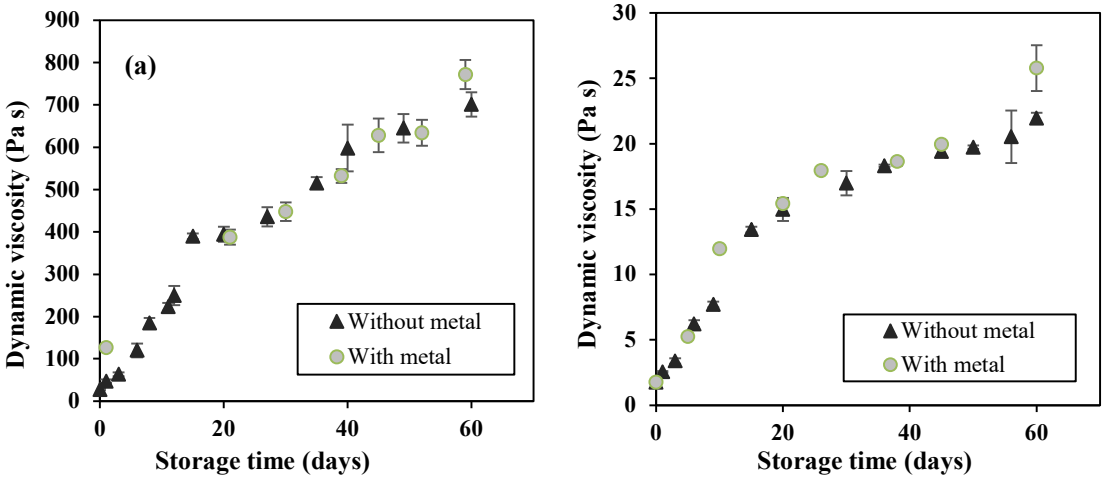

Figure 5-4. Thermogravimetric analysis (TGA) of *C. vulgaris* biocrude stored for several days. (a) Ch300 stored at 35 °C, (b) Ch350 stored at 35 °C, (c) Ch300 stored at 20 °C, (d) Ch350 stored at 20 °C, (e) Ch300 stored at 4 °C, and (f) Ch350 stored at 4 °C.

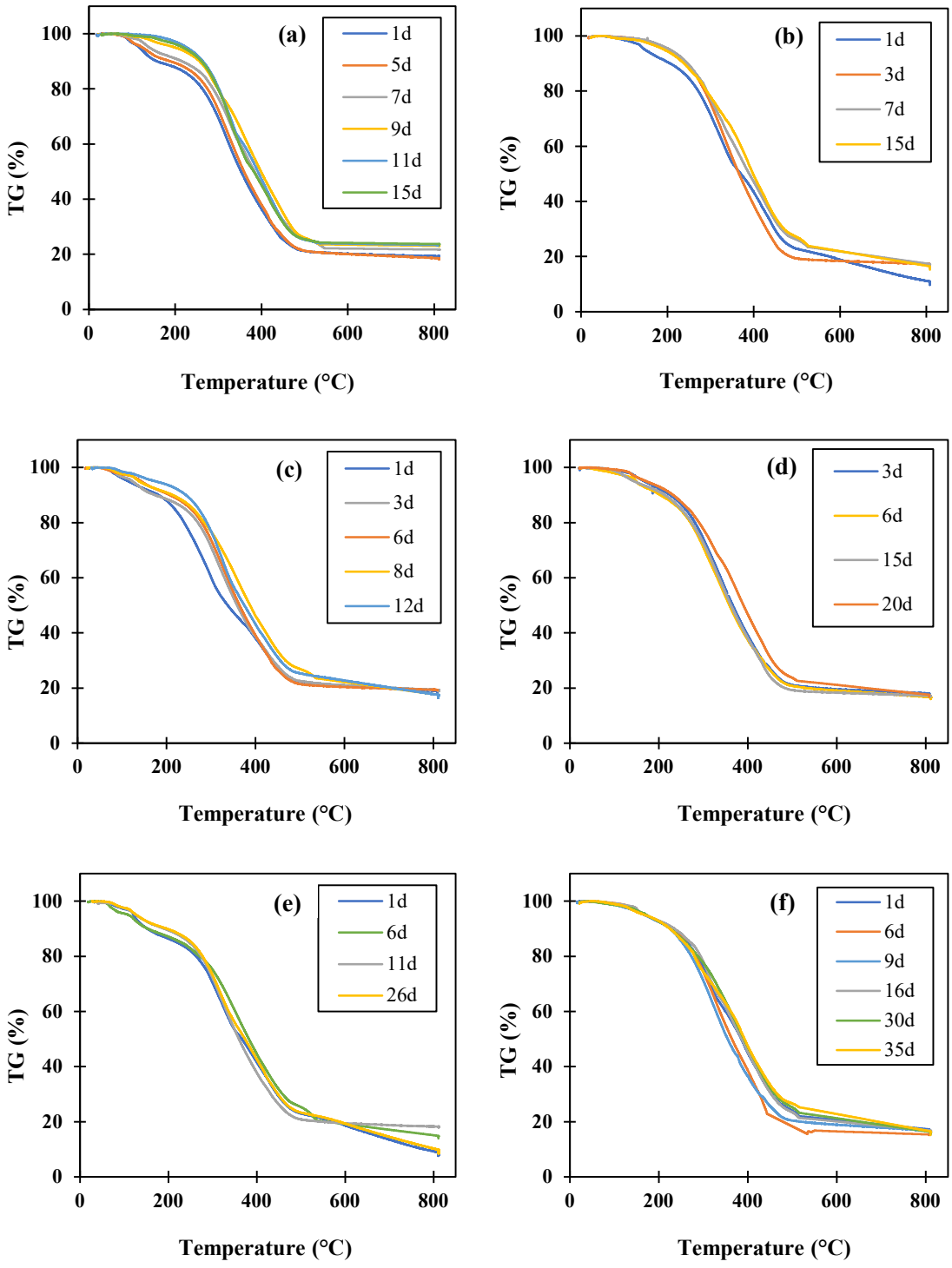

Figure 5-5. Change in HHV of microalgae biocrude before and after 60 days of storage.

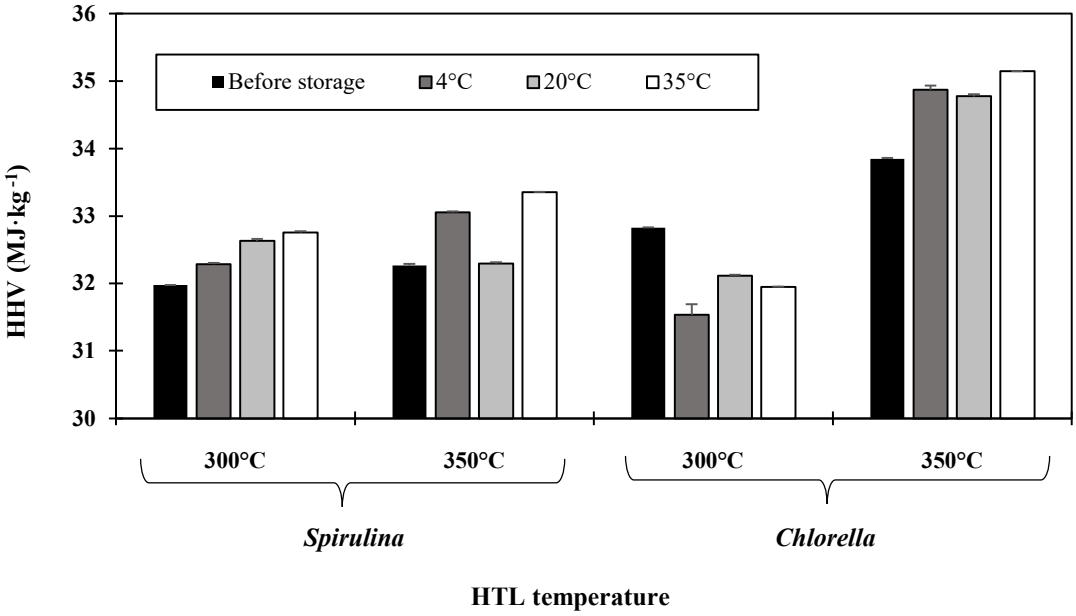

Figure 5-6. GC-MS of biocrude of microalgae before and after 60 days of storage. (a) Ch300. (b) Ch350. (c) Sp300. (d) Sp350. (e) Ch300 and Ch300m. (f) Ch350 and Ch350m.

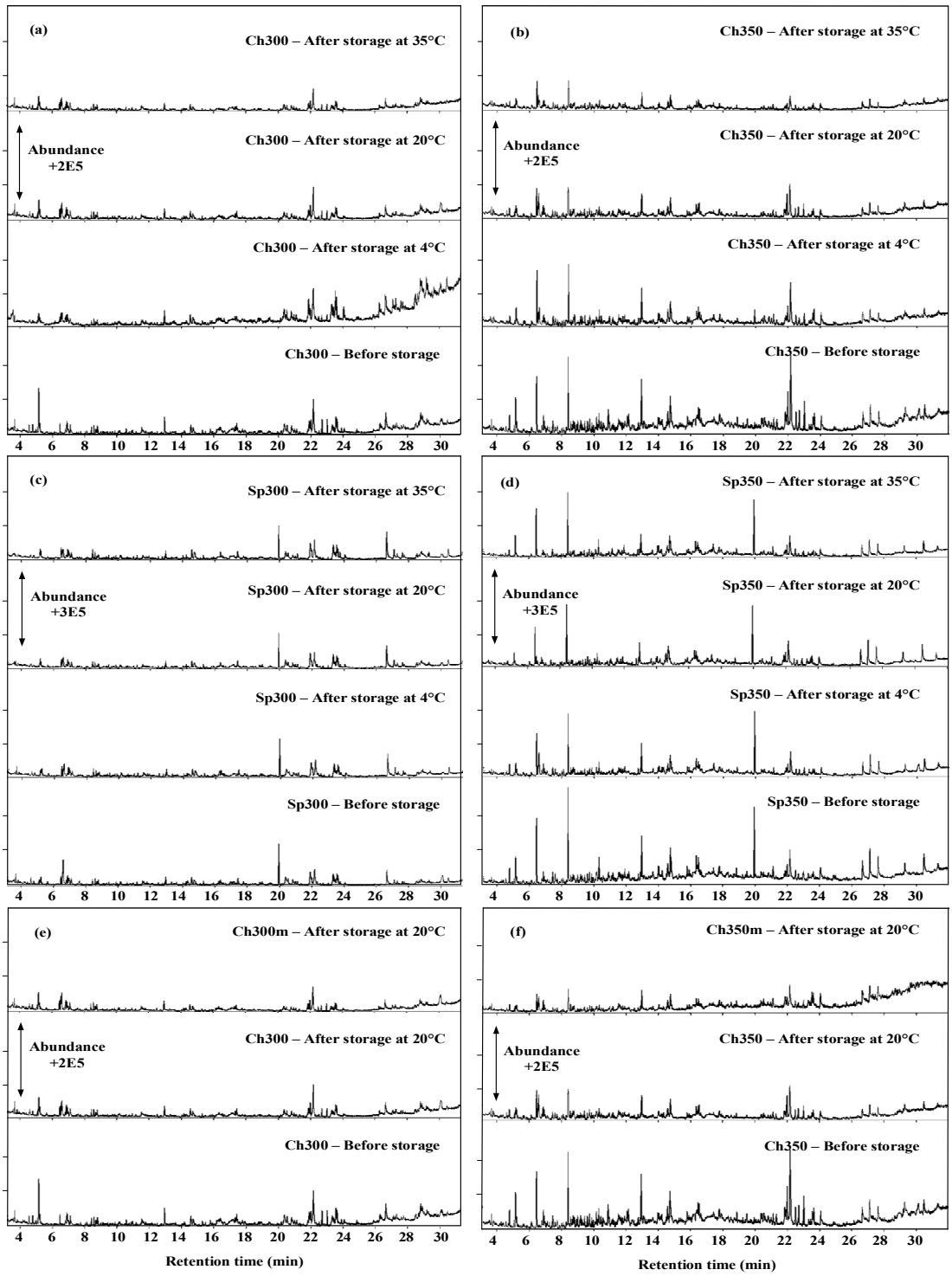

6. Conclusions and recommendations

6.1 Conclusions

In this research work, The HTL of microalgae was performed as an effective way to convert wet biomass into biocrude. The main conclusions are summarized below:

(1) The microalgae *Parachlorella kessleri* was converted to biocrude, aqueous products, gases, and solids. The composition of the biomass was manipulated by varying the culture conditions. Two types of biomass were obtained: the first with a lipid ratio of 0.15 (approximately 70 % protein) and the second with a lipid ratio of 0.65 (approximately 40 % protein). The Lr (lipid ratio) factor was defined as the relationship between lipids and the sum of proteins and carbohydrates in biomass. The effect of reaction temperature (250–350 °C), retention time (0–60 min), initial total solids (5–15 %) and lipid ratio (0.15–0.65) on the yield and quality of the biocrude was analyzed. The elemental composition, TAN and HHV were used as indicators of the biocrude quality. All the factors had a positive and significant effect on the biocrude yield. The maximum biocrude yield was obtained between 315–325 °C and 40–45 min. The increase in the lipid ratio and ITS improved the yield of the biocrude. However, in the range studied, the optimization of these two factors was not achieved. Under these conditions, the HHV was 35 $MJ \cdot kg^{-1}$, the value of TAN was 70 mg $KOH \cdot g^{-1}$ and the carbon, nitrogen and oxygen contents were 72 %, 3.7 % and 13 %, respectively. Although the increase of the Lr factor significantly improved the biocrude TAN, it was not enough to reach the maximum limit allowed by the ASTM standard. The Lr factor had no significant influence on the elementary composition of the biocrude in the range studied. The increase in the lipid content in the biomass and the manipulation of the reaction conditions were not enough to improve the quality of the biocrude. Due to the high values of TAN, oxygen, and nitrogen, the biocrude of microalgae must be upgraded.

(2) From the analysis of the main reaction conditions using the response surface methodology, a regression model was obtained for the calculation of the yield and the elementary composition of the

biocrude. The inclusion of the Lr factor in the design of experiments allowed validating the regression model using a large number of data sets published by other authors.

(3) A one-of-a-kind analysis was performed of the main models to predict biocrude yield. Based on the analysis, a new combined model was proposed and tested with more than 800 published data sets. The new model improved its prediction capacity up to 15 %, compared to previously existing models. The combined model was also able to predict yields greater than 50 % for lipid-rich microalgae. A multivariable regression model was proposed for the calculation of the elemental composition of the algae biocrude. For the first time, the reaction temperature and retention time were included as independent variables for the calculation of the elemental composition of biocrude. Likewise, a model was included for the calculation of the elemental composition of the biocrude of macroalgae, with a success rate greater than 81 %. This model is the first known approximation for the calculation of the quality of macroalgae biocrude.

(4) A study on the storage stability of microalgae biocrude was performed. For the first time, the effect of reaction temperature, storage temperature, microalgae species and the type of vial on stability of biocrude was analyzed. Dynamic viscosity, elemental and chemical composition and thermogravimetric analysis were used as indicators to measure biocrude stability. The reaction temperature and the biomass species had a significant impact on the aging of the biocrude. On the one hand, the viscosity of the biocrude increased during storage, due to the esterification and polymerization reactions that occur between the oxygenated and nitrogenated compounds in the biocrude. On the other hand, no significant changes were observed in the HHV biocrude or the elemental composition in all storage conditions.

6.2 Recommendations

The liquefaction of microalgae to produce biocrude was studied in this work. First, the effect of the main reaction conditions, temperature, retention time, STI and chemical composition of the biomass was analyzed on the yield and quality of the biocrude. Second, a model was developed and validated to predict the yield and quality of the biocrude. Third, the stability of the biocrude during storage was analyzed. Although this research work included an extensive analysis of the yield and quality of the biocrude, from its obtention to storage, there are still many areas that need more studies in order to improve several aspects:

(1) The microalgae biocrude has a higher oxygen and nitrogen content than petroleum. The quality of the biocrude greatly restricts its application for obtaining biofuel. Although the reaction conditions and the increase in lipids in the biomass affect the yield and quality of the biocrude, they are not enough to reduce the oxygen and nitrogen content of the biocrude to levels close to those of petroleum. Therefore, it is necessary to upgrade biocrude, before it can be used as fuel. The use of catalysts during liquefaction has proven to be another alternative that helps improving the quality of the biocrude. However, this approach poses other challenges such as the useful life of the catalyst, the type, size and recovery of the catalyst, contact between the catalyst and the biocrude, among others.

(2) In the development of new mathematical models to predict the yield and quality of the biocrude, it is necessary to include more detailed information on the characterization of biomass, such as amino acid and fatty acid profiles, for proteins and lipids, respectively. Currently, the biomass characterization includes the identification of macromolecules (lipids, protein and carbohydrates), using different techniques and patterns. The use of different techniques in the characterization of biomass may indicate that the immediate analysis of the biochemical compositions of the macromolecules of biomass does not always provide enough information for accurate predictions.

(3) The stability of the biocrude during storage is affected by the high content of oxygenated compounds that react with each other, increasing the biocrude viscosity. The biocrude of microalgae is also different from petroleum because of its high nitrogen content, hence it is necessary to study polymerization reactions between nitrogenated compounds. The stability analysis of the microalgae biocrude can also include the monitoring of other variables, such as water content. It has been shown that an increase in the water content of the biocrude decreases its viscosity, which could lead to erroneous conclusions about the stability of the biocrude. The water content in the biocrude can increase during storage because of the esterification of fatty and organic acids.

A. Annex: Supplementary information for chapter 2

Table A 1. Determination of protein content by the Bradford method - calibration curve

<table>
<tr><th colspan="2">Determination of protein content by the Bradford method - calibration curve</th></tr>
<tr><td>Equipment</td><td>Cytation 3 (BioTek®), analytical balance, vortex stirrer</td></tr>
<tr><td>Reagents</td><td>Bradford Reagent (Dye Reagent Concentrate, Bio-Rad), NaH_2PO_4, Na_2HPO_4, albumin</td></tr>
<tr><td>Calibration standard</td><td>Weigh 0.130 g of albumin
Dissolve with 10 mL of distilled water
Make up to 100 mL (albumin = 1.3 mg/mL)
Store the solution at 4ºC</td></tr>
<tr><td>Sodium phosphate buffer (0.02 M, pH 6)</td><td>Weigh 0.0344 g Na_2HPO_4 and 0.2412 g NaH_2PO_4
Dissolve with 80 mL of distilled water
Adjust the pH to 6
Make up to 100 mL
Store the solution at 4ºC</td></tr>
<tr><td>Calibration curve</td><td>Typical test:
Mix 5 µL of the calibration standard, 395 µL of the sodium phosphate buffer and 100 µL of the Bradford reagent
Agitate vigorously in a vortex for one minute.
Measure the absorbance at 595 nm
The mixture is stable for 1 hour.

Reaction mixtures for the calibration curve of protein
<table>
<tr><th>#</th><th>Albumin (µL)</th><th>Buffer (µL)</th><th>Bradford reagent (µL)</th><th>Total protein (µg/µL)</th></tr>
<tr><td>1</td><td>5</td><td>395</td><td>100</td><td>16.25</td></tr>
<tr><td>2</td><td>10</td><td>390</td><td>100</td><td>32.50</td></tr>
<tr><td>3</td><td>12</td><td>388</td><td>100</td><td>39.00</td></tr>
<tr><td>4</td><td>15</td><td>385</td><td>100</td><td>48.75</td></tr>
<tr><td>5</td><td>17</td><td>383</td><td>100</td><td>55.25</td></tr>
<tr><td>6</td><td>20</td><td>380</td><td>100</td><td>65.00</td></tr>
<tr><td>7</td><td>25</td><td>375</td><td>100</td><td>81.25</td></tr>
<tr><td>8</td><td>30</td><td>370</td><td>100</td><td>97.50</td></tr>
<tr><td>B</td><td>0.0</td><td>400</td><td>100</td><td>0.00</td></tr>
</table>
Graph total protein(µg/µL) vs. Absorbance</td></tr>
</table>

Table A 2. Determination of lipids content by the SFV method - calibration curve

<table>
<tr><th colspan="2">Determination of lipids content by the SFV method - calibration curve</th></tr>
<tr><td>Equipment</td><td>Cytation 3 (BioTek®), analytical balance, vortex stirrer</td></tr>
<tr><td>Reagents</td><td>Concentrated sulfuric acid > 98 %, phosphoric acid (17 % v/v), vanillin (99 %), canola oil (commercial), chloroform: methanol (1:1)</td></tr>
<tr><td>Calibration standard</td><td>Weigh 0.015 g of oil
Make up to 10 mL with chloroform: methanol (oil = 1.5 mg/mL).
Store the solution at 4ºC.</td></tr>
<tr><td>Phosphoric acid - vanillin reagent</td><td>Weigh 50 mg of vanillin
Dissolve with 250 mL of phosphoric acid (17 % v/v)
Store in an amber bottle at 4ºC.</td></tr>
<tr><td>Calibration curve</td><td>Typical test:
Mix 10 µL of the calibration standard and 300 µL of sulfuric acid
Agitate vigorously in a vortex for one minute
Heat at 90 °C for 20 minutes
Cool quickly in an ice bath
Add 500 µL of phosphoric acid-vanillin reagent
Agitate vigorously in a vortex for one minute
Measure the absorbance at 540 nm
The mixture is stable for 1 hour.

Reaction mixtures for the calibration curve of lipis
<table>
<tr><th>#</th><th>Oil (µL)</th><th>H_2SO_4 (µL)</th><th>H_3PO_4 – Vainillin (µL)</th><th>Total lipids (µg/µL)</th></tr>
<tr><td>1</td><td>10</td><td>300</td><td>500</td><td>10</td></tr>
<tr><td>2</td><td>20</td><td>300</td><td>500</td><td>20</td></tr>
<tr><td>3</td><td>30</td><td>300</td><td>500</td><td>30</td></tr>
<tr><td>4</td><td>40</td><td>300</td><td>500</td><td>40</td></tr>
<tr><td>5</td><td>50</td><td>300</td><td>500</td><td>50</td></tr>
<tr><td>6</td><td>60</td><td>300</td><td>500</td><td>60</td></tr>
<tr><td>B</td><td>0.0</td><td>300</td><td>500</td><td>0.0</td></tr>
</table>
Graph total lipids (µg/µL) vs. Absorbance</td></tr>
</table>

Table A 3. Determination of carbohydrates content by the Dubois method - calibration curve

<table>
<tr><th colspan="2">Determination of carbohydrates content by the Dubois method - calibration curve</th></tr>
<tr><td>Equipment</td><td>Cytation 3 (BioTek®), analytical balance, vortex stirrer</td></tr>
<tr><td>Reagents</td><td>Concentrated sulfuric acid > 98 %, phenol, D-glucose</td></tr>
<tr><td>Calibration standard</td><td>Weigh 0.100 g of D-glucose
Dissolve with 10 mL of distilled water
Make up to 100 mL (D-glucose = 1.0 mg/mL)
Store the solution at 4ºC</td></tr>
<tr><td>Phenol solution (80% w/w)</td><td>Weigh 8 g of phenol
Dissolve with 10 mL of distilled water
Prepare the solution in an amber bottle
Do not store</td></tr>
<tr><td>Calibration curve</td><td>Typical test:
Mix 10 µL of the standard, 95 µL of distilled water and 100 µL of phenol (80% w/w)
Agitate vigorously in a vortex for one minute
Add quickly 500 µL of sulfuric acid
Agitate vigorously in a vortex for one minute
Let cool in the dark (exothermic reaction)
Measure the absorbance at 485 nm
The mixture is stable for 36 hours.

Reaction mixtures for the calibration curve of carbohydrates
<table>
<tr><th>#</th><th>Distilled water (µL)</th><th>Glucose (µL)</th><th>Phenol (µL)</th><th>H_2SO_4 (µL)</th><th>Total Sugar (µg/µL)</th></tr>
<tr><td>1</td><td>100</td><td>5</td><td>100</td><td>500</td><td>0.71</td></tr>
<tr><td>2</td><td>95</td><td>10</td><td>100</td><td>500</td><td>1.42</td></tr>
<tr><td>3</td><td>90</td><td>15</td><td>100</td><td>500</td><td>2.13</td></tr>
<tr><td>4</td><td>85</td><td>20</td><td>100</td><td>500</td><td>2.84</td></tr>
<tr><td>5</td><td>80</td><td>25</td><td>100</td><td>500</td><td>3.55</td></tr>
<tr><td>6</td><td>75</td><td>30</td><td>100</td><td>500</td><td>4.26</td></tr>
<tr><td>7</td><td>70</td><td>35</td><td>100</td><td>500</td><td>4.96</td></tr>
<tr><td>8</td><td>65</td><td>40</td><td>100</td><td>500</td><td>5.67</td></tr>
<tr><td>9</td><td>60</td><td>45</td><td>100</td><td>500</td><td>6.38</td></tr>
<tr><td>10</td><td>55</td><td>50</td><td>100</td><td>500</td><td>7.09</td></tr>
<tr><td>B</td><td>105</td><td>0,0</td><td>100</td><td>500</td><td>0.00</td></tr>
</table>

Graph total sugar (µg/µL) vs. Absorbance</td></tr>
</table>

Table A 4. Determination of ash content

Determination of ash content	
Equipment	Muffle (Tmim. 600 °C), analytical balance and glass desiccator
Reagents	Freeze-dried microalgae
The capsules	Weigh the empty capsules Heat the empty capsules at 575 °C for 4 hours Let cool (approximately 20 hours) Remove the capsules with tweezers and put in a desiccator. Weigh again
Ashes	Weigh 0.5 g of lyophilized microalgae (capsules + biomass) Heat the empty capsules at 575 °C for 4 hours Let cool (approximately 20 hours) Remove the capsules with tweezers and put in a desiccator. Weigh again Ash content: $$\%\, ash \;=\; \frac{W_2}{W_1\,(100-H)}\, x\; 100$$ W_2: weight of microalgae sample after heating at 575 °C (g) W_1: weight of the microalgae sample before heating at 575 °C (g) H: percentage of moisture of the microalgae in g water/g biomass

Table A 5. Determination of ash content

Determination of ash content	
Equipment	Moisture balance AMB 50
Reagents	Freeze-dried microalgae
Ashes	Weigh 0.2 g of lyophilized microalgae, Set the balance temperature to 105 °C Heat the sample to constant weight. Moisture content: $\% \, moisture = \frac{W_1 - W_2}{W_1} x \, 100$ W_2: weight of microalgae sample after heating at 105 °C (g) W_1: weight of the microalgae sample before heating at 105 °C (g)

Table A 6. Reported experimental chemical and elemental compositions of microalgae, HTL operating conditions and yield and quality of biocrude used for model prediction analysis.

This table is in a separate Excel file**.** The file can be found at:
https://drive.google.com/file/d/1NhJn6CPLl-sPQE4GtRFLuF1Msw3V6O_U/view?usp=sharing

Table A 7. Chemical composition of microalgae without normalization.

Properties[1]	***P. kessleri* (P-aut)**	***P. kessleri* (P-myx)**
Neutral Lipids (%)	9.2 ± 0.1	8.8 ± 0.2
Protein (%)	56.1 ± 1.9	6.7 ± 0.1
Soluble carbohydrates (%)	5.4 ± 0.3	7.0 ± 0.2

[1]daf: dry ash free

Table A 8. Parameters of biocrude RSM model.

Factor (Xi)[1]	Parameter	Response variable (Y_i)[2]					
		Yield (%)	TAN (mg KOH·g^{-1})	Carbon (%)	Nitrogen (%)	Oxygen (%)	HHV (MJ·kg^{-1})
Constant	a_0	32.27	90.83	71.92	3.30	15.30	34.36
A: T	a_1	8.07	-11.39	2.51	0.67	-3.38	1.30
B: tr	a_2	3.47	-12.64	1.22	0.30	-1.22	0.48
C: IST	a_3	1.52	-8.02	-1.00	0.11	0.95	-0.71
D: Lr	a_4	1.65	-4.27	-0.04	-0.04	0.11	0.01
AA	a_5	-6.72	2.07	0.54	-0.16	-0.44	0.32
AB	a_6	-2.73	2.40	-0.23	-0.28	0.30	-0.06
AC	a_7	-0.38	-1.63	0.58	0.06	-0.39	0.26
AD	a_8	-1.68	11.27	0.11	0.02	0.00	0.01
BB	a_9	-6.27	1.62	0.43	-0.11	-0.20	0.27
BC	a_{10}	0.59	3.57	-0.42	0.08	0.20	-0.08
BD	a_{11}	1.39	-4.61	-0.24	-0.04	-0.09	0.00
CC	a_{12}	1.93	0.87	-0.96	-0.06	1.16	-0.58
CD	a_{13}	-0.39	-3.85	0.06	-0.03	0.06	0.07
DD	a_{14}	5.18	0.67	0.97	-0.01	-1.26	0.59

[1]The factors were normalized from -1 to 1

[2]Response surface model:

$$Y_i = a_0 + a_1A + a_2B + a_3C + a_4D + a_5AA + a_6AB + a_7AC + a_8AD + a_9BB + a_{10}BC + a_{11}BD + a_{12}CC + a_{13}CD + a_{14}DD$$

Table A 9. ANOVA of the response variables of RSM.

Factor	Response variables											
	Yield (%)		TAN (mg KOH·g^{-1})		Carbon (%)		Nitrogen (%)		Oxygen (%)		HHV (MJ·kg^{-1})	
	Σ[1]	P-value[2]	Σ	P-value	Σ	P-value	Σ	P-value	Σ	P-value	Σ	P-value
A: T	1498.59	0.000	2743.40	0.000	124.94	0.000	10.63	0.000	235.62	0.000	36.23	0.000
B: tr	278.00	0.000	3563.94	0.000	30.73	0.002	2.08	0.000	31.56	0.005	4.98	0.026
C: IST	53.29	0.020	1359.37	0.001	19.98	0.010	0.28	0.033	18.41	0.025	10.60	0.002
D: Lr	64.98	0.011	389.09	0.045	0.04	0.899	0.04	0.431	0.26	0.777	0.00	0.943
AA	121.66	0.001	11.46	0.717	0.80	0.570	0.06	0.291	0.53	0.683	0.27	0.577
AB	162.95	0.000	116.27	0.256	0.91	0.544	1.68	0.000	1.62	0.479	0.08	0.769
AC	3.17	0.547	52.84	0.439	5.92	0.133	0.07	0.281	2.77	0.357	1.27	0.235
AD	59.92	0.014	2440.80	0.000	0.21	0.770	0.01	0.656	0.00	0.999	0.00	0.968
BB	105.91	0.002	8.77	0.751	0.63	0.615	0.03	0.469	0.14	0.837	0.19	0.638
BC	7.67	0.352	256.92	0.097	3.19	0.263	0.14	0.129	0.75	0.630	0.11	0.719
BD	40.72	0.039	418.35	0.038	1.07	0.512	0.04	0.399	0.15	0.830	0.00	0.997
CC	10.04	0.288	2.01	0.879	2.60	0.311	0.01	0.698	3.78	0.284	0.91	0.314
CD	3.23	0.544	284.58	0.082	0.06	0.871	0.01	0.626	0.06	0.893	0.10	0.741
DD	89.39	0.004	1.19	0.907	3.23	0.260	0.00	0.962	5.49	0.200	1.15	0.258
R squared (R^2)	0.9420		0.8895		0.8300		0.9301		0.8500		0.7929	
Adjusted R^2	0.9051		0.8121		0.7047		0.8894		0.7394		0.6403	

[1]Σ: sum of squares. [2]P-value: p value for F test.

Figure A 1. Response surface analysis for elemental composition and HHV of biocrude. (a) interactions for carbon content, (b) interactions for nitrogen content, (c) interactions for oxygen content, and (d) interactions for HHV. In each graph, the first factor was varied of its lowest level to its highest level. on one line, the second factor remains in its lowest level (red medium-dashed line). On the other line, the second factor remains at its highest level (black solid line). All other factors except those involved in the interaction remain constant in their central values.

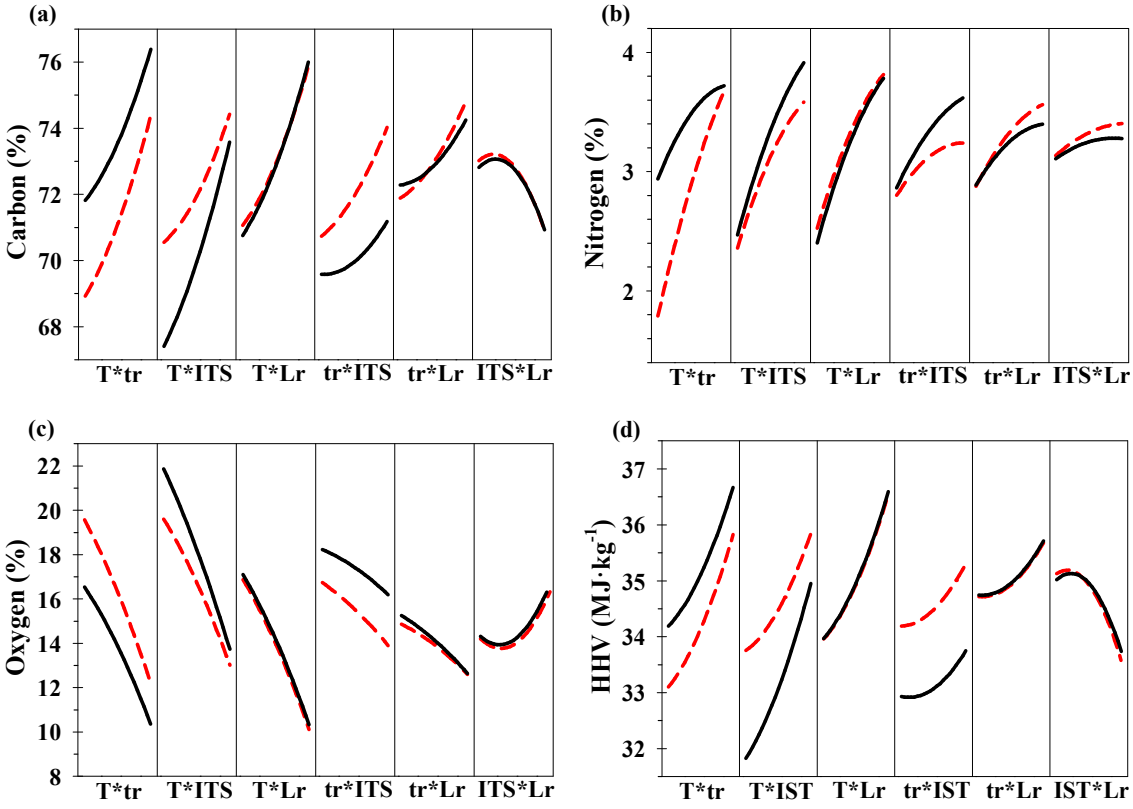

B. Annex: Supplementary information for chapter 3

Table B 1. Values of the rate constants for correlating biocrude yields from the kinetic models.

Pathway (Fig. 1b)	**k_i (min^{-1})**											
	250 °C	**300 °C**	**350 °C**	**400 °C**	**250 °C**	**300 °C**	**350 °C**	**400 °C**	**250 °C**	**300 °C**	**350 °C**	**400 °C**
[1]P → AP	0.0095	0.20	0.28	0.33	0.085	0.180	0.270	0.340	1.1173	3.2542	7.9837	17.1420
L → AP	0.15	0.35	0.35	0.35	0.180	0.210	0.300	0.380	0.0587	0.1864	0.4918	1.1230
CH → AP	0.25	0.35	0.35	0.35	0.078	0.184	0.282	0.294	0.0234	0.0747	0.1980	0.4541
P → B	0.13	0.13	0.28	0.32	0.066	0.156	0.318	0.468	1.2822	3.6311	8.7008	18.3104
L → B	0.031	0.11	0.33	0.35	0.840	0.180	0.312	0.450	0.0562	0.2105	0.6374	1.6372
CH → B	0.0001	0.0001	0.001	0.0032	0.047	0.126	0.306	0.456	0.0025	0.0122	0.0459	0.1415
B → AP	0.0044	0.14	0.30	0.35	0.096	0.174	0.300	0.300	0.0007	0.0027	0.0082	0.0209
AP → B	0.003	0.12	0.26	0.26	0.09	0.180	0.342	0.348	0.0008	0.0031	0.0094	0.0242
AP → G	0.0001	0.0004	0.0014	0.0014	0.000032	0.000071	0.0010	0.0015	0.0000	0.0000	0.0000	0.0000
B → G	0.0001	0.0002	0.0009	0.0053	0.00022	0.00091	0.0020	0.0096	0.0000	0.0003	0.0013	0.0046
Kinetic model	**Valdez et al.** [19]				**Vo et al.** [85]				[2]**Sheehan & Savage** [106]			

[1] P: proteins. L: Lipids. CH: Carbohydrates. AP: aqueous-phase products. B: biocrude. G: gas. [2] The kinetics constants of the Sheehan & Savage model are calculated from their Arrhenius parameters [106].

Table B 2. Experimental reported of biochemical compositions of microalgae, HTL operating conditions and biocrude yields used for model prediction analysis.

This table is in a separate Excel file**.** The file can be found at:
https://drive.google.com/file/d/1HeA3o4K8ahFBqGIKi8zptFcE68t8V4Bd/view?usp=sharing

Figure B 1. Chemical composition of the microalgae in different publishes articles. n = 184. The box represents the range where 50 % of the data is located. The black and red lines inside the box mark the median and the average, respectively. The whiskers (error bars) above and below the box indicate the 90th and 10th percentiles. The black dots represent the 5th and 95th percentiles. L: lipids, P: proteins, CH: carbohydrates and A: ash.

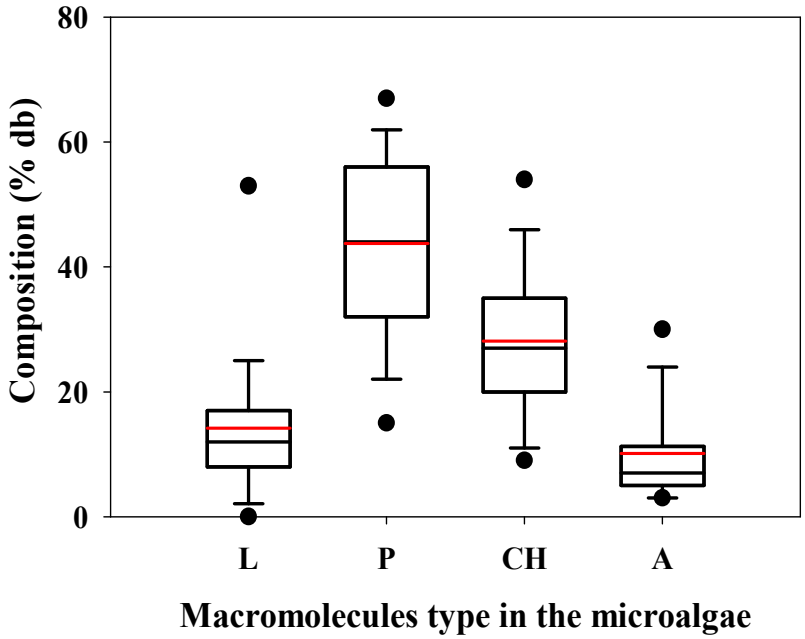

Figure B 2. Comparison of yield predictions obtained by the component additivity model from Wagner et al. [101] at 300 °C. All experimental data were obtained at 300 °C and retention times between 1–90 min. The continuous black line represents an exact match between the model and the experimental data. The red dotted lines represent a SD of ± 5 %. The r^2 explains the variance of the experimental and predicted data for a linear regression with the intercept equal to zero.

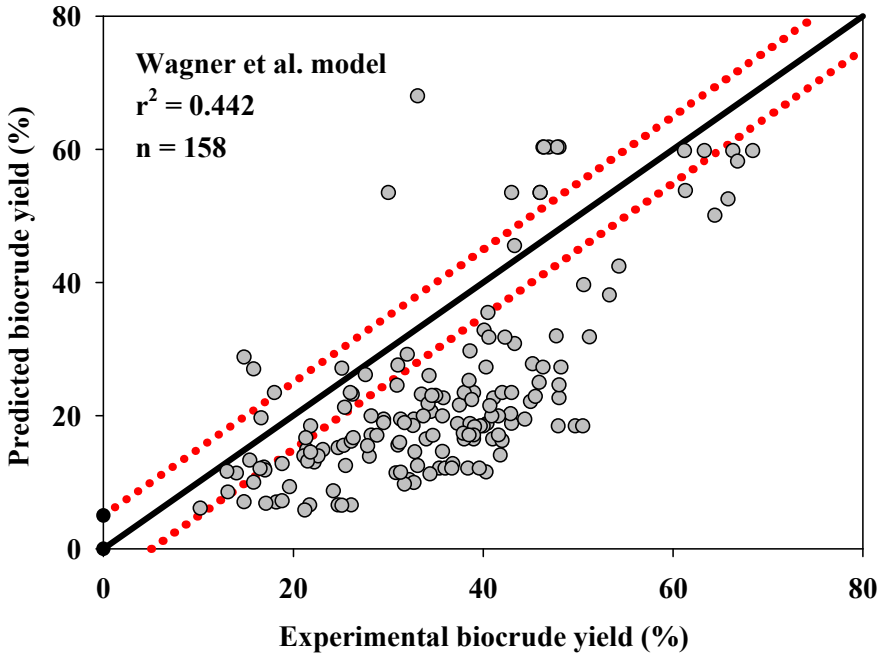

Figure B 3. Effect of temperature and retention time on calculated biocrude yields by the model of Vo et al. [85] for hydrothermal liquefaction of four hypothetical biomasses. (a) – (d) at constant temperature and (e) – (h) at constant retention time. Biomass 1: 10 % lipids, 60 % proteins and 25 % carbohydrates. Biomass 2: 35 % of each lipids and proteins and 25 % carbohydrates. Biomass 3: 60 % lipids, 10 % proteins and 25 % carbohydrates. Biomass 4: 60 % carbohydrates and 17.5 % of each lipids and proteins.

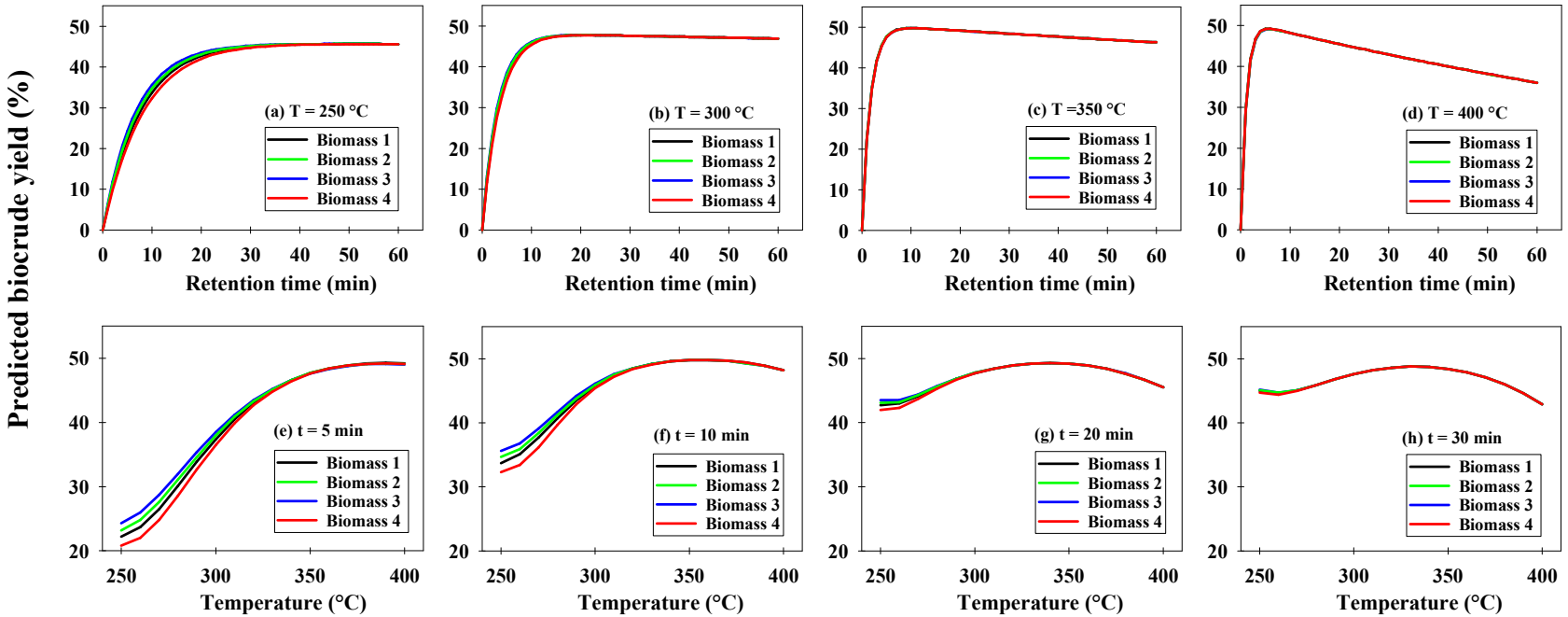

Figure B 4. Effect of lipids content of microalgae on the biocrude yield calculated at 300 °C using different kinetic models. n = 158. Black triangle: Valdez et al. [19]. Gray circle: Vo et al. [85]. White circle: Sheehan & Savage [106]. db: dry basis. Absolute error = Predicted yield – Experimental yield.

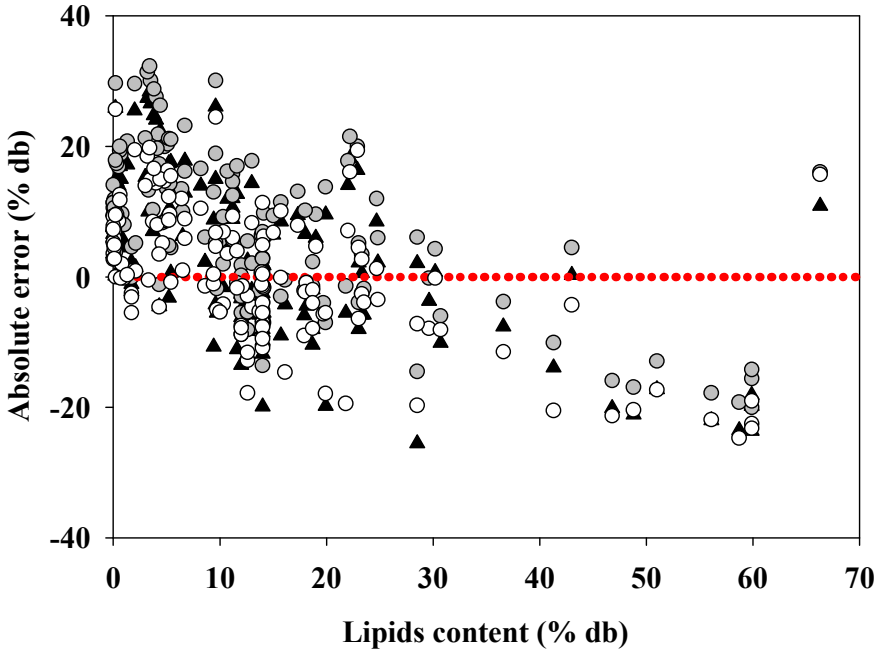

Figure B 5. Effect of protein content of microalgae on the biocrude yield calculated using the model from Sheehan & Savage [106] at different HTL temperature. Black triangle: 250 °C (n = 74). Gray circle: 300 °C (n = 158). db: dry basis. Absolute error = Predicted yield – Experimental yield.

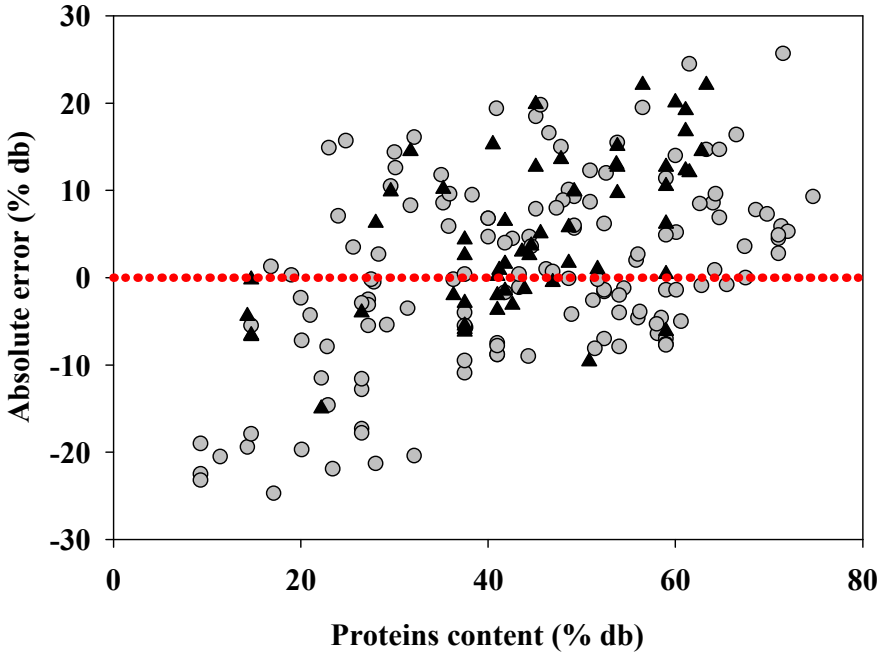

Figure B 6. Comparison of yield predictions obtained using the kinetic model from Sheehan & Savage [106] with interactions at different HTL temperatures: (a) 250 °C, (b) 300 °C, (c) 350 °C and (d) 400 °C. The continuous black line represents an exact match between the model and the experimental data. The red dotted lines represent a SD of ± 5 %. The r^2 explains the correlation between the experimental and the predicted data.

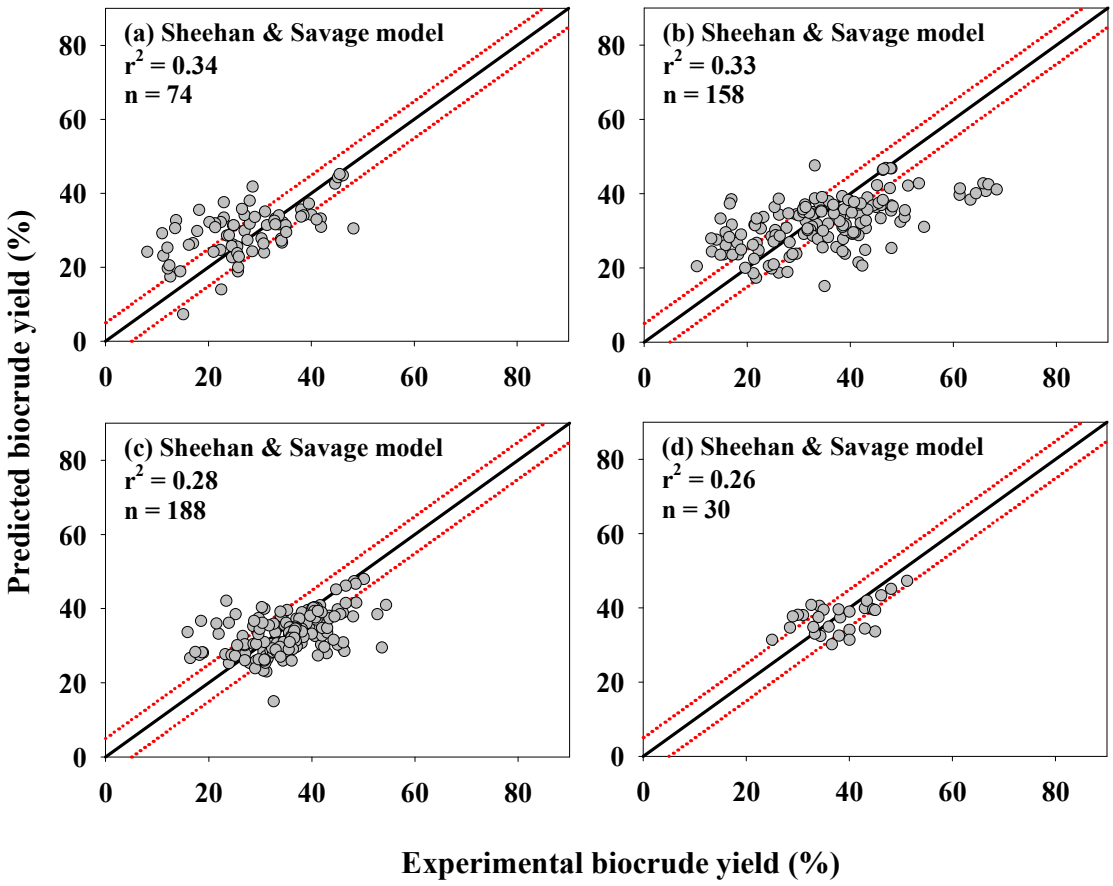

Figure B 7. Comparison of yield predictions obtained from different models. (a) Leow et al. [59], (b) Sheehan & Savage [106] and (c) model proposed by this study (n = 830). The continuous black line represents linear regression of data. The red dotted lines represent a 95 % prediction interval. The r^2 explains the correlation between the experimental and the predicted data.

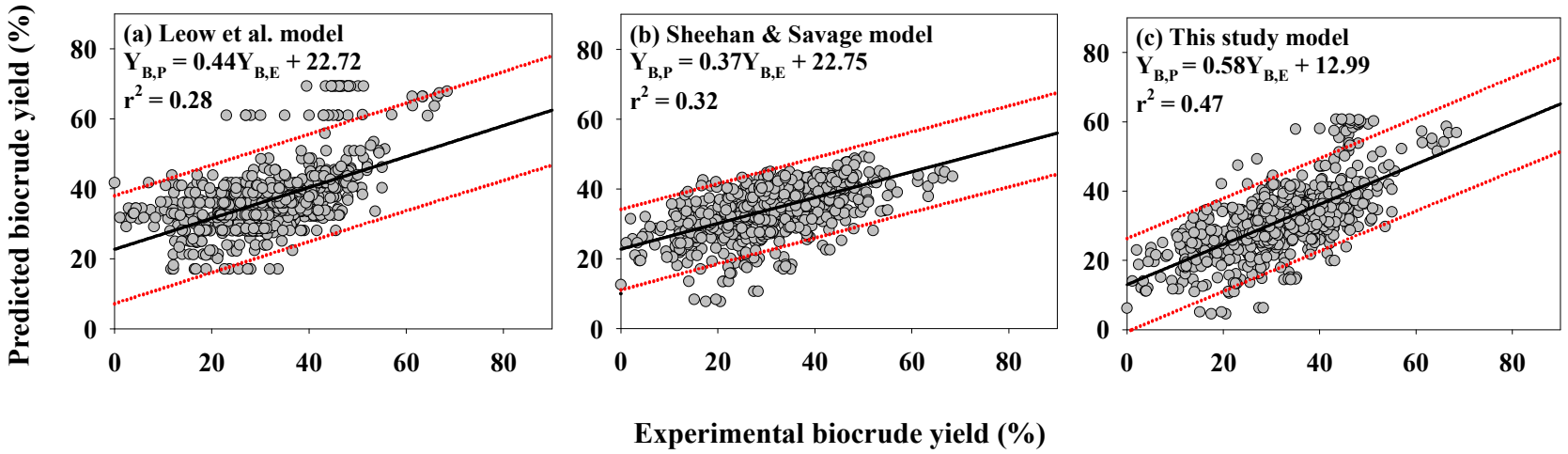

C. Annex: Supplementary information for chapter 4

Table C 1. Experimental reported about chemical and elemental compositions of macroalgae, HTL operating conditions and yield and quality of biocrude used for model prediction analysis.

This table is in a separate Excel file**.** The file can be found at:
https://drive.google.com/file/d/15cHWO9DyJBar0q-ezEtWQeeaisa8IQNX/view?usp=sharing

Table C 2. Experimental reported about chemical and elemental compositions of microalgae, HTL operating conditions and yield and quality of biocrude used for model prediction analysis.

This table is in a separate Excel file**.** The file can be found at:
https://drive.google.com/file/d/15cHWO9DyJBar0q-ezEtWQeeaisa8IQNX/view?usp=sharing

Table C 3. Important statistic parameters for the elementary composition of algae and biocrude.

Type	Element	n	Minimum	Maximum	Average	Median	Percentiles					
							5th	10th	25th	75th	90th	95th
Biomass	C (%)[1]	59	30.7	59.6	44.4	42.7	33.4	37.2	40.5	49.3	53.6	56.5
(Macroalgae)	H (%)	59	5.4	9.6	7.0	6.8	5.8	6.0	6.4	7.9	7.9	9.0
	O (%)	59	22.8	57.2	42.3	44.6	26.9	33.1	38.4	46.2	49.9	53.8
	N (%)	59	1.0	8.1	4.5	4.5	1.1	1.8	3.1	5.8	6.6	7.5
	S (%)	40	0.1	7.1	2.6	2.2	0.2	0.2	0.9	4.3	5.6	6.0
Biocrude	C (%)	59	69.5	80.9	74.9	74.1	70.4	72.4	73.2	77.1	79.0	79.6
(Macroalgae)	H (%)	59	6.5	11.5	8.4	8.2	7.0	7.1	7.6	8.9	10.2	10.7
	O (%)	59	5.2	17.6	11.1	11.4	5.9	6.4	9.2	13.4	15.2	16.3
	N (%)	59	2.1	7.2	5.0	5.1	2.3	3.0	3.9	6.2	6.8	6.9
	S (%)	37	0.0	4.9	0.9	0.7	0.0	0.1	0.4	1.2	2.0	2.6
Biomass	C (%)	404	43.2	78.2	53.6	52.9	47.2	49.3	50.6	56.0	58.8	61.6
(Microalgae)	H (%)	404	4.3	9.9	7.7	7.6	6.4	6.9	7.3	8.0	8.8	9.1
	O (%)	404	8.8	48.6	30.1	30.3	22.3	24.5	26.7	33.8	36.3	36.7
	N (%)	404	1.5	12.6	8.0	8.8	2.7	3.3	6.9	9.5	11.1	11.7
	S (%)	289	0.0	3.3	0.8	0.6	0.2	0.2	0.6	0.9	1.8	2.2
Biocrude	C (%)	404	62.7	82.2	72.8	73.1	65.6	67.4	70.9	75.1	76.9	78.2
(Microalgae)	H (%)	404	4.7	14.4	9.6	9.3	8.3	8.6	8.8	10.0	10.8	12.1
	O (%)	404	0.6	27.0	12.2	11.7	4.8	7.1	9.1	14.2	19.0	22.0
	N (%)	404	0.3	9.1	5.0	5.4	1.0	2.0	3.9	6.4	7.3	7.7
	S (%)	285	0.0	3.1	0.6	0.6	0.0	0.1	0.3	0.9	1.2	1.6

[1]daf: dry ash free

Figure C 1. Example of data processing. (a) Group of experimental data to analyze the effect of reaction temperature on the nitrogen content of the biocrude. Each letter of figure (a) identifies the average of the experimental nitrogen content for every type of algae (gray triangles for microalgae, black circles for macroalgae) reported in 84 articles (n = 59 for macroalgae and n = 404 for microalgae) and grouped in subsets (a, b, c, …k) by reaction temperature. The experimental data of every subset are identified by letter in Table C 1 (macroalgae) and Table C 2 (microalgae). (b) Analysis of the effect of reaction temperature on nitrogen content of the biocrude. Red triangles represent the calculated nitrogen content in microalgae biocrude using the proposed model (Equation 3-1 and Equation 3-2 and Table 4-1 and Table 4-2) for every data published in every subset described in (a) and then averaged. The red dotted line is the second order regression from the calculated averages of nitrogen content of microalgae biocrude. Blue circles mean nitrogen content in macroalgae biocrude using the proposed model (Equation 3-1 and Equation 3-2 and Table 4-1 and Table 4-2) for every data published in every subset described in (a) and then averaged. The blue dotted line is the second order regression from the averages of calculated nitrogen content of macroalgae biocrude.

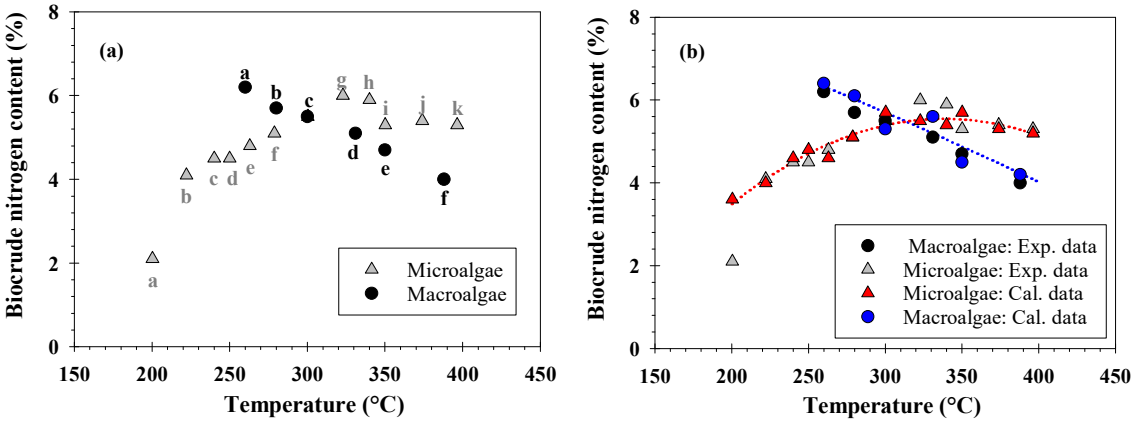

Figure C 2. Hydrogen content in the biocrude via algae HTL: (a) Effect of reaction temperature on H content of the biocrude, (b) effect of retention time on H content of the biocrude and (c) effect of algae H content on H content of the biocrude. The dotted lines represent H content predicted by the model.

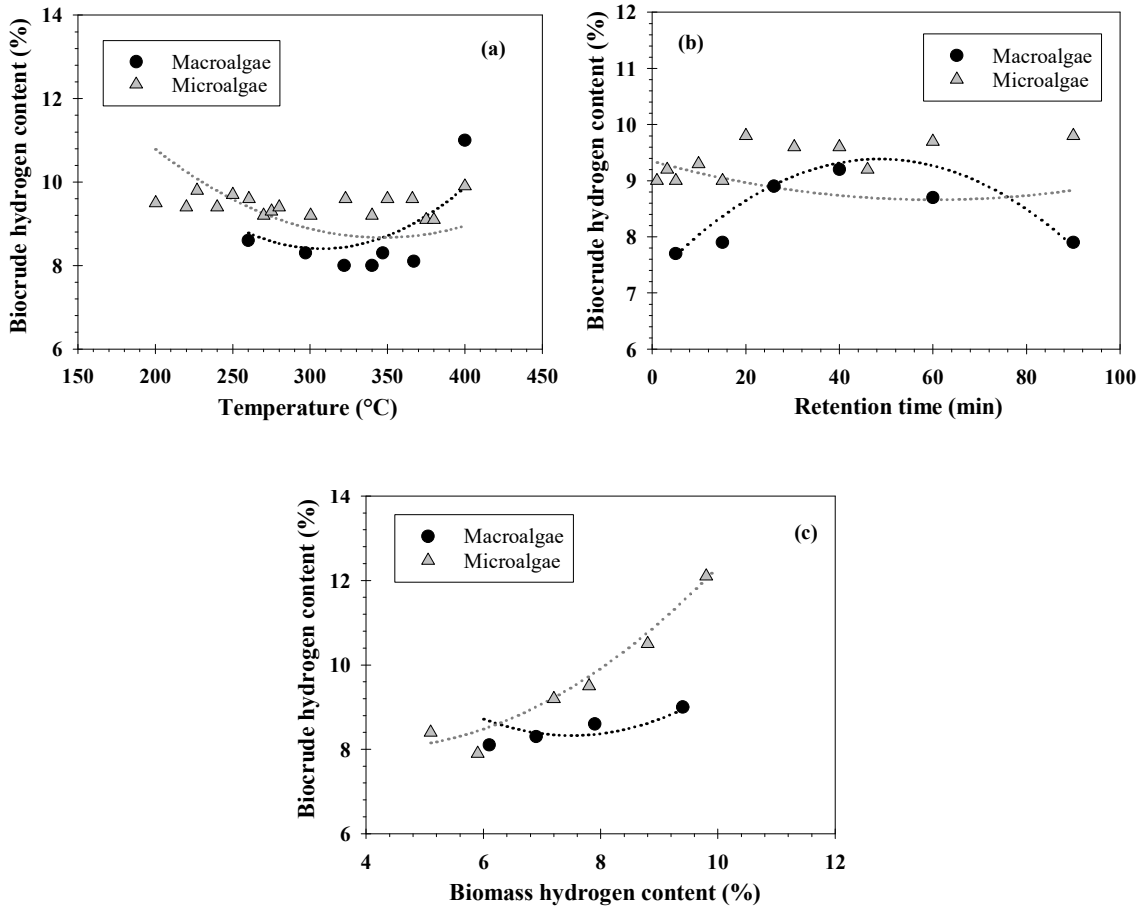

D. Annex: Supplementary information of chapter 5

Figure D 1. Thermogravimetric analysis (TGA) of microalgae. Black circle: Spirulina; gray square: *C. vulgaris*.

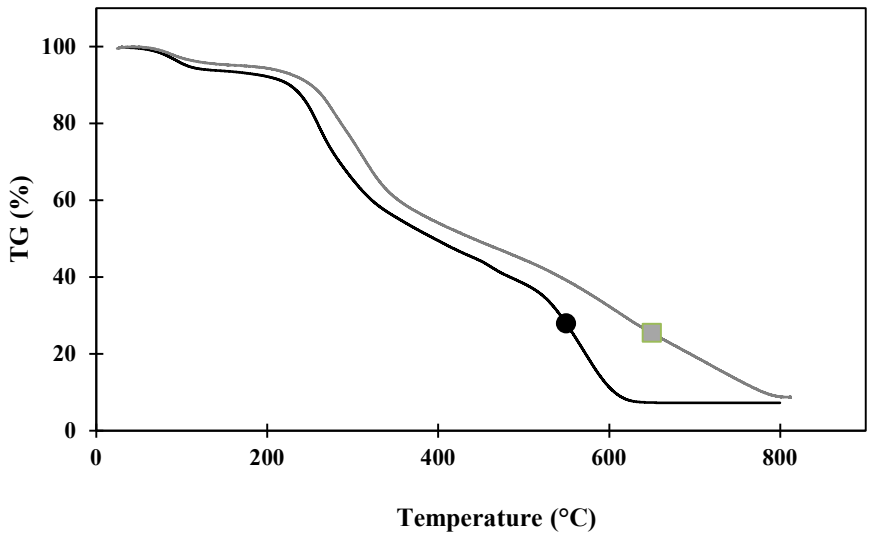

Figure D 2. Typical thermal profile inside the reactor during HTL. Black circle: 300 °C; gray square: 350 °C.

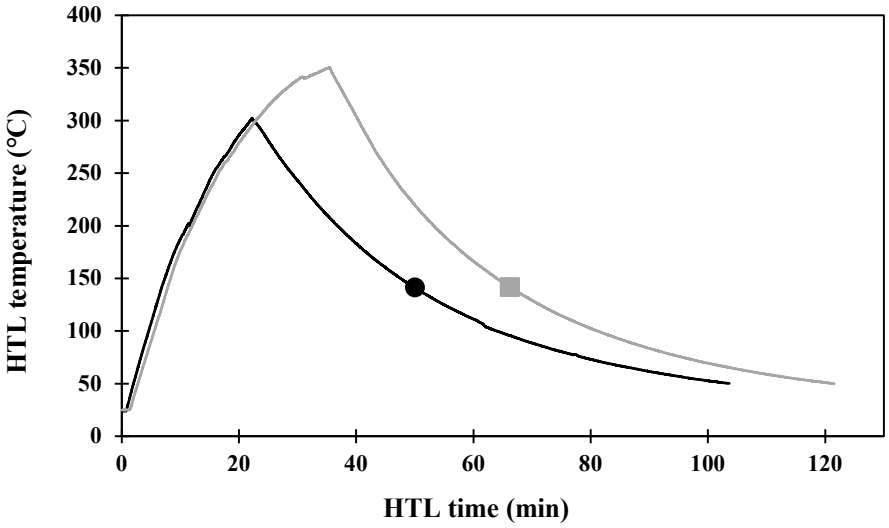

Figure D 3. Thermogravimetric analysis (TGA) of Spirulina biocrude obtained at 350 °C and stored for a several days at (a) 4 °C, (b) 20 °C, and (c) 35 °C.

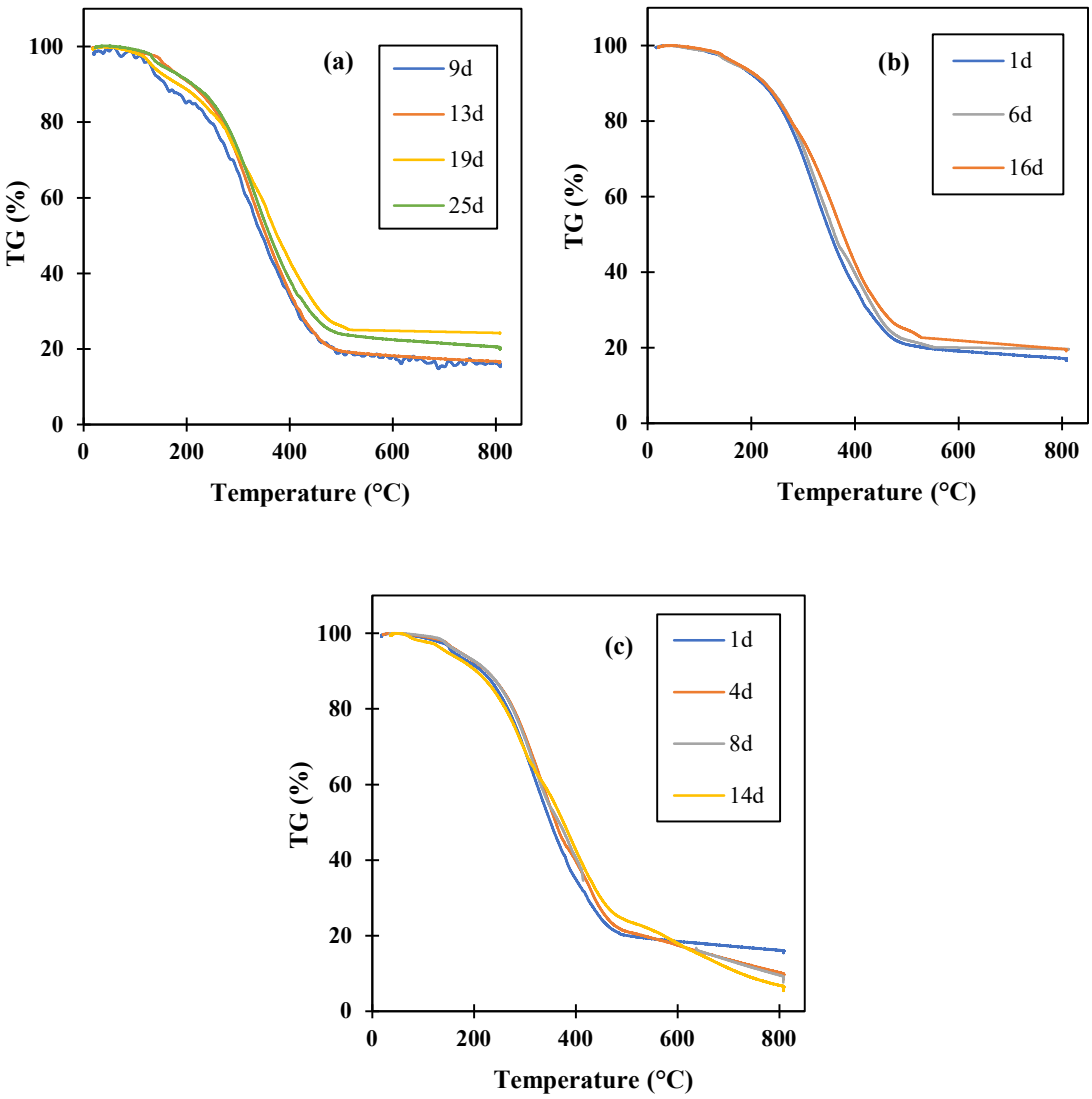

References

[1] International Energy Agency (IEA), Technology Roadmap Biofuels for Transport, 2011.

[2] L. Gouveia, Microalgae as a Feedstock for Biofuels, in: SpringerBriefs Microbiol., 2011: pp. 1–69.

[3] S. Kumar, Sub- and Supercritical Water Technology for Biofuels, in: J.W. Lee (Ed.), Adv. Biofuels Bioprod., Springer New York, 2013: pp. 147–183.

[4] N.S. Lewis, D.G. Nocera, Powering the planet: Chemical challenges in solar energy utilization, Proc. Natl. Acad. Sci. 103 (2006) 15729–15735.

[5] J.P. Maity, J. Bundschuh, C.-Y. Chen, P. Bhattacharya, Microalgae for third generation biofuel production, mitigation of greenhouse gas emissions and wastewater treatment: Present and future perspectives – A mini review, Energy. (2014).

[6] G.C. Dismukes, D. Carrieri, N. Bennette, G.M. Ananyev, M.C. Posewitz, Aquatic phototrophs: efficient alternatives to land-based crops for biofuels., Curr. Opin. Biotechnol. 19 (2008) 235–40.

[7] A.E. Harman-Ware, T. Morgan, M. Wilson, M. Crocker, J. Zhang, K. Liu, J. Stork, S. Debolt, Microalgae as a renewable fuel source: Fast pyrolysis of Scenedesmus sp., Renew. Energy. 60 (2013) 625–632.

[8] R. Thilakaratne, M.M. Wright, R.C. Brown, A techno-economic analysis of microalgae remnant catalytic pyrolysis and upgrading to fuels, Fuel. 128 (2014) 104–112.

[9] R. Halim, M.K. Danquah, P.A. Webley, Extraction of oil from microalgae for biodiesel production: A review., Biotechnol. Adv. 30 (2012) 709–32.

[10] R. Halim, B. Gladman, M.K. Danquah, P.A. Webley, Oil extraction from microalgae for biodiesel production., Bioresour. Technol. 102 (2011) 178–85.

[11] D. López Barreiro, W. Prins, F. Ronsse, W. Brilman, W. Prins, F. Ronsse, W. Brilman, Hydrothermal liquefaction (HTL) of microalgae for biofuel production: State of the art review and future prospects, Biomass and Bioenergy. 53 (2013) 113–127.

[12] C. Tian, Z. Liu, Y. Zhang, Hydrothermal liquefaction (HTL): A promising pathway for biorefinery of algae, 2017.

[13] S. Kumar, Sub- and Supercritical Water-Based Processes for Microalgae to Biofuels, in: R. Gordon, J. Seckbach (Eds.), Sci. Algal Fuels SE - 25, Springer Netherlands, 2012: pp. 467–493.

[14] G. Yu, Y. Zhang, B. Guo, T. Funk, L. Schideman, Nutrient Flows and Quality of Bio-crude Oil Produced via Catalytic Hydrothermal Liquefaction of Low-Lipid Microalgae, BioEnergy Res. 7 (2014) 1317–1328.

[15] H. Li, Z. Liu, Y. Zhang, B. Li, H. Lu, N. Duan, M. Liu, Z. Zhu, B. Si, Conversion efficiency and oil quality of low-lipid high-protein and high-lipid low-protein microalgae via hydrothermal liquefaction., Bioresour. Technol. 154 (2014) 322–9.

[16] L. Leng, J. Li, Z. Wen, W. Zhou, Use of microalgae to recycle nutrients in aqueous phase derived from hydrothermal liquefaction process, Bioresour. Technol. (2018).

[17] M. Saber, B. Nakhshiniev, K. Yoshikawa, A review of production and upgrading of algal bio-oil, Renew. Sustain. Energy Rev. 58 (2016) 918–930.

[18] P. Biller, A.B. Ross, Potential yields and properties of oil from the hydrothermal liquefaction of microalgae with different biochemical content., Bioresour. Technol. 102 (2011) 215–25.
[19] P.J. Valdez, V.J. Tocco, P.E. Savage, A general kinetic model for the hydrothermal liquefaction of microalgae., Bioresour. Technol. 163 (2014) 123–7.
[20] K. Anastasakis, A.B.B. Ross, Hydrothermal liquefaction of four brown macro-algae commonly found on the UK coasts: An energetic analysis of the process and comparison with bio-chemical conversion methods, Fuel. 139 (2015) 546–553.
[21] R. Singh, B. Balagurumurthy, T. Bhaskar, Hydrothermal liquefaction of macro algae: Effect of feedstock composition, Fuel. 146 (2015) 69–74.
[22] N. Neveux, A.K.L. Yuen, C. Jazrawi, M. Magnusson, B.S. Haynes, A.F. Masters, A. Montoya, N.A. Paul, T. Maschmeyer, R. de Nys, Biocrude yield and productivity from the hydrothermal liquefaction of marine and freshwater green macroalgae., Bioresour. Technol. 155 (2014) 334–41.
[23] D. Zhou, L. Zhang, S. Zhang, H. Fu, J. Chen, Hydrothermal Liquefaction of Macroalgae Enteromorpha prolifera to Bio-oil, Energy & Fuels. 24 (2010) 4054–4061.
[24] P.S. Christensen, G. Peng, F. Vogel, B.B. Iversen, Hydrothermal Liquefaction of the Microalgae Phaeodactylum tricornutum: Impact of Reaction Conditions on Product and Elemental Distribution, Energy & Fuels. 28 (2014) 5792–5803.
[25] D. López Barreiro, C. Zamalloa, N. Boon, W. Vyverman, F. Ronsse, W. Brilman, W. Prins, Influence of strain-specific parameters on hydrothermal liquefaction of microalgae., Bioresour. Technol. 146 (2013) 463–71.
[26] U. Jena, K.C. Das, J.R. Kastner, Comparison of the effects of Na2CO3, Ca3(PO4)2, and NiO catalysts on the thermochemical liquefaction of microalga Spirulina platensis, Appl. Energy. 98 (2012) 368–375.
[27] W.-T. Chen, Y. Zhang, J. Zhang, L. Schideman, G. Yu, P. Zhang, M. Minarick, Co-liquefaction of swine manure and mixed-culture algal biomass from a wastewater treatment system to produce bio-crude oil, Appl. Energy. 128 (2014) 209–216.
[28] W.-T.W.-T.. Chen, Y. Zhang, J.J.. b Zhang, G.. G. Yu, L.C.L.C.. Schideman, P.P.. P. Zhang, M.M.. M. Minarick, Hydrothermal liquefaction of mixed-culture algal biomass from wastewater treatment system into bio-crude oil., Bioresour. Technol. 152 (2014) 130–9.
[29] B. Jin, P. Duan, Y. Xu, F. Wang, Y. Fan, Co-liquefaction of micro- and macroalgae in subcritical water., Bioresour. Technol. 149 (2013) 103–10.
[30] Q.-H. Shen, Y.-P. Gong, W.-Z. Fang, Z.-C. Bi, L.-H. Cheng, X.-H. Xu, H.-L. Chen, Saline wastewater treatment by Chlorella vulgaris with simultaneous algal lipid accumulation triggered by nitrate deficiency, Bioresour. Technol. 193 (2015) 68–75.
[31] C. Safi, B. Zebib, O. Merah, P.-Y. Pontalier, C. Vaca-Garcia, Morphology, composition, production, processing and applications of Chlorella vulgaris: A review, Renew. Sustain. Energy Rev. 35 (2014) 265–278.
[32] L.M. Serrano, Estudio de cuatro cepas nativas de microalgas para evaluar su potencial uso en la producción de biodiesel, Universidad Nacional de Colombia, 2012.
[33] K. Anastasakis, A.B. Ross, Hydrothermal liquefaction of the brown macro-alga Laminaria saccharina: effect of reaction conditions on product distribution and composition., Bioresour. Technol. 102 (2011) 4876–83.
[34] U. Jena, K.C. Das, J.R. Kastner, Effect of operating conditions of thermochemical liquefaction on biocrude production from Spirulina platensis., Bioresour. Technol. 102 (2011) 6221–9.
[35] D. Li, L. Chen, D. Xu, X. Zhang, N. Ye, F. Chen, S. Chen, Preparation and characteristics of bio-oil from the marine brown alga Sargassum patens C. Agardh., Bioresour. Technol. 104 (2012) 737–42.

[36] S. Zou, Y. Wu, M. Yang, C. Li, J. Tong, Thermochemical Catalytic Liquefaction of the Marine Microalgae Dunaliella tertiolecta and Characterization of Bio-oils, Energy & Fuels. 23 (2009) 3753–3758.
[37] B.E. Eboibi, D.M. Lewis, P.J. Ashman, S. Chinnasamy, Effect of operating conditions on yield and quality of biocrude during hydrothermal liquefaction of halophytic microalga Tetraselmis sp., Bioresour. Technol. 170 (2014) 20–9.
[38] P. Duan, P.E. Savage, Hydrothermal Liquefaction of a Microalga with Heterogeneous Catalysts, Ind. Eng. Chem. Res. 50 (2010) 52–61.
[39] P. Biller, R. Riley, A.B. Ross, Catalytic hydrothermal processing of microalgae: decomposition and upgrading of lipids., Bioresour. Technol. 102 (2011) 4841–8.
[40] Y. Xu, X. Zheng, H. Yu, X. Hu, Hydrothermal liquefaction of Chlorella pyrenoidosa for bio-oil production over Ce/HZSM-5., Bioresour. Technol. 156 (2014) 1–5.
[41] C. Torri, D. Fabbri, L. Garcia-Alba, D.W.F. Brilman, Upgrading of oils derived from hydrothermal treatment of microalgae by catalytic cracking over H-ZSM-5: A comparative Py–GC–MS study, J. Anal. Appl. Pyrolysis. 101 (2013) 28–34.
[42] J. Li, G. Wang, M. Chen, J. Li, Y. Yang, Q. Zhu, X. Jiang, Z. Wang, H. Liu, Deoxy-liquefaction of three different species of macroalgae to high-quality liquid oil., Bioresour. Technol. 169 (2014) 110–8.
[43] C. Tian, B. Li, Z. Liu, Y. Zhang, H. Lu, Hydrothermal liquefaction for algal biorefinery: A critical review, Renew. Sustain. Energy Rev. 38 (2014) 933–950.
[44] Y. Guo, T. Yeh, W. Song, D. Xu, S. Wang, A review of bio-oil production from hydrothermal liquefaction of algae, Renew. Sustain. Energy Rev. 48 (2015) 776–790.
[45] G. Yu, Y. Zhang, L. Schideman, T.L. Funk, Z. Wang, Hydrothermal liquefaction of low lipid content microalgae into bio-crude oil, Am. Soc. Agric. Biol. Eng. 54 (2011) 239–246.
[46] Q.-V. Bach, M.V. Sillero, K.-Q. Tran, J. Skjermo, Fast hydrothermal liquefaction of a Norwegian macro-alga: Screening tests, Algal Res. 6 (2014) 271–276.
[47] L. Garcia Alba, C. Torri, C. Samorì, J. van der Spek, D. Fabbri, S.R.A. Kersten, D.W.F. (Wim) Brilman, Hydrothermal Treatment (HTT) of Microalgae: Evaluation of the Process As Conversion Method in an Algae Biorefinery Concept, Energy & Fuels. 26 (2011) 642–657.
[48] T. Minowa, S. Yokoyama, M. Kishimoto, T. Okakura, Oil production from algal cells of Dunaliella tertiolecta by direct thermochemical liquefaction, Fuel. 74 (1995) 1735–1738.
[49] T.T.-O. Matsui, A. Nishihara, C. Ueda, M. Ohtsuki, N. Ikenaga, T. Suzuki, Liquefaction of micro-algae with iron catalyst, Fuel. 76 (1997) 1043–1048.
[50] P.J. Valdez, M.C. Nelson, H.Y. Wang, X.N. Lin, P.E. Savage, Hydrothermal liquefaction of Nannochloropsis sp.: Systematic study of process variables and analysis of the product fractions, Biomass and Bioenergy. 46 (2012) 317–331.
[51] P.J. Valdez, J.G. Dickinson, P.E. Savage, Characterization of Product Fractions from Hydrothermal Liquefaction of Nannochloropsis sp. and the Influence of Solvents, Energy & Fuels. 25 (2011) 3235–3243.
[52] H. Li, J. Hu, Z. Zhang, H. Wang, F. Ping, C. Zheng, H. Zhang, Q. He, Insight into the effect of hydrogenation on efficiency of hydrothermal liquefaction and physico-chemical properties of biocrude oil., Bioresour. Technol. 163 (2014) 143–51.
[53] J. Zhang, Y. Zhang, Z. Luo, Hydrothermal Liquefaction of Chlorella pyrenoidosa in Ethanol-water for Bio-crude Production, Energy Procedia. 61 (2014) 1961–1964.
[54] D.R. Vardon, B.K. Sharma, J. Scott, G. Yu, Z. Wang, L. Schideman, Y. Zhang, T.J. Strathmann, Chemical properties of biocrude oil from the hydrothermal liquefaction of Spirulina algae, swine manure, and digested anaerobic sludge., Bioresour. Technol. 102 (2011) 8295–303.

[55] B. Patel, K. Hellgardt, Hydrothermal upgrading of algae paste in a continuous flow reactor, Bioresour. Technol. 191 (2015) 460–468.
[56] P. Duan, B. Wang, Y. Xu, Catalytic hydrothermal upgrading of crude bio-oils produced from different thermo-chemical conversion routes of microalgae, Bioresour. Technol. 186 (2015) 58–66.
[57] D. López Barreiro, C. Samorì, G. Terranella, U. Hornung, A. Kruse, W. Prins, Assessing microalgae biorefinery routes for the production of biofuels via hydrothermal liquefaction., Bioresour. Technol. 174C (2014) 256–265.
[58] N. Neveux, A.K.L. Yuen, C. Jazrawi, Y. He, M. Magnusson, B.S. Haynes, A.F. Masters, A. Montoya, N.A. Paul, T. Maschmeyer, R. de Nys, Pre- and post-harvest treatment of macroalgae to improve the quality of feedstock for hydrothermal liquefaction, Algal Res. 6 (2014) 22–31.
[59] S. Leow, J.R. Witter, D.R. Vardon, B.K. Sharma, J.S. Guest, T.J. Strathmann, Prediction of microalgae hydrothermal liquefaction products from feedstock biochemical composition, Green Chem. 17 (2015) 3584–3599.
[60] E.U. Franck, Fluids at high pressures and temperatures, Pure Appl. Chem. 59 (1987) 25.
[61] C. Jazrawi, P. Biller, Y. He, A. Montoya, A.B. Ross, T. Maschmeyer, B.S. Haynes, Two-stage hydrothermal liquefaction of a high-protein microalga, Algal Res. 8 (2015) 15–22.
[62] Z. Shuping, W. Yulong, Y. Mingde, I. Kaleem, L. Chun, J. Tong, Production and characterization of bio-oil from hydrothermal liquefaction of microalgae Dunaliella tertiolecta cake, Energy. 35 (2010) 5406–5411.
[63] J. Li, G. Wang, Z. Wang, L. Zhang, C. Wang, Z. Yang, Conversion of Enteromorpha prolifera to high-quality liquid oil via deoxy-liquefaction, J. Anal. Appl. Pyrolysis. 104 (2013) 494–501.
[64] S.S. Toor, H. Reddy, S. Deng, J. Hoffmann, D. Spangsmark, L.B. Madsen, J.B. Holm-Nielsen, L.A. Rosendahl, Hydrothermal liquefaction of Spirulina and Nannochloropsis salina under subcritical and supercritical water conditions., Bioresour. Technol. 131 (2013) 413–9.
[65] B.E.-O. Eboibi, D.M. Lewis, P.J. Ashman, S. Chinnasamy, Hydrothermal liquefaction of microalgae for biocrude production: Improving the biocrude properties with vacuum distillation., Bioresour. Technol. 174C (2014) 212–221.
[66] Z. Li, P.E. Savage, Feedstocks for fuels and chemicals from algae: Treatment of crude bio-oil over HZSM-5, Algal Res. 2 (2013) 154–163.
[67] P. Duan, X. Bai, Y. Xu, A. Zhang, F. Wang, L. Zhang, J. Miao, Catalytic upgrading of crude algal oil using platinum/gamma alumina in supercritical water, Fuel. 109 (2013) 225–233.
[68] C. Gai, Y. Zhang, W.-T. Chen, P. Zhang, Y. Dong, An investigation of reaction pathways of hydrothermal liquefaction using Chlorella pyrenoidosa and Spirulina platensis, Energy Convers. Manag. 96 (2015) 330–339.
[69] H. Huang, X. Yuan, The migration and transformation behaviors of heavy metals during the hydrothermal treatment of sewage sludge, Bioresour. Technol. 200 (2016) 991–998.
[70] D.C. Hietala, C.M. Godwin, B.J. Cardinale, P.E. Savage, The independent and coupled effects of feedstock characteristics and reaction conditions on biocrude production by hydrothermal liquefaction, Appl. Energy. (2019) 714–728.
[71] Y. Huang, Y. Chen, J. Xie, H. Liu, X. Yin, C. Wu, Bio-oil production from hydrothermal liquefaction of high-protein high-ash microalgae including wild Cyanobacteria sp. and cultivated Bacillariophyta sp., Fuel. 183 (2016) 9–19.
[72] K.P.R. Dandamudi, T. Muppaneni, J.S. Markovski, P. Lammers, S. Deng, Hydrothermal liquefaction of green microalga Kirchneriella sp. under sub- and super-critical water conditions, Biomass and Bioenergy. 120 (2019) 224–228.

[73] Y. Li, S. Leow, A.C. Fedders, B.K. Sharma, J.S. Guest, T.J. Strathmann, Quantitative multiphase model for hydrothermal liquefaction of algal biomass, Green Chem. 19 (2017) 1163–1174.
[74] D.C. Hietala, C.K. Koss, A. Narwani, A.R. Lashaway, C.M. Godwin, B.J. Cardinale, P.E. Savage, Influence of biodiversity, biochemical composition, and species identity on the quality of biomass and biocrude oil produced via hydrothermal liquefaction, Algal Res. 26 (2017) 203–214.
[75] W. Song, S. Wang, Y. Guo, D. Xu, Bio-oil production from hydrothermal liquefaction of waste Cyanophyta biomass: Influence of process variables and their interactions on the product distributions, Int. J. Hydrogen Energy. 42 (2017) 20361–20374.
[76] C. Gai, Y. Zhang, W.-T. Chen, P. Zhang, Y. Dong, Energy and nutrient recovery efficiencies in biocrude oil produced via hydrothermal liquefaction of Chlorella pyrenoidosa, RSC Adv. 4 (2014) 16958–16967.
[77] D. Xu, G. Lin, S. Guo, S. Wang, Y. Guo, Z. Jing, Catalytic hydrothermal liquefaction of algae and upgrading of biocrude: A critical review, Renew. Sustain. Energy Rev. 97 (2018) 103–118.
[78] S. Xiu, A. Shahbazi, Bio-oil production and upgrading research: A review, Renew. Sustain. Energy Rev. 16 (2012) 4406–4414.
[79] R. Shakya, J. Whelen, S. Adhikari, R. Mahadevan, S. Neupane, Effect of temperature and Na2CO3 catalyst on hydrothermal liquefaction of algae, Algal Res. 12 (2015) 80–90.
[80] R. Shakya, S. Adhikari, R. Mahadevan, S.R. Shanmugam, H. Nam, E.B. Hassan, T.A. Dempster, Influence of biochemical composition during hydrothermal liquefaction of algae on product yields and fuel properties, Bioresour. Technol. 243 (2017) 1112–1120.
[81] S.A. Channiwala, P.P. Parikh, A unified correlation for estimating HHV of solid, liquid and gaseous fuels, Fuel. 81 (2002) 1051–1063.
[82] M. DuBois, K.A. Gilles, J.K. Hamilton, P.A. Rebers, F. Smith, Colorimetric Method for Determination of Sugars and Related Substances, Anal. Chem. 28 (1956) 350–356.
[83] Y.S. Cheng, Y. Zheng, J.S. VanderGheynst, Rapid quantitative analysis of lipids using a colorimetric method in a microplate format, Lipids. 46 (2011) 95–103.
[84] T.K. Vo, S.-S. Kim, H.V. Ly, E.Y. Lee, C.-G. Lee, J. Kim, A general reaction network and kinetic model of the hydrothermal liquefaction of microalgae Tetraselmis sp., Bioresour. Technol. 241 (2017) 610–619.
[85] T.K. Vo, O.K. Lee, E.Y. Lee, C.H. Kim, J.-W. Seo, J. Kim, S.-S. Kim, Kinetics study of the hydrothermal liquefaction of the microalga Aurantiochytrium sp. KRS101, Chem. Eng. J. 306 (2016) 763–771.
[86] X. Bai, P. Duan, Y. Xu, A. Zhang, P.E. Savage, Hydrothermal catalytic processing of pretreated algal oil: A catalyst screening study, Fuel. 120 (2014) 141–149.
[87] Y.-P. Xu, P.-G. Duan, F. Wang, Q.-Q. Guan, Liquid fuel generation from algal biomass via a two-step process: Effect of feedstocks, Biotechnol. Biofuels. 11 (2018).
[88] ASTM, ASTM International Designation: Standard Specification for Biodiesel Fuel Blend Stock (B100) for Middle Distillate, ASTM Int. D6751-19 (2019) 1–10.
[89] T.M. Brown, P. Duan, P.E. Savage, Hydrothermal Liquefaction and Gasification of Nannochloropsis sp., Energy & Fuels. 24 (2010) 3639–3646.
[90] R.C. Selley, S.A. Sonnenberg, Chapter 2 - The Physical and Chemical Properties of Petroleum, in: R.C. Selley, S.A. Sonnenberg (Eds.), Elem. Pet. Geol., Third Edit, Academic Press, Boston, 2015: pp. 13–39.
[91] F. Obeid, T. Chu Van, R. Brown, T. Rainey, Nitrogen and sulphur in algal biocrude: A review of the HTL process, upgrading, engine performance and emissions, Energy Convers. Manag. 181 (2019) 105–119.

[92] S. Oh, H.S. Choi, U.-J. Kim, I.-G. Choi, J.W. Choi, Storage performance of bio-oil after hydrodeoxygenative upgrading with noble metal catalysts, Fuel. 182 (2016) 154–160.
[93] Z. Yang, A. Kumar, R.L. Huhnke, Review of recent developments to improve storage and transportation stability of bio-oil, Renew. Sustain. Energy Rev. 50 (2015) 859–870.
[94] Z. He, D. Xu, L. Liu, Y. Wang, S. Wang, Y. Guo, Z. Jing, Product characterization of multi-temperature steps of hydrothermal liquefaction of Chlorella microalgae, Algal Res. 33 (2018) 8–15.
[95] B.P. Hollebone, Oil Physical Properties: Measurement and Correlation, Handb. Oil Spill Sci. Technol. (2015) 37–50.
[96] D. Chen, J. Zhou, Q. Zhang, X. Zhu, Evaluation methods and research progresses in bio-oil storage stability, Renew. Sustain. Energy Rev. 40 (2014) 69–79.
[97] M.S. Haider, D. Castello, K.M. Michalski, T.H. Pedersen, L.A. Rosendahl, Catalytic Hydrotreatment of Microalgae Biocrude from Continuous Hydrothermal Liquefaction: Heteroatom Removal and Their Distribution in Distillation Cuts, Energies. 11 (2018).
[98] D. López Barreiro, F.J. Martin-Martinez, C. Torri, W. Prins, M.J. Buehler, Molecular characterization and atomistic model of biocrude oils from hydrothermal liquefaction of microalgae, Algal Res. 35 (2018) 262–273.
[99] L. Gouveia, A.C. Oliveira, Microalgae as a raw material for biofuels production, J Ind Microbiol Biot. 36 (2009).
[100] S. Jones, Y. Zhu, D. Anderson, R.T. Hallen, D.C. Elliott, Process Design and Economics for the Conversion of Algal Biomass to Hydrocarbons : Whole Algae Hydrothermal Liquefaction and Upgrading, 2014.
[101] J. Wagner, R. Bransgrove, T.A. Beacham, M.J. Allen, K. Meixner, B. Drosg, V.P. Ting, C.J. Chuck, Co-production of bio-oil and propylene through the hydrothermal liquefaction of polyhydroxybutyrate producing cyanobacteria, Bioresour. Technol. 207 (2016) 166–174.
[102] G. Teri, L. Luo, P.E. Savage, Hydrothermal Treatment of Protein, Polysaccharide, and Lipids Alone and in Mixtures, Energy & Fuels. 28 (2014) 7501–7509.
[103] J. Lu, Z. Liu, Y. Zhang, P.E. Savage, Synergistic and Antagonistic Interactions during Hydrothermal Liquefaction of Soybean Oil, Soy Protein, Cellulose, Xylose, and Lignin, ACS Sustain. Chem. Eng. 6 (2018) 14501–14509.
[104] L. Sheng, X. Wang, X. Yang, Prediction model of biocrude yield and nitrogen heterocyclic compounds analysis by hydrothermal liquefaction of microalgae with model compounds, Bioresour. Technol. 247 (2017) 14–20.
[105] P.J. Valdez, P.E. Savage, A reaction network for the hydrothermal liquefaction of Nannochloropsis sp., Algal Res. 2 (2013) 416–425.
[106] J.D. Sheehan, P.E. Savage, Modeling the effects of microalga biochemical content on the kinetics and biocrude yields from hydrothermal liquefaction, Bioresour. Technol. 239 (2017) 144–150.
[107] D.C. Hietala, J.L. Faeth, P.E. Savage, A quantitative kinetic model for the fast and isothermal hydrothermal liquefaction of Nannochloropsis sp., Bioresour. Technol. 214 (2016) 102–111.
[108] Z. Liu, H. Li, J. Zeng, M. Liu, Y. Zhang, Z. Liu, Influence of Fe/HZSM-5 catalyst on elemental distribution and product properties during hydrothermal liquefaction of Nannochloropsis sp., Algal Res. 35 (2018) 1–9.
[109] H.K. Reddy, T. Muppaneni, S. Ponnusamy, N. Sudasinghe, A. Pegallapati, T. Selvaratnam, M. Seger, B. Dungan, N. Nirmalakhandan, T. Schaub, F.O. Holguin, P. Lammers, W. Voorhies, S. Deng, Temperature effect on hydrothermal liquefaction of Nannochloropsis gaditana and Chlorella sp., Appl. Energy. 165 (2016) 943–951.
[110] S. Chaudry, P.A. Bahri, N.R. Moheimani, Pathways of processing of wet microalgae for liquid fuel production: A critical review, Renew. Sustain. Energy Rev. 52 (2015) 1240–1250.

[111] H. Chen, D. Zhou, G. Luo, S. Zhang, J. Chen, Macroalgae for biofuels production: Progress and perspectives, Renew. Sustain. Energy Rev. 47 (2015) 427–437.
[112] T. Suganya, M. Varman, H.H. Masjuki, S. Renganathan, Macroalgae and microalgae as a potential source for commercial applications along with biofuels production: A biorefinery approach, Renew. Sustain. Energy Rev. 55 (2016) 909–941.
[113] U. Jena, K.C. Das, Comparative Evaluation of Thermochemical Liquefaction and Pyrolysis for Bio-Oil Production from Microalgae, Energy & Fuels. 25 (2011) 5472–5482.
[114] A. Palomino, L.C. Montenegro-Ruíz, R.D. Godoy-Silva, Evaluation of yield-predictive models of biocrude from hydrothermal liquefaction of microalgae, Algal Res. 44 (2019).
[115] Y. Chen, Y. Huang, J. Xie, X. Yin, C. Wu, Hydrothermal reaction of phenylalanine as a model compound of algal protein, J. Fuel Chem. Technol. 42 (2014) 61–67.
[116] L. Luo, J.D. Sheehan, L. Dai, P.E. Savage, Products and Kinetics for Isothermal Hydrothermal Liquefaction of Soy Protein Concentrate, ACS Sustain. Chem. Eng. 4 (2016) 2725–2733.
[117] E. Barbarino, S.O. Lourenço, An evaluation of methods for extraction and quantification of protein from marine macro- and microalgae, J. Appl. Phycol. 17 (2005) 447–460.
[118] C. Safi, M. Charton, O. Pignolet, F. Silvestre, C. Vaca-Garcia, P.-Y. Pontalier, Influence of microalgae cell wall characteristics on protein extractability and determination of nitrogen-to-protein conversion factors, J. Appl. Phycol. 25 (2013) 523–529.
[119] M. Bjarnadóttir, B.V. Aðalbjörnsson, A. Nilsson, R. Slizyte, M.Y. Roleda, G.Ó. Hreggviðsson, Ó.H. Friðjónsson, R. Jónsdóttir, Palmaria palmata as an alternative protein source: enzymatic protein extraction, amino acid composition, and nitrogen-to-protein conversion factor, J. Appl. Phycol. 30 (2018) 2061–2070.
[120] J. Cheng, R. Huang, T. Yu, T. Li, J. Zhou, K. Cen, Biodiesel production from lipids in wet microalgae with microwave irradiation and bio-crude production from algal residue through hydrothermal liquefaction., Bioresour. Technol. 151 (2014) 415–8.
[121] A.R.K. Gollakota, N. Kishore, S. Gu, A review on hydrothermal liquefaction of biomass, Renew. Sustain. Energy Rev. (2016) 1–15.
[122] A. Galadima, O. Muraza, Hydrothermal liquefaction of algae and bio-oil upgrading into liquid fuels: Role of heterogeneous catalysts, Renew. Sustain. Energy Rev. 81 (2018) 1037–1048.
[123] K.O. Albrecht, Y. Zhu, A.J. Schmidt, J.M. Billing, T.R. Hart, S.B. Jones, G. Maupin, R. Hallen, T. Ahrens, D. Anderson, Impact of heterotrophically stressed algae for biofuel production via hydrothermal liquefaction and catalytic hydrotreating in continuous-flow reactors, Algal Res. 14 (2016) 17–27.
[124] D. Elliott, T. Hart, A. Schmidt, G. Neuenschwander, L. Rotness, M. Olarte, A. Zacher, K. Albrecht, R. Hallen, J. Holladay, Process development for hydrothermal liquefaction of algae feedstocks in a continuous-flow reactor, Algal Res. 2 (2013) 445–454.
[125] D.C. Elliott, T.R. Hart, G.G. Neuenschwander, L.J. Rotness, G. Roesijadi, A.H. Zacher, J.K. Magnuson, Hydrothermal Processing of Macroalgal Feedstocks in Continuous-Flow Reactors, ACS Sustain. Chem. Eng. 2 (2013) 207–215.
[126] Y.. Chen, N.. Zhao, Y.. b Wu, K.. Wu, X.. Wu, J.. Liu, M.. Yang, Distributions of organic compounds to the products from hydrothermal liquefaction of microalgae, Environ. Prog. Sustain. Energy. 36 (2017) 259–268.
[127] S. Czernik, D.K. Johnson, S. Black, Stability of wood fast pyrolysis oil, Biomass and Bioenergy. 7 (1994) 187–192.
[128] R.N. Hilten, K.C. Das, Comparison of three accelerated aging procedures to assess bio-oil stability, Fuel. 89 (2010) 2741–2749.
[129] O.D. Mante, F.A. Agblevor, Storage stability of biocrude oils from fast pyrolysis of poultry litter, Waste Manag. 32 (2012) 67–76.

[130] J. Kosinkova, J.A. Ramirez, Z.D. Ristovski, R.J. Brown, T.J. Rainey, Physical and Chemical Stability of Bagasse Bio-crude from Liquefaction Stored in Real Conditions, Energy &Fuels. (2016).
[131] T.-S. Kim, J.-Y. Kim, K.-H. Kim, S. Lee, D. Choi, I.-G. Choi, J.W. Choi, The effect of storage duration on bio-oil properties, J. Anal. Appl. Pyrolysis. 95 (2012) 118–125.
[132] J.P. Diebold, A Review of the Chemical and Physical Mechanisms of the Storage Stability of Fast Pyrolysis Bio-Oils, NREL, 2000.
[133] M.. Boucher, A. Chaala, H. Pakdel, C. Roy, Bio-oils obtained by vacuum pyrolysis of softwood bark as a liquid fuel for gas turbines. Part II: Stability and ageing of bio-oil and its blends with methanol and a pyrolytic aqueous phase, Biomass and Bioenergy. 19 (2000) 351–361.
[134] H. Li, S. Xia, Y. Li, P. Ma, C. Zhao, Stability evaluation of fast pyrolysis oil from rice straw, Chem. Eng. Sci. 135 (2015) 258–265.
[135] A. Oasmaa, J. Korhonen, E. Kuoppala, An Approach for Stability Measurement of Wood-Based Fast Pyrolysis Bio-Oils, Energy & Fuels. 25 (2011) 3307–3313.
[136] A. Oasmaa, E. Kuoppala, Fast pyrolysis of forestry residue. 3. Storage stability of liquid fuel, Energy and Fuels. 17 (2003) 1075–1084.
[137] J. Meng, A. Moore, D.C. Tilotta, S.S. Kelley, S. Adhikari, S. Park, Thermal and Storage Stability of Bio-Oil from Pyrolysis of Torrefied Wood, Energy & Fuels. 29 (2015) 5117–5126.
[138] L. Zhu, K. Li, H. Ding, X. Zhu, Studying on properties of bio-oil by adding blended additive during aging, Fuel. 211 (2018) 704–711.
[139] S. Raikova, H. Smith-Baedorf, R. Bransgrove, O. Barlow, F. Santomauro, J.L. Wagner, M.J. Allen, C.G. Bryan, D. Sapsford, C.J. Chuck, Assessing hydrothermal liquefaction for the production of bio-oil and enhanced metal recovery from microalgae cultivated on acid mine drainage, Fuel Process. Technol. 142 (2016) 219–227.
[140] J.-H. Yang, H.-Y. Shin, Y.-J. Ryu, C.-G. Lee, Hydrothermal liquefaction of Chlorella vulgaris: Effect of reaction temperature and time on energy recovery and nutrient recovery, J. Ind. Eng. Chem. 68 (2018) 267–273.
[141] Y. Dote, S. Sawayama, S. Inoue, T. Minowa, S. Yokoyama, Recovery of liquid fuel from hydrocarbon-rich microalgae by thermochemical liquefaction, Fuel. 73 (1994) 1855–1857.
[142] Y. He, X. Liang, C. Jazrawi, A. Montoya, A. Yuen, A.J. Cole, N. Neveux, N.A. Paul, R. de Nys, T. Maschmeyer, B.S. Haynes, Continuous hydrothermal liquefaction of macroalgae in the presence of organic co-solvents, Algal Res. 17 (2016) 185–195.
[143] S. Ren, X.P. Ye, Stability of crude bio-oil and its water-extracted fractions, J. Anal. Appl. Pyrolysis. 132 (2018) 151–162.
[144] M. Garcìa-Pèrez, A. Chaala, H. Pakdel, D. Kretschmer, D. Rodrigue, C. Roy, Evaluation of the Influence of Stainless Steel and Copper on the Aging Process of Bio-Oil, Energy & Fuels. 20 (2006) 786–795.
[145] S. Liu, M. Chen, Q. Hu, J. Wang, L. Kong, The kinetics model and pyrolysis behavior of the aqueous fraction of bio-oil, Bioresour. Technol. 129 (2013) 381–386.
[146] T.N. Trinh, P.A. Jensen, K. Dam-Johansen, N.O. Knudsen, H.R. Sørensen, S. Hvilsted, Comparison of Lignin, Macroalgae, Wood, and Straw Fast Pyrolysis, Energy & Fuels. 27 (2013) 1399–1409.
[147] H. Jo, D. Verma, J. Kim, Excellent aging stability of upgraded fast pyrolysis bio-oil in supercritical ethanol, Fuel. 232 (2018) 610–619.
[148] H. Hwang, J.-H. Lee, J. Moon, U.-J. Kim, I.-G. Choi, J.W. Choi, Influence of K and Mg Concentration on the Storage Stability of Bio-Oil, ACS Sustain. Chem. Eng. 4 (2016) 4346–4353.

[149] J.D. Adjaye, R.K. Sharma, N.N. Bakhshi, Characterization and stability analysis of wood-derived bio-oil, Fuel Process. Technol. 31 (1992) 241–256.
[150] H. Talbi, G. Monard, M. Loos, D. Billaud, Theoretical study of indole polymerization, J. Mol. Struct. THEOCHEM. 434 (1998) 129–134.
[151] F. Yu, S. Deng, P. Chen, Y. Liu, Y. Wan, A. Olson, D. Kittelson, R. Ruan, Physical and chemical properties of bio-oils from microwave pyrolysis of corn stover, Appl. Biochem. Biotechnol. 137 (2007) 957–970.